The Calibration of a Robotic Workstation

by

© Woon Kong Thong, B Eng (McGill University)

March 1986

Computer Vision and Robotics Laboratory
Department of Electrical Engineering
McGill University
Montréal Québec Canada

A thesis submitted to the Faculty of Graduate Studies and Research
in partial fulfillment of the requirements
for the degree of
Master of Engineering

Postal Address 3480 University Street Montreal Québec Canada H3A 2A7

Abstract

This thesis addresses the subject of calibrating a robotic workstation to allow a robotic manipulator a greater degree of adaptability in carrying out its tasks The specific task being carried out at the Computer Vision and Robotics Laboratory is the visual inspection and repair of hybrid Integrated Circuits An ECUREUIL Microbo robot and a Unimation PUMA 260 are used but the procedures developed here can readily be adapted to other applications The procedures involve external tactile and visual feedback to aid in the positioning of the tools carried by the arm The nature of the tactile sensing involves electrical contact, while visual feedback is derived from multiple *Charge Coupled Device* (CCD) cameras and a microscope with motorized zoom and focus These calibration techniques are programmed to automatically measure the tool calibration transformations associated with a variety of interchangeable tools used in the execution of its repair tasks The underlying philosophy in this procedure of calibration of the workstation is one of adaptability in which any minor re-positioning of the peripherals of the workstation such as the microscope, feeder, camera, etc can be efficiently updated and accommodated by the robot programs with minimal operator intervention Larger variations are handled by interactive graphic displays to assist the operator in setting up the workstation

Résumé

Cette these aborde le sujet de la calibration d une station robotique Le but est de permettre à un manipulateur robot d oeuvrer avec plus d aisance dans l exécution de ses fonctions Les principaux sujets de recherches au *Computer Vision and Robotics Laboratory*" sont l inspection visuelle et la reparation de circuits hybrides Les méthodes de calibration présentees ont éte developpees dans le but d être utilisees avec un robot Ecureuil de Microbo et un robot PUMA 260 de Unimation Cependant ces methodes peuvent être facilement adaptees a des applications n'impliquant aucun robot La connaissance des outils par le manipulateur est obtenue par l entremise de senseurs tactiles externes et de rétroaction visuelle Le fonctionnement des senseurs tactiles est basé sur l utilisation de contacts électriques alors que la rétroaction visuelle est obtenue à l aide d une caméra CCD (*Charge-Coupled Device*") et d un microscope muni de zoom et de focus motorises Ces techniques de calibration ont eté programmees afin d evaluer automatiquement les equations de transformation pour la calibration des outils interchangeables disponibles pour l execution des tâches de reparation L avantage de ces techniques de calibration est qu elles augmentent de façon importante la flexibilite d une station robotique Elles permettent de minimiser le nombre d'interventions de l opérateur de la station en corrigeant automatiquement les valeurs mémorisées des positions des peripheriques de la station lorsque ceux-ci subissent de faibles déplacements L'utilisation interactive de graphiques par ordinateur est requise dans le cas de déplacement majeur

Acknowledgements

I would like to thank FCAC and NSERC for their generous support of this work and the Computer Vision and Robotics Laboratory

I would like to thank the many people in the laboratory who have assisted me with advice and encouragement throughout the course of my work here

I would like to thank very much my parents for seeing me through this quest for tertiary education I could not have carried it out without their generous support and unfailing encouragement

Most of all I would like to thank my supervisor, Dr Alfred S Malowany for his constant encouragement and guidance of my research His is an epitome of patience

March 1985

Table of Contents

List of figures

1. Introduction and Robotics Survey

Since the very dawn of civilization man has attempted every so often to create tools that would expedite his task Initially those tools were used solely for hunting food for survival Later, with the advent of further civilization, the concept of survival took on an economic face The Industrial Revolution brought about tremendous advances in the automated methods of large volume productions The programmable weaving machine was an invention of that period BRITANNICA81 The quest towards faster and better machines however did not end there

There were a few attempts to create robotic devices in the 17th century but these were largely ornamental in nature and were essentially limited to remotely-controlled mechanisms which could write and draw and even play musical instruments BRITANNICA81 Some writers cite the *clepsydra* BRITANNICA81 or the water clock as the earliest forerunner of industrial robot devices but the trace is barely tangible

Faced with the need to produce advanced aircraft parts which were designed to be machined rather than riveted, the United States Air Force in 1947 funded research for the development of a numerically-controlled NC for short milling machine ROSEN72 It called for the implementation of sophisticated feedback techniques using digital technology which had just arrived on the scene The result of that effort was a machine that produced a workpiece which was cut according to the instructions punched out on a paper tape It was first demonstrated at the Radiation Laboratory of the Massachusetts Institute of Technology in 1953 PAUL81 Later refinements led to the Automatically Programmed Tool (APT) allowing the machine to be programmed in a more natural language BROWN63 ROSS59

Extrapolating the discoveries made in the construction of the NC milling machine and the teleoperator George Devol in 1960, produced Unimate's first industrial robot ENGELBERGER80 The robot first incorporated a feature now commonly found in today s robots it could be taught a simple task by leading it by the hand, literally, moving it through the sequence of task positions UNIMATION83 A year later, in 1961, at MIT's Lincoln's Laboratory a teleoperator with touch sensing was developed ERNST61 It incorporated touch sensors which were connected to the computer controlling the arm. This allowed the arm to be guided through the performance of its task by touch sensing, rather than by its absolute position Its task then was defined as a series of touch states ERNST61.

The word **robot** was first used in 1920 PFISTER82 in the play *Rossum's Universal Robots* written by the Czechoslovak dramatist Karel Čapek, who had derived it from the Czech word **robota** meaning *forced labour* BRITANNICA81 Unavoidably, the word *automaton* surfaces when the topic is discussed and is taken generally, to mean "a machine or control mechanism designed to follow automatically a predetermined sequence of operations or respond to encoded instructions" WEBSTER73 The word however, has fallen into disuse and been gradually superseded by the word *robot* An *android*, on the other hand, is used to describe a robot that has taken on a human-like appearance WEBSTER73, and is often the subject of many science fiction movies STAR79 EMPIRE81 RETURN83, BLADE82

One very obvious motivation for the advancement of robotics is definitely economics With human workers there is always the question of safety involved, and this often incurs a considerable expense for its provision ACHMATOWICZ82 Then, there are the fringe benefits the medical benefits the unemployment benefits, the retirement benefits, and the list goes on There are also the usual breaks that a human worker needs Very very few industries can lay claim to a totally tranquil labour-management relationship Disputes often lead to millions of lost man-hours of labour lost earnings and lost customers But with robots, this does not have to be so They are able to work tirelessly performing the same monotonous task over and over again with every piece handled exactly as the very first one LEVINTHAL82 The recent line of "J" cars by General Motors is painted and welded by robots ACHMATOWICZ82 In the consumer industries, there is very often a need to bring out a new product line every so often to satisfy new customer trends and demands RAUSA82 With older production technologies this is often a very expensive occurrence, for it involves re-tooling, and retraining of workers The latter is often very time-consuming Robots, on the other hand, can be re-programmed with a new sequence of maneuvers in next to no time LEVINTHAL82 Besides, robots are a very attractive option in filling the gap between laborious hand assembly for prototypes, and hard automation for large production runs STEWART82, BORTZ84

Serious development, however, did not take place until the second world war when R C Goertz developed the *teleoperator* to handle radioactive materials, when it was discovered that radioactivity was hazardous to human life GEORTZ63. R. Paul described it as thus "An operator was separated from a radioactive task by a concrete wall with one or more viewing ports through which the task could be observed The teleoperator was to substitute for the operator's hands, it consisted of a pair of tongs on the inside (the slave), and two handles on the outside (the master) Both tongs and handles were connected together by six degree of freedom mechanisms to provide for the arbitrary positioning and orienting of the master and slave The mechanism was provided to control the slave in order to replicate the motion of the master" PAUL81

Industry was quick to realize the importance of robots. It sought greater precision and speed in the control of motion to economically justify the use of robots. At the same time, digital computer technology had arrived on the scene With it, Cincinnati Milacron HOHN76 developed the world's first computer-controlled robot

1.1 Robot Vision

Significant in-roads were made into robot vision when L G Roberts demonstrated in 1963 the feasibility of obtaining a mathematical description of block-like objects which comprised a scene from a digitized half-tone image of the scene ROBERTS63 He further showed that he could represent their location and orientation by homogeneous coordinate transformations ROBERTS65

Recently, numerous attempts have been made to incorporate vision into robots, and there have been varying degrees of success Vision is the most complex, and yet, most powerful of our senses LEVINE85, KAK76 Nature has developed it to an extent that, just by looking at a scene, we are able to infer so many things about it Researchers have implemented into computational algorithms some of the ways they think we are extracting our information from the scene LEVINE85 KAK76 These algorithms are often computationally very expensive PAUL81, and by no means anywhere near what we achieve with our own eyes Nonetheless, by 1970 vision-controlled robots reached a stage of development when the "insanity puzzle" - a puzzle in which 4 cubes with coloured faces must be stacked so that no identical colours appear on any one side - was solved at Stanford FELDMAN82 The solution of the "missing" vision feedback link had one valuable attendant benefit Today's robots are often very repeatable but not accurate If, for example, a robot is made to traverse a certain distance, it can replicate that distance moved very nearly exactly However, that distance moved as determined by the robot, is a poor representation of the *actual* distance FOULLOY84 With vision feedback it is possible to guide the robot to the desired position in space to within its repeatability FOULLOY84 This is very much in accordance with how humans solve trajectory problems Humans do not perform any trigonometric calculations to obtain the position of their hand PAUL81 Rather they do it by a series of corrections supported by visual information of the scene obtained by their eyes, and finally when the object is sufficiently close, by their touch

Despite the short-comings of current techniques, there are a number of commercial machine vision systems CARLISLE81 available on the market all of them using some variation of the algorithm developed by G J Agin which extracts features from binary images AGIN79 A more modern approach is taken by **CONTEXT**VISION, based on grey-scale, color and contextual information of the pixels CONTEXTVISION85

1.2 Force Sensing

Force feedback is often overshadowed when it is juxtaposed with robot vision, but nonetheless it is a very important building block in the solution of the robot puzzle Vision can guide a robot to the proximity of a target However any closer approaches to the target can only be made with the provision of force sensing to enable tactile exploration with specifiable pressure of contact RAIBERT82 This is particularly important in assembly where parts have to be brought together and fitted WHITNEY76 In the early seventies, Stanford University developed a system in which the joints of a manipulator arm were force-servoed, rather than position-servoed with the degree of compliance specified in an instruction Further work there gave birth to a robot control command language called WAVE, which for the first time ever, brought force touch and vision together in a single comprehensive system PAUL77. The assembly of a water pump was demonstrated using this approach BOLLES73.

Under the same title of force sensing, one could probably include tactile sensing Tactile sensing can provide information regarding the texture of the object touched, and also, to a certain extent, force sensing too While some researchers have been experimenting with pressure conductive plastics BEJCZY78, SYNDER78, some have adopted a more novel approach with the sensor fabricated on a VLSI RAIBERT82 This implementation has the advantage that the transduced information is already processed by the VLSI before being communicated RAIBERT82

1.3 Artificial Intelligence

Research into the area of artificial intelligence too has been going on for some time now, ever since the advent of computers NILSSON80, WINSTON82 The rapid development of robotics however has given a tremendous impetus to further its advancement Artificial intelligence is the formulation of computer algorithms for the process of abstract thought WINSTON82 and this augurs well with robots as they are computer controlled With few exceptions much that has gone on in the field of artificial intelligence is done in a piece-meal ad-hoc fashion Part of the problem lies in that it is difficult for man to articulate every variable considered in reaching his decision and also that man does not reach his decision by the brute consideration of all the alternatives - though he may do so for a small fraction of them - but rather by a heuristic approach in which man draws upon his experience to narrow the decision considerably NILSSON82 From there on an exhaustive search may then take over However there has not been a comprehensive expansion of the work in this area that would take it a quantum leap forward Nevertheless under some unambiguous controlled situations JORDAN82 these systems can be made to think, sense and effect a course of action NILSSON82 In a narrow sharply-defined area of expertise - thereby earning the name "expert systems" JORDAN82 systems such as MYCIN and PROSPECTOR, in the areas of medicine and prospecting for minerals respectively have achieved a considerable measure of success NILSSON80

The process from which one goes from not knowing to knowing is learning Artificial Intelligence researchers have been trying to incorporate this learning process into some of their expert systems and some foresee the next generation of robots being able to learn from experience and using accrued experience to formulate plans KEMPF82, BALZER85

1.4 Collision Avoidance

The problem of path/trajectory planning and its attendant velocity planning GUPTA84, SCHWARTZ83, has been the focus of researchers in order to lay the ground work for semi-autonomous and autonomous robots LEVINTHAL82 LEIGHTY82 This is necessary for increased autonomy so that the robot itself CROWLEY84 BROWN82 can determine the path and velocity with which it has to take to avoid static and dynamic obstacles GUPTA84 This requires the robot to have a dynamic model of the world CROWLEY84, SHNEIER84 Some researchers are concentrating solely on the path planning problem GUPTA84 SCHWARTZ83, while others are examining methods for gathering the trajectory information of the objects to be avoided UDUPA77 Often the solution cannot be computed in polynomial time[1], but simplifications can be made that will allow a more reasonable time response SCHWARTZ83, HOPCROFT83

1.5 Locomotion

Ever since the advent of robots, there have been attempts to make them more mobile Wheels proved to be the easiest to implement, but it restricted movement only to places on which the wheels could travel HARMON82 This ruled out any travel over soft and irregular terrains DEKKER69 The development of a more versatile mode of carriage, in the form of a multi-legged robot HARMON82 MOSHER69 had to wait for the arrival of digital technology, in particular, it had to wait for the development of microprocessors CHAO79 This was so

[1] If a problem can be solved in polynomial time it means that the time to reach the solution is a polynomial function of the variables of the problem

because of the tremendous complexity involved in the independent control of a number of these legs each again with a number of degrees of freedom SUN74 S R Harmon terms this as articulated locomotion Much work has been done on an experimental hexapod vehicle at the Ohio State University by R B McGhee in 1977 McGHEE77 C A Klein and Maney in 1979 KLEIN83 In the same year C S Chao introduced real-time microprocessor control to the vehicle CHAO79 In 1976, D E Orin researched interactive control ORIN76 and implemented supervisory control in 1982 ORIN82 while Klein Olson, and Pugh used attitude and force sensors to maneuver through irregular terrain KLEIN83

1.6 Robot Languages

Much research is currently being carried out to design robot control command languages VANDERBRUG81 HAYWARD83, LOZANO77, BONNER82 To describe each and every move down to the last variable in the command primitives, can be a time consuming and burdensome task for all but the simplest of maneuvers KEMPF82 It seems obvious that some form of hierarchical command structure has to be developed in which the user would describe his objective prefably in a natural language and this hierarchical structure of command interpretation should then be able to parse it into a concise and unique set of primitive directives LOZANO83 This structure too, apart from receiving direction from the top, must also be able to accept information from levels further down the hierarchy TAYLOR82 Force feedback information from the various joints and fingers and visual information from any number of perspectives, for example are inputs which must be accepted at some level VANDERBRUG81 Robot languages are, to a certain extent a function of the intelligence of the machine If the robot incorporated a sufficiently large amount of intelligence, it would be able to understand spoken language, define the task, and also execute it HARMON82 The US

Defense Advanced Research Projects Agency (DARPA) is heavily involved in the research and funding of the development of such robots HARMON82 In the mean time, however there is an urgent need for the development of powerful and comprehensive robot simulators that will allow for an accurate depiction of the robot movements under program control With such simulators it would then be possible to develop programs off-line with a shorter down-time and with much less chance of damaging the robot in the process This would be especially useful in the testing of multi-robot programs SOROKA83 .

1.7 Impact of Automation on Society

Much has been written about the impact of automation on society THOMAS78 BRONOWSKI78 HAYES84 Philosophers, thinkers and sociologists, have at one time time or another discussed the ramifications of increased automation in society They pondered upon the effects on the average factory worker and what he would be doing if he were displaced by advances in automation The same probably happened when the world headed for its industrial revolution It is true that people got displaced from occupations directly related to agriculture, but somehow, other forms of occupation came along to fill those lost HAYES84 Probably, one of the more interesting views in this matter comes from the author of "The Medusa and the Snail", Dr Lewis Thomas, who likens the relationship between man and computers, and by extension robots, to the medusa and the snail These two life-forms carry on a symbiotic relationship in which one species is dependent on the other for survival THOMAS74 In the same way too, computers and robots should not be looked upon as man's nemesis, but rather as an entity - the use of the word "entity" here may be disputed - that would complement and enrich man's existence. Man can look after the needs of the machines by supplying it with parts, power, and maintenance, and in return the machines can relieve us of the drudgery of more mundane tasks and better look after the complex socio-economic structure of our society In relieving us of the more mundane of tasks, we are free to better seek out our creative and artistic tendencies HAYES84

1.8 Future Direction

There has been some enthusiasm lately about holding an international robotics competition to come up with an integrated robotic system that will allow a pair of robots to engage themselves in a game of ping pong LOEWENSTEIN84 At present, this task presents a very demanding set of specifications for the image processing, optical or otherwise, and trajectory calculations which have to be performed at millisecond speeds LOEWENSTEIN84 This is still very much beyond the capabilities of today's hardware LEVINE85, DUDA72, AMBLER73 and software PIPITONE83

The US Department of Defense is spearheading some of the state-of-art developments in robotics and robotics intelligence (artificial intelligence as applied to robots) LEVINTHAL82, LEIGHTY82 HARMON82 In the future, the army hopes to have autonomous and semi-autonomous vehicles - planes, drones, tanks, etc - to fight wars LEVINTHAL82 In the near term future they envisage automated munitions loaders, automatic ware-housing, teleoperated devices, and flight display and warning systems LEIGHTY82 The army hopes that in the long-term future, they will be able to develop fighting machines like one-man helicopters, two-man tanks, and one-man artillery pieces LEIGTHY82

1.9 Robot Calibration Techniques

Robots like most instruments of precision, have to be calibrated, and much more frequently than others because of their articulated linkage construction Calibration is required in each of the domains in which sensing is performed to effect the robotic task Calibration is of particular importance in robotic environments because the robot actually uses these inputs to coordinate itself For unattended operations, these become the *only* aids to its operation Failure or more often incorrect interpretation of these stimuli could well lead to an entire batch of incorrectly assembled parts

1.10 Tactile Sensing

Besides our vision, in our daily solution of the "pick-and-place" problem, we depend heavily on our touch to subconsciously gain insight to the nature of the object we are picking up SANDERSON83 So it is no accident that with the advent of more intelligent robots we often incorporate some form of tactile sensing, and thereby exploration to lend it some measure of adaptability SANDERSON83 Furthermore as mentioned earlier vision alone cannot complete the task of assembly force/torque sensing is prerequisite when parts have to be fitted together WHITNEY76 BOLLES73 There are instances too, when force/torque sensing is necessary when the fingers of the robot - the end effectors - obscure its vision system NITZAN81 The most fundamental of the application of force sensing is its use in tactile sensing Initially most of these methods are electrical in nature having only a binary condition which is essentially limited to describing whether there is indeed a contact or not MALOWANY85 In more critical applications however, this response is inadequate because a contact can either mean that the robot is touching the target or that it has smashed into it Some researchers have attempted to remedy this through the use of multiple contacts, with designs somewhat resembling cat's whiskers This still remained inadequate, and has led some researchers to explore inductive proximity sensors sensors whose inductance is a function of its proximity to the target NITZAN81 SANDERSON83 Another form of proximity sensing is to use photodiode detectors to sense the reflections off a target from Light Emitting Diodes (LED s) This method of proximity sensing, however, is dependent upon the reflectance of the target NITZAN81, but can be accommodated by calibration

To completely describe all the forces, and or torques exerted at a particular location, a force/torque sensor must measure six components in all three components of force, and three components of torque PAUL81. As applied to robots, this sensor measures these components between the last link of the robot and its end effector, which can be thought of as the wrist GOTO72 WATSON75 The strains generated here through contact between the end-effector and the work piece are transduced by strain gauges into electrical signals which are analyzed for the direction and magnitude of these stresses NITZAN81 The strain gauges used take on a variety of forms, but those which are currently preferred are the semiconductor variety NITZAN81 They are robust - able to withstand sudden jarring motions and harsh environmental conditions - and generate a large output for the same amount of stress when compared to a wire strain gauge NITZAN81 Some researchers, however, are experimenting with the use of mylar films with metallization on both sides as force sensors Contact with any object will compress the mylar film, and thereby increase its capacitance, the harder the contact, the greater will be the increase in capacitance Other researchers are concentrating their efforts on piezoelectric force sensors BARDELLI83, and also on ansiotropic conducting materials SYNDER78

An attendant of force sensing is active compliance With active compliance, it is possible to servo the arm until a certain force is reached PAUL76 This has proven to be especially useful in the assembly of parts without the use of chamfers SANDERSON83, and also in manufacturing processes which requires following the contour of the workpiece such as grinding, deburring, and seam-tracking SANDERSON83, SELTZER82

1.11 Scanning Laser Interferometer

There exists a class optical measurement methods that come under the generic term of time-of-flight ranging While tactile exploration may solve some of the problems associated with robotics, it is still primitive, and often inflexible because the discovery path has to be known to some extent before it can be traversed in order to gather the needed information As with man, vision is turning out to be the most powerful, as well as the most complex, tool in robotic applications In robotic applications, the term vision is not exclusively used for the sensing of information in the visible region of the electromagnetic spectrum, but also in the infrared and ultraviolet regions Coherent light, especially laser light, is often used for visible region sensing because it affords a greater depth of field PARTHASARATHY82, RIOUX84 Time-of-flight methods usually make on the configuration shown in figure 1 A pulsed laser beam is directed at the target in question, and the reflected beam is collected by a fast receiver, usually a photomultiplier With the elapsed time between the emission of the pulse, and its return, and the knowledge of the speed of light, the range information can be computed Time-of-flight methods are not without problems, however, especially when very short distances are involved Light takes only about 7 picoseconds to traverse 1 millimeter This requires extremely fast circuits to measure this duration, and repeated averaging is often necessary to reduce the statistical scattering PARTHASARATHY82 Also, this scheme tends to be slow if the target is dark Dark targets require repeated averaging to improve the upon the low reflected signal amidst noise This may be solved by increasing the power of the laser, but in doing so the power of the laser may be raised to a hazardous level NITZAN81 The main disadvantage of such a system is the severe speed-accuracy trade-off PIPITONE83, RIOUX84

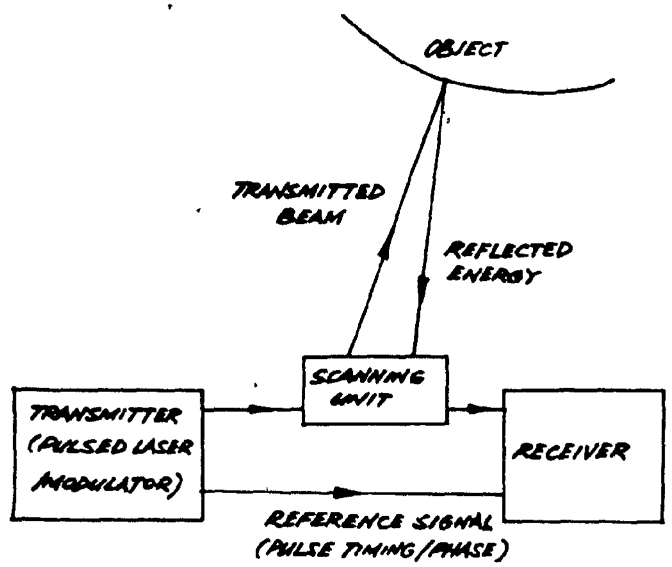

Figure 1 Time of flight ranging

The use of lasers in range determination is not limited to time-of-flight methods Range determination by triangulation is another well-researched method CONNAH82, NIMROD82, PARTHASARATHY82 In triangulation (see figure 2), the range of the target is determined by bouncing a laser beam off a mirror to reflect off the target and then bringing the reflected beam to focus on a detector array D is the baseline distance, the distance between the z-axis of the laser and the principal axis of the lens The laser rangefinder is first calibrated by directing the laser at a known point, say $(\frac{D}{2}, l)$, and observing the location of the beam on the sensor array. The angle that the beam makes when reflected off the mirror with the x-axis is θ Once the rangefinder is calibrated, any subsequent point such as (x, z) can be readily determined CONNAH82, PIPITONE83, RIOUX84 The name triangulation comes from the fact that the directions of the incident and reflected beams - the angles of two sides of a triangle - together with the length of the baseline have to be known to determine the third point

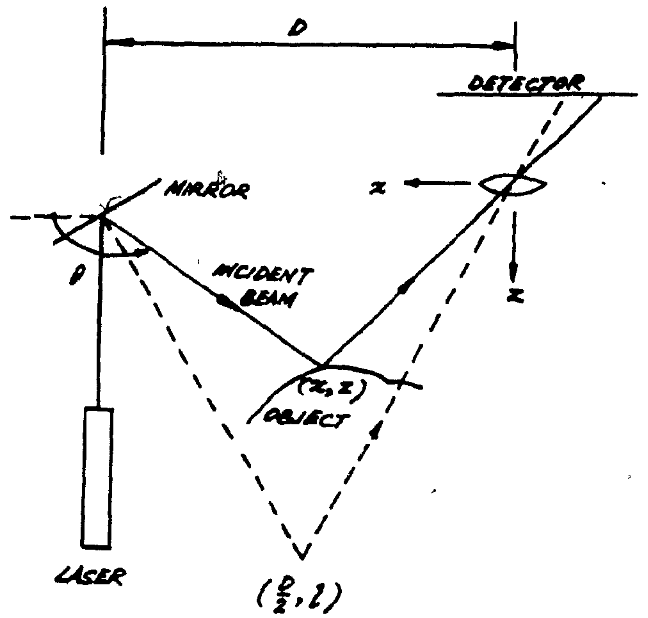

Figure 2 Ranging by triangulation

Laser interferometry is another different yet related method of time-of-flight ranging ANDERSON82 Interferometry has been in use for the last few decades now The technique was used in X-ray crystallography in which X-rays of a known wavelength are bounced off a sample of the crystal to be examined Since the phase is a linear function of round-trip time, it becomes also a linear function of range PIPITONE83 Large displacements are generally more difficult to perform, but this technique is excellent for small displacements with precisions of up to 0 03 microns ANDERSON82

1.12 Ultrasonic Sensing

There have been recent attempts to develop ultrasonic sensing techniques for use in calibration Very much like the way a bat sees its way in the dark, these methods are essentially time-of-flight methods, whereby a source of ultrasonic vibration of a known frequency is emitted, and the time between its emission and its returning echo is measured NITZAN81 Knowledge of the group velocity of the vibration at that particular air pressure, density, and temperature will allow the distance to the target to be measured. For the position of the target to uniquely known in 3-D space, measurements from at least two different locations are required There are two main variables here that directly affect the accuracy of this method It can shown mathematically that the minimum distance that can be resolved by illuminating a target with any emission, can at best be equal to half the wavelength of that emitting radiation This means that, for example, if the wavelength of the radiation is 1.0mm, its position cannot be resolved to better than 0 5mm On the face of it, the solution would be to use a vibration of a sufficiently high frequency - thereby affording a correspondingly shorter wavelength - but it turns out that materials readily absorb high frequency vibrations NITZAN81. Another major source of error comes from the fact that ultrasonic sensing systems are very prone to noise This can be remedied to a large extent by repeating the measurement a large number of times and then performing a statistical analysis on the resultant data as to locate the volume with the highest probability of containing the target

1.13 Monocular, Binocular, Polycular Vision

Vision has long fascinated and intrigued researchers Early researchers concentrated on the elements of vision, and on how low-level vision is performed The advent of digital computers gave rise to the study of *computer vision* LEVINE85, KAK76 There have been numerous attempts to incorporate vision into robots AGIN79 This, in large part, is due to the flexibility afforded by vision However, there still remain many unanswered questions leaving only a poor realization of what could be One reason for this is that man is the only creature that can articulate the sensation of seeing LEVINE85. Coupled to this is the difficulty of divorcing the physics of seeing from the perception of seeing KAK76 This has somewhat hampered the research in the field of computer vision

Monocular vision, as the term implies, is vision based on the view obtained from only one point of view Often, the 3-D information, or the "depth map", is invariably lost because it cannot be inferred from the scene This can be made up to a certain extent through the use of structured light sources, in which the light sources are collimated, and their angles of incidence known With the knowledge of resultant shadows generated by occluding structures, the depth map can be partially filled OKADA82 In some methods, the structured light sources are projected as a slit onto the target, and from the resultant line traced out by the light source, the depth map of the target can be computed PORTER82 Hovanesian and Hung, on the other hand, used moire light patterns on the targets These are concentric light and dark bands of illumination which are projected onto the target HOVANESIAN82 The particular distortion of these patterns on the target is indicative of the contour of the target HOVANESIAN82.

Binocular vision is best known in man The two different views obtained in each eye are integrated in the brain to generate a 3-D model of the world There are occasions, however, when the target is sufficiently far way that the information is no longer 3-D, but compressed into 2-D This happens when the distance to the target is considerably greater than the distance between the two eyes, also known as the base-line However, this problem can be alleviated to an extent by increasing this baseline, by physically moving to a different viewing location, or by having multiple viewing positions as in the case of polycularvision The ways in which the 3-D information is inferred from the 2-D images are many, but it is generally accepted that the process in man makes use of tokens in the target, whose dimensions are known, or at least estimated, which when viewed from different perspectives, presents different, yet related, views from which the distance to target can be inferred LOEWENSTEIN84. What the algorithm does basically, is to find a correspondence between the two (or many) views LOEWENSTEIN84 Implementations of this algorithm, however, are particularly difficult and computationally very expensive DUDA73, MUDGE82 and have yet to fill the need for a fast and reliable method of detection A possible way of cutting down the computational complexity would be to use "partial token matching", matching only part of the image LOEWENSTEIN84

There are some attempts to categorize vision into either those utilizing ambient illumination, and those utilizing active - eg projected light planes - illumination NITZAN81 This distinction tends to be rather weak in that, for example, there is no such thing as ambient illumination in the laboratory Illumination there is always active Rather, the distinction should be made differently Although illumination in the laboratory is always active, some techniques use a *structured* form, while others do not. Structured light sources refer to sources where some geometrical or planar attributes are attached to the illumination

Today vision sensing is achieved by solid state linear, or area photo-sensitive arrays In its early days, these arrays were limited to 128 X 128 elements FAIRCHILD82, but recently arrays of 2048 X 2048 have been fabricated, and reportedly used in spy satellites by the United States Light falling on each element of these arrays is converted into an electrical signal, either charge or voltage By scanning these arrays in a predetermined fashion, a serial stream of signals corresponding to the image is generated and can then be transmitted to a computer for processing As with all solid-state devices, they also boast of a more robust nature, able to well withstand the rigors of the environment and also of usage NITZAN81 They also offer a much larger dynamic range to input illumination and have a much quicker response time NITZAN81 In addition, these devices are sensitive to a larger portion of the electromagnetic spectrum but can also be tailored to have a response very close to the photopic sensitivity of the human eye NITZAN81 Because these devices are solid state, they are often very compact and light-weight, thereby earning their places in spacecraft payloads, satellites, robotics, and many other applications where space and weight are premium

Recent research in VLSI has produced special function chips which embody image processing algorithms in hardware that allow for the execution of these algorithms at hardware speeds Hughes and the University of Southern California have developed such chips that run at 10MHz MILGRAM78 Some common image processing functions that have been hardwired this way are edge detection, correlation masking and convolution BOUDREAULT85 Because some of these functions operate on pixel information independent of its neighbours, Single-Instruction-Multiple-Data (SIMD) LOWRY82 architectures have been implemented in silicon to do the task Hardware implementation of these algorithms is necessary because of the tremendous throughput involved in the processing of images The delegation of low-level processing to dedicated processors is a necessity to maintain some semblance real-time response NITZAN81

1.14 Thesis Overview

This thesis addresses the subject of calibrating a robotic workstation Here in the Electrical Engineering department at McGill University we are in the process of developing a robotic work/repair station for the inspection and repair of hybrid Integrated Circuits (IC's) We have a production model of the Unimation PUMA 260, a recently acquired ECUREUIL Microbo, and a brand new IBM 7565 robot Chapter 1 surveys the current robotics literature, the state-of-the-art developments and provides an insight to future direction Chapter 2 looks at some of the problems that have to be solved in order to accomplish the workstation calibration.

inspection and repair task It will also examine some of the calibration techniques currently used their applicability and their limitations Chapter 3 develops the mathematics used to control the robot arm and to derive the calibration results obtained in this thesis Chapter 4 presents the experimental results obtained from a production model of Unimation's PUMA 260 Chapter 5 concludes by summing up the salient points researched in this thesis

2. The Hybrid IC Inspection/Repair Task

2.1 Hybrid Integrated Circuits

The term "hybrid" IC's comes from the fact that the circuit is constructed using a hybrid of components it incorporates both active and passive components JONES82 It is fabricated on an insulating substrate together with some thin- or thick-film components, monolithic semiconductor devices, and discrete components JONES82 The substrate is usually alumina or ceramic JONES82 Metallic interconnect and passive components, like fired resistors, capacitors dielectric and solder pads are then transferred to the substrate Unlike conventional printed circuit boards in which the conductor pattern is formed by removal of conductor material, the conductors are *fabricated* on to the substrate Also unlike the conventional printed circuit board which uses drilled and plated through mounting holes, the use of solder pads greatly increases circuit integrity and reliability as well as eliminating the cost involved in the production of the mounting holes MARCOUX84 Components are attached to the circuit board with epoxy adhesive and then soldered to the solder pads Strong demand for higher circuit densities and functional varieties JONES82, MARKSTEIN84 has prompted nearly every major semiconductor manufacturer to offer their current line of products in miniaturized chip carriers BROWN84 Referred to in the industry as "small outline" (SO) packages, this has led to electronic assemblies which are up to 60% smaller, and up to a third less costly than comparable PCB's MARCOUX84

Because hybrid IC's boards have all their components mounted on the surface of the substrate, they are also called Surface Mount Assemblies (SMA) MARCOUX84 SMA's have the attractive advantage being easily assembled by robots or special automation as it is essentially a pick-and-place task with none of the problems associated with the insertion of components and leads into specific holes JONES82 MARKSTEIN84 Current SMA automatic assembly devices however are rather simple and rely heavily upon the precise registration of the substrate MARKSTEIN84 Any problems with the registration of the substrate could result in the misplacement of components for an entire batch Barring any misalignments however these hard automation machines with multi-placement heads reach remarkable speeds of up to 140 000 components per hour[1]

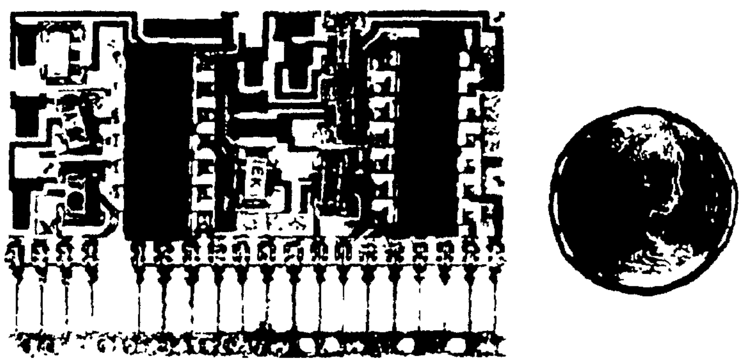

Figure 3 A Hybrid integrated circuit

2.2 The Inspection/Repair Task

The Computer Vision and Robotics Laboratory of the Department of Electrical Engineering here at McGill University is currently involved in a program to inspect for manufacturing defects in hybrid Integrated Circuits (IC's) using computer vision, and robots to physically perform the repair if the repair can be effected Figure 3 shows a typical hybrid IC that will be inspected by such a system The penny next to it gives an indication of its size Figure 4 shows the configuration of the robotic workstation The robot seen on the right is the PUMA 260 and that in the center is the MICROBO

There are a number of problems specific to the repair of manufacturing defects in hybrid IC s (This is not to be confused with any problems with the electrical performance of the circuit) LEVINE82 The defects are physical in nature and are a direct result of an aberration in the manufacturing process The following is a list, though not exhaustive, of the possible defects that can be currently accommodated by the inspection/repair system -

i) missing components

ii) bridged/open conductors

iii) solder defects excess/insufficient

iv) misaligned/inverted components

Figure 4 The inspection/repair workstation

The obvious prerequisite of the repair task is the inspection task The *a priori* knowledge of the scene. in this case the hybrid IC. allows grey-scale processing of the image to be sufficient The number of grey-scales needed is dependent upon the task to be performed Generally anywhere between 64 (2^6) and 256 (2^8) levels are the most often used Commercially available visual inspections systems have all implemented in one form or another algorithms that have been developed by Agin and Gleason for Automatix AGIN79 Agin and Gleason used high contrast images - a target against a lighted background - to obtain a *binary* image of the item to be inspected The binary images are then converted to edges and approximated by straight lines or curves as the case may be PAVLIDIS82 Once the polygonal approximation has been made. the shape and orientation of the object can then be deduced. and a decision made as to whether it has a defect. or if it is indeed of the right dimensions PAVLIDIS82

For more complex scenes without the aid of back-lighting. however. a definitive binary image cannot be easily obtained Resort has to be made to more complex image processing algorithms In the low-level processing of the raw image. edge operators have proven themselves to be very useful On a background of noise or clutter. an edge operator has the effect of enhancing the edges. and at the same time lowering the noise content Thresholding can then be effectively used to produce a cleaner binary image

Another algorithm that is often used after the generation of a suitable binary image is horizontal and vertical profiling In horizontal and vertical profiling. a signature is obtained of the horizontal and vertical profiles of the sub-image under study This signature is then compared with that of a reference Rejection or acceptance is often a function of its deviation from the reference Paul Merrill. one of our former researchers. has used this method quite effectively in his method to inspect solder joints visually MERRILL84 In his program. one joint at a time is presented to the vision system. and its horizontal and vertical signatures compared to a reference While it does not represent a perfect verification of the joint. it is successful about 75% of the time MERRILL84 P J Besl et al. used features of the intensity surface of the solder joint to carry out their inspection BESL85

Although a 100% reliable solder joint inspection technique does not yet exist, there are two other methods whose performance borders on that When a solid is subjected to a point source of heat, and then removed from it the resulting heat distribution is very much dependent upon its thermal coefficient density and porosity Thus the thermal distribution of a blow-hole solder joint (a hole through the body of the solder, which is a solder defect), is different from a good solder joint It is this information that will allow for the verification of a solder joint Thermal imaging devices have been on the market for a number of years now, but are only now seeing use in computer vision HUGHES85

The other method that provides a satisfactory solution to the problem is acoustic microscopy This method uses a very high frequency, sub-micron wavelength *sound* wave to penetrate into the body of the material to explore it, without subjecting it to damage or destruction MEULLER82 Very high resolution acoustic waves can be used to provide planar reconstruction of the nature of the material inside the specimen MEULLER82 Thus, if a bubble occurs within the body of the solder it can be detected by such a method It would show up because it is of a different acoustic density than the surrounding material At the time of writing, acoustic microscopy is still very much being researched, and probably will not be available commercially for a few years The above methods however, can be argued, probably successfully, as *not* being vision

2.3 Bare Board Inspection

Basic in each hybrid IC is the substrate itself, with all the conductors, and in some cases resistors fired in place When fully assembled, a board can have gained considerably in value. and can represent a substantial loss if it has to be discarded Problems can and do appear on the boards in the form of bridged or open conductors THIBADEAU85 In state-of-the-art manufacturing now. the complexity and fine definition of the conductors has made it too strenuous to be visually inspected by humans for any length of time A growing number of these boards are now inspected by commercially available computer vision systems THIBADEAU85. JARVIS80 Computer vision inspection systems fall into two categories referencing and non-referencing STERLING79 These systems use binary image processing algorithms FU82 In referencing systems the image of the board obtained under inspection is compared with the image of what is considered a "good" board BOLHOUSE85 Any significant deviation from the reference would then be considered to be an unacceptable aberration. and the board in question is rejected The main disadvantage with the referencing scheme and it is a serious one is the generation of the reference The reference has to be as perfect as possible because all subsequent references are made to it LEONARD85 The inspection of the reference is done by a human operator. and a reference has to be produced for each different board to be inspected Production of the reference can be a very painstaking and laborious task

On the other hand. the non-referencing method. is somewhat like an "expert system" in that it has a set of stored rules of. for example. how a good conductor should look like. what sort of blemishes are acceptable. and what joined conductors should look like FU82 Different scaling options can be selected to accommodate different magnifications and conductor widths The non-referencing method is extremely versatile because virtually any board can be inspected without first generating the reference. but it tends to be slow especially when it has a large number of rules to apply A compromise between these two methods would represent the best of both worlds THIBADEAU85 Such a system would incorporate an expert system to first generate the reference. Subsequent boards would then be compared to this reference, which is a much more rapid operation than the purely rule-based one

Once a board has been determined to be defective, an assessment has to be made to decide if the board can be repaired If there is bridging of the traces, for example, a decision has to be made as to whether the board can be saved. There is nothing that can be done about open conductors or cracked boards because they are fired, but excess, bridged conductors can often be worked upon Such aberrations can be removed by grinding with a high-speed tool Grinding is a contour-following operation, and, as such, requires the provision of force-sensing Force and torque sensing in our environment is provided by a force sensor manufactured by Regeltechnik This also requires accurate knowledge of the dimensions of the tools used because the point of contact with the workpiece is offset from the point of sensing Thus the torque measured at the sensor has to be transformed to the point of contact to correctly determine the actual forces involved

2.4 Automated Visual Component Inspection

The generally cluttered surface of the hybrid IC precludes the use of just binary vision to inspect the surface mounted components Straight binary vision, on the other hand, can be used to determine the orientation of the board placed when it is placed against a lighted background GONZALEZ82 With the orientation of the board known, a database can be consulted so as to limit the search to a small portion of the image This synthetic limitation of the search area is critical to increase the chances for a successful search Once the search area is determined, a number of inspection tasks can be carried out Search is first performed to verify that there is indeed some component there Upon successful verification of that fact, and that the component which is there is of similar dimensions to the component that is supposed to be there, the orientation of the component can be determined For surface mounted capacitors, for the most part, they are non-polarized and can be mounted either way The capacitor has only to be inspected to determine if the solder joints holding it in place are well formed If however, there is no component where there should be one, a component will be placed accordingly

Inspection of a chip on the other hand, is considerably more difficult For example, the chip can be longitudinally *symmetrical*, and the only polarization mark is a notch at one end of the chip Finding the notch consistently may prove to be difficult because some manufacturers do not have the notch all the way through the thickness the chip, while others use a dot instead[1] The most consistent - still not perfect though - indications of orientation are the markings on the chip Optical Character Recognition (OCR) can be used to read the markings, to determine the orientation of the chip, and also to verify that the chip is indeed what it should be BERGER85 As for now component manufacturers ship out their devices and components in tape form or in tubes so that they can all be handled correctly, without ambiguity

The area surrounding the capacitor or chip is often cluttered with conductor traces, resistors, and other components The algorithm has to locate the chip or capacitor reliably despite these The success of the search has already been increased by limiting the search to an area where it is most likely to be found Under these conditions, the Sobel operator LEVINE85, JARVIS82 provides the necessary first level of processing The dimension of the Sobel operator, whether it is a 3 X 3 or a 5 X 5 GONZALEZ82 is dependent upon tradeoff between the amount of filtering necessary and the computation time that can be afforded It is assumed here that a database containing containing the physical dimensions of the components and their relative locations has already been set up and can be accessed by the inspection program as needs be Together with the magnification with which the scene is viewed, the associated scaling factors can be computed From the data derived by the Sobel operator, straight line segments are fitted to as many points thought to be forming a line From these line segments, a transformation is made to the Hough domain LEVINE85 The Hough domain plots the frequency of the line segments with a particular orientation A high frequency at a particular orientation is indicative of an edge For a rectangular object, there are two distinct peaks at 90° apart for the only two possible orientation of the edges Note that the Hough transform does not distinguish between parallel lines

With the orientation of the rectangle now known, a number of well-known techniques in image processing such as line-finding, connectivity, neighbourhood-operations PAVLIDIS82 can be used to detect the exact location of the rectangular object sought. The above operations, in part, achieve their goal by minimizing the effects of spurious data introduced into the image For any spurious points still remaining in the image, an exhaustive process will have to be employed to eliminate them It can be seen from the above description that analysis of other than binary images requires tremendous computational power Given the size of the average image to be analyzed to be 242 X 256, there are nearly 64 000 pixels involved so that every operation that has to be performed on one pixel has to be repeated 64,000 times

Recent experiments have shown that there remains some longitudinal uncertainty when determining the position of the capacitor because of the specular reflections caused by the solder joints at the ends This amount of uncertainty can be accommodated by the tweezer tool. Alternatively, a vacuum pickup tool with a sufficiently large end face would suffice

2.5 World Modeling

Inspecting and performing the repair task in a structured and efficient manner requires the design and implementation of a comprehensive and flexible database This database contains information describing the components of the hybrid IC, their locations relative to calibration points and relative to the edges of the board, the locations of the solder joints, profiles of good solder joints, and acceptable tolerances. It also serves to contain the locations of all task peripherals that are accessible by the two robots. The locations are described relative to calibration points to facilitate updating the database should any peripheral be moved around. This database is referenced by the inspection programs, by the repair programs, and by the trajectory and path generation programs of the robots

The term *path generation* refers to the generation of a path through a set of *static* obstacles, obstacles that remain stationary throughout the time needed to negotiate the obstacles GILBERT85 Trajectory generation on the other hand, requires the generation of a collision-free path between moving obstacles It includes both *path and velocity* generation. In moving the robot from one position to another, a trajectory has to be formulated such that its path will avoid any obstacles, moving or stationary, between those positions To this end, in trajectory generation, the database will be consulted for the locations and trajectories (if known) of the obstacles If the trajectories of the obstacles are not known, the database will be consulted repeatedly to ensure that the obstacles are not in the way while movement of the robot arm is in progress (note that the database is constantly updated) The complexity of the collision avoidance trajectory formulation is both a function of the number of obstacles to be avoided and the proximity with which the obstacles can be approached GILBERT85 The closer the allowed approach, the more computations will have to be performed

The need to move both robots simultaneously requires a comprehensive collision avoidance strategy One collision avoidance strategy for two moving robots presents one robot as a moving obstacle to the other MICHAUD85 Thus, not only path generation is needed, but also trajectory generation so that the moving robots will not collide into each other BROOKS83.

The inspection and repair task requirement here is best met using a hierarchical structure of command directives To describe every movement in their primitives is a very tedious task, and utterly inefficient Faulty components, and solder joints are first located, and a decision made as to whether they can be repaired or not Those that cannot will be rejected, but those that can, will have to be evaluated to determine how it can best be performed. At the top level, the repair task of each faulty component is described by "verbs" LEVINE82, SANDERSON83 These verbs are then parsed into movement primitives, and with the appropriate parameters, transmitted to the robot controllers There is need for a supervisory program too, that ensures that the movement primitives so generated accurately reflect the verb at the top level, and that the movements are of a reasonable nature If this is not so, the supervisory program can stop the execution, initiate the error recovery, and inform the user as to the extent and source of the error

2.6 Multi-Robot Operation

The environment in which the inspection and repair is carried out is unique in that it involves not one, but *two* robots Conventional ideas applicable to one robot environment will have to be modified, or revamped entirely for the operation of two or more robots It requires provision for multi-branch control, and efficient communication not only between the host and the robots, but also between the robots Valetz described the use of a production system in multi-robot control VALETZ82 The particular environment here will use some form of a production system because of its inherent capability to perform symbolic processing. Symbolic processing as opposed to numerical computation, refers to manipulation of symbols, character strings in this case Elements, or variables in a program are treated as symbols rather than numbers Using symbolic processing the task at hand can be very compactly described by a set of rules, which again are a set of character strings Incidentally, there are some empirical examples which show that human reasoning is a form of symbolic processing WINSTON82

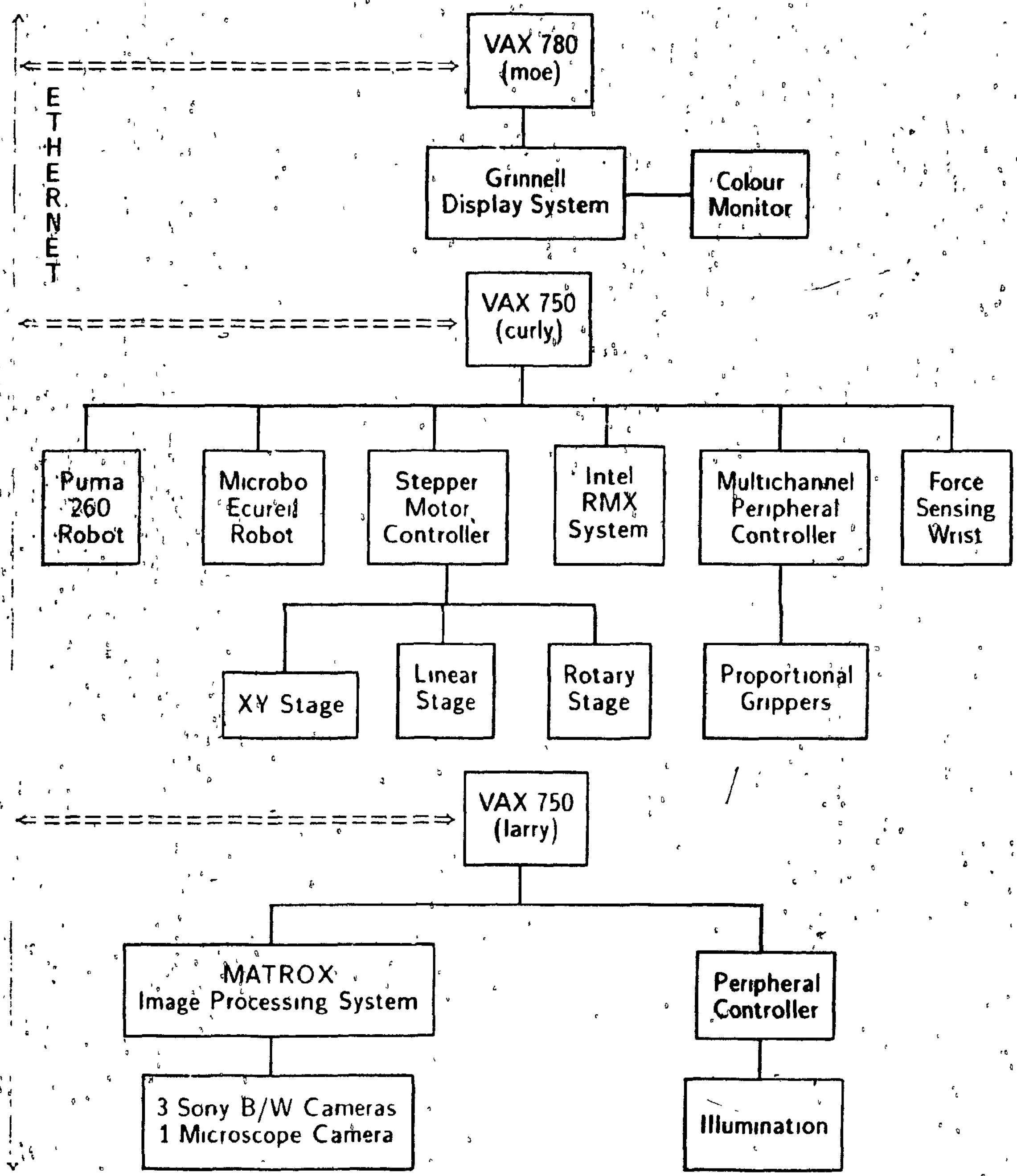

Figure 5 The CVaRL research environment

The requirement that the two robots do not collide into each other is only a small facet of multi-robot operation At some point, the many robots arms will have to be working at a single task in collaboration with each other Humans perform such operations routinely, like clapping, or washing of hands, with complete ease Such a dextrous use of hands requires an understanding as to how such dexterity is achieved, and how a machine can be instructed to perform with the same dexterity

2.7 Network Environment

In the environment in which the inspection and repair task is to be performed, we have three Digital Equipment Corporation VAX s one VAX-11/780 and two VAX-11/750's networked in the manner depicted shown in figure 5 GAUTHIER85, FREEDMAN85 The interconnect system is ETHERNET The VAX-11/780 runs VMS, the operating system supplied by the manufacturer while the VAX-11/750's run BSD UNIX version 4 2, supplied by the University of California at Berkely Under VMS a UNIX emulator called EUNICE can be run The current assignment of roles for the computers may be varied, but, at the moment the VAX-11/780 will handle the overall supervision of the inspection and repair task It will be the so-called "repair consultant" LEVINE82 It will contain a database describing the world - a world model - which will be consulted by the repair consultant itself, and also by the two VAX-11/750's In the sub-division of tasks one of the VAX-11/750's is assigned the task of the robot vision It will have the function of gathering visual information via CCD (Charged-Coupled Device) cameras and will interpret this information The CCD cameras are connected to two MATROX RGB GRAPH and one VAF512 boards which contain a frame grabber and video memory These are located in an INTEL system 310 unit provided with an 80286 CPU and running the INTEL RMX operating system An interesting feature of the Matrox boards is that while resolutions of up to 512 X 512 pixels can be handled, it can be programmed to sample only 128 X 128 pixels Thus, when only low resolution inspection is needed, the sampling rates can be adjusted so that the throughput rates are acceptable for real-time responses One of the four video inputs is selectable by software Various cameras are available for example, the tiny Sony XC-37, which weighs just 250 grams, or a Fairchild CCD-3000 camera weighing over 600 grams The Fairchild camera is connected to a viewing port of a Wild Leitz 6-50X microscope from which fine inspection of the hybrid IC can be carried out The microscope is fitted with a motorized zoom and a vertical motorized stage for focusing Both can be controlled by software The algorithms for auto-focusing are many, but the focusing could be carried out by analog means to increase focusing speed Currently, the algorithm used is the squared-gradient operator LIGTHART82 It looks for the maximum in the squared-gradient operation, and the location at which that occurred is the point of optimal focus

The other VAX-11/750 is assigned the task of performing trajectory calculations for the two robots Implicit in its task too, is the problem of collision-avoidance By consulting the database, and with the knowledge of the positions of the two robot arms, a trajectory will be calculated to avoid all obstacles, and also *each other* The part of the database containing the positions of the robots will be constantly updated whenever a motion is performed to ensure that the information in the database is current. Movement of various motorized stages is treated in the same way

2.8 Robot Control 'C' Library

The Unimation PUMA 260 is supplied with a proprietary language called VAL, for Versatile Assembly Language The controller is configured in a master-slave configuration, in which an LSI-11 is the master and six Signetics 6502's for the slave processors, one for each joint

Currently, control of the PUMA 260 from the VAX-11/780 is achieved by using a command interpreter to form the VAL string and then port it over to the PUMA controller via an RS-232 line at 9600 baud In effect the PUMA appears to the VAX-11/780 as a terminal and vice versa This procedure is sufficient for simple motions, but for more complicated motions, more sophisticated control of the robot arm is necessary Resort is being made to another language to provide enhanced capabilities needed for sensor-based robotic control

A robot language called RCCL (for Robot Control 'C' Library) developed at Purdue University for the PUMA 560 running on a VAX-11/780 HAYWARD83, HAYWARD84, is currently undergoing tests and modification to run a PUMA 260 using a VAX-11/750 RCCL offers the basic functions afforded by VAL, but with a some very important additions Because it communicates directly with the LSI-11 instead of first being processed by the VAL kernel, it allows for very sophisticated control of the PUMA arm The user is not hampered by the limitations of VAL If the robot geometry and specifications can support a particular motion, RCCL can carry out the motion Intrinsic in RCCL is a facility to measure the currents controlling the joints HAYWARD83 The current of a particular joint motor is related to the torque exerted Monitoring this current provides a measure of the *torque*, and hence the force, exerted

The complexity of the trajectory calculations, in particular that of the inverse kinematics for motion, may prevent the VAX-11/750 from providing adequate control for the two robots Besides computing the trajectory the motion has to be sufficiently sampled to ensure that it is adequately smooth for interpolated or extrapolated motion Experimentation is currently underway to move the trajectory computations for the MICROBO from the VAX-11/750 to a MULTIBUS based INTEL 80286 processor with an INTEL 80287 math co-processor Currently it is linked by a RS-232 line but future plans are to link it using a parallel port and eventually with the Ethernet In distributed processing of information, the segmentation of task is of particular importance to reduce the need for inter-processor communications Inefficient segmentation will result in needless communication that will significantly reduce the computational power available

The proprietary language of the MICROBO robot is called IRL, for Intuitive Robot Language Users of both IRL and VAL have pointed to numerous deficiencies in IRL. This is not to say that VAL is perfect but it is closer to being task-oriented than IRL is. To alleviate these inadequacies, IRL, as with VAL, is being replaced by a version RCCL that is compatible with it Major changes are involved because of the different geometries of the robots, and also because the MICROBO uses the INTEL 8085 for all its processors, including the master With the different geometries too, come different control algorithms

2.9 Repair Tools

The particular nature of the repairs, and the manner in which they are to be effected precludes the use of conventional tools The PUMA 260 and the MICROBO are being fitted with special end-effectors to enable them to carry out the repair task McCONNEY86 The standard gripper supplied with the PUMA 260 has been modified to realize a set of pneumatically operated jaws with a special built-in coupling for supplying a feed of compressed air to the various pneumatic tools that will be picked up by the robot An electrically operated proportional gripper is also under development

In the event that a soldered component has to be re-oriented, or be removed entirely, conventional desoldering techniques are not applicable to hybrid IC's Conventional desoldering techniques work well only with through holes, or traditional types of components For hybrid IC's, because of their miniaturization and surface mounted nature, heat has to be applied evenly to all the solder joints, and the component lifted off when the solder has liquefied

While it is possible to design a specially shaped soldering iron, the problem of assuring good thermal contact remains. One solution is to use a stream of superheated gas. The flow nature of a gas will ensure even heating of the joints. At the same time the joints are being heated, a vacuum pickup tool is placed over the component to be removed. After a sufficiently long interval - to be determined experimentally - the vacuum is activated, and a lift operation attempted. A micro-switch built into the tip of the vacuum tool, indicates if the pickup operation was successful. The advantage of this method of removal is that compliance is automatically achieved. If the component is still soldered to the board, the vacuum pickup will fail. If the same operation were to be carried out by a gripper, it may end up ripping the component out of the board. It is much harder to implement compliance with the gripper than with the vacuum tool.

Once the misaligned (or wrong) component has been removed, a vacuum-assisted desoldering tool will be passed over all the solder pads to remove the excess solder. The source of heat for this operation could come from the super-heated stream of gas, or from the desoldering tool itself. The desoldering tool in this case is a soldering iron with a bore in the soldering tip that is connected to a vacuum. Solder paste with built-in flux will then be applied to the solder pads with a syringe that will be maneuvered by one of the robots. The correct component is placed with its pins aligned with the solder pads. Following this, the solder pads are again re-heated to melt the solder and bond the component in place.

2.10 The Calibration Task

To perform the inspection and repair task adequately, it becomes necessary to operate the robot arm with known precision and repeatability STAUFFER85. When a tool is picked up, its end point has to be known and also compensated for in the event of tool wear, from perturbations in the robot geometry that come from misuse, or from the need to move some of the robot workstation peripherals

Tactile calibration is one technique to achieve the discovery of the end point It has the attraction of being economical and can be engineered to be sufficiently rugged to withstand the harsh conditions of an industrial environment Tactile calibration can be extended to tactile sensing, in which the robot arm can be made to handle an object with a certain force The need for force sensing in certain circumstances is indispensable Contour-following operations are examples In tactile sensing, calibration too has to be performed to correlate the currents sent to the joint motors and the tactile transducer signals

The use of vision in the calibration task is very attractive for it affords a flexibility and adaptability unmatched by other methods of sensing There are numerous occasions in which it is not possible, or desirable to perform tactile calibration The object that is being carried, for example, could be fragile and susceptible to surface contamination In such circumstances, the use of vision in calibration is unsurpassed for its simplicity and unobtrusive nature STAUFFER85 Before vision can be used as an aid in any task, it has first to be calibrated to obtain correct dimension and depth perception The need to use different optics on occasions (different lenses) and changes in the viewing positions (different camera positions) also require recalibration for correct perception, and hand-eye coordination TREPAGNIER85

With the successful application and evolution of the above-described techniques, a comprehensive hybrid IC inspection and repair program could develop and render needless much of the inspection carried out today by humans The philosophy common to the developed programs is that the programs will not be applied rigidly Rather, they will be adaptive, adapting to small perturbations in its setup and environment, and perhaps even learning to perform the task better each time Such a development would have significant contribution for inspection and repair programs because it involves subordinating a higher intelligence to production machines than ever before.

In this chapter we have outlined the general direction of the Computer Vision and Robotics Laboratory, and explained the current application involving the hybrid circuit board inspection and repair. The calibration requirements for these robot tasks were also outlined.

3. Robot Arm Kinematics and Dynamics

This chapter presents the robot arm kinematics formulations and equations required in the calculations associated with the calibration study

3.1 Robot Geometries

Current industrial robots are general-purpose manipulators that consist of a number of rigid bodies, called links, connected together in a series fashion by revolute and/or prismatic joints They are generally six-jointed, therefore affording six degrees of freedom, with three of degrees of freedom controlling the arm sub-assembly, and the other three forming the wrist sub assembly All of the general purpose manipulators now available fall into 4 categories depending on how motion is performed.

- Cartesian (three linear axes).
- Cylindrical (two linear, one rotary),
- Spherical or polar (one linear, two rotary), and
- Revolute or articulated (three rotary)

Figure 6 shows the different categories The Unimation PUMA 260 is a six-degree-of-freedom revolute robot arm, while the ECUREUIL Microbo is a six-degree-of-freedom cylindrical robot arm

Much of the mathematics now used to compactly describe the kinematics of articulated serial-linkage robots were formalized as far back as 1955 by Denavit and Hartenberg in a landmark paper titled "A Kinematic Notation for Lower-Pair Mechanisms Based on Matrices" DENAVIT55 It has been brought to the current level of refinement by R P Paul in two

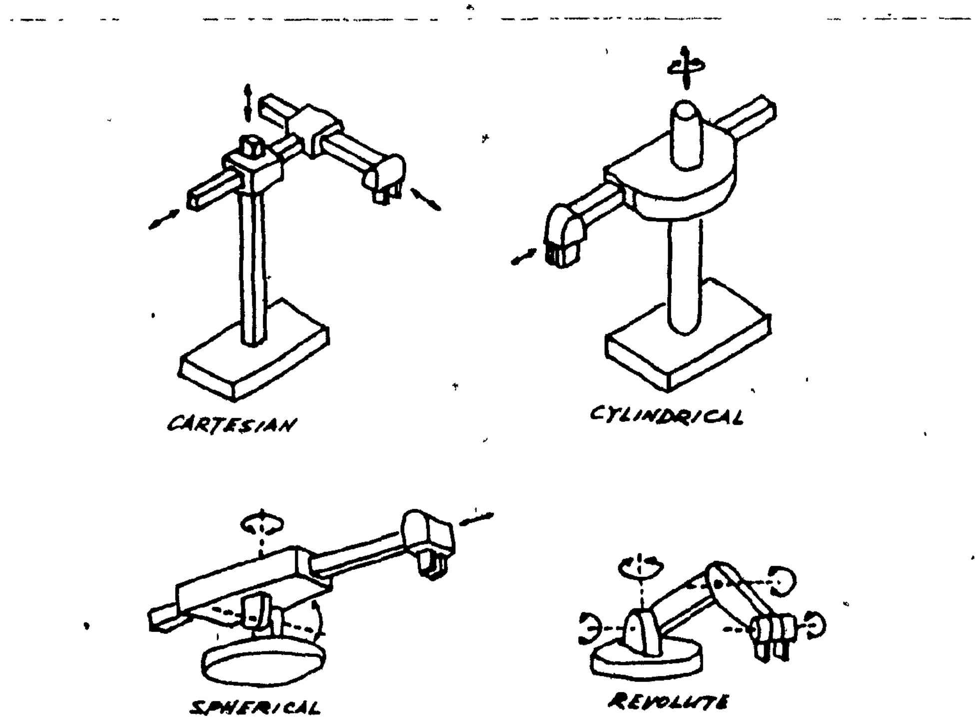

Figure 6 Different robot geometries

papers PAUL78, PAUL81 and a book PAUL81 In the first paper, Paul gives a comprehensive introduction, while the book presents a very thorough treatment of the formulations

3.2 Setting up the Denavit-Hartenberg coordinate system

Denavit and Hartenberg proposed a convention to uniquely and consistently describe each link of a serially-linked arm, and their associated coordinate frames The rules for setting up the coordinate systems are as follows

1 An n-link manipulator will require n coordinate systems, one for each link
2. The motion of a given joint i will produce a motion of link i with respect to link i - 1 (or the base if $i = 0$) The i-th coordinate system is fixed in link i and hence moves with it
3 The z_{i-1} axis lies along the axis of motion of the i-th joint
4 The x_{i-1} axis is normal to the z_{i-1} axis Its direction is away from the (i - 1)th origin

5 y_i is chosen to form a right-handed coordinate system with respect to z_i and x_i

With the link-manipulator coordinate system now set up, the following parameters are used describe each link, and relate one coordinate system to another

θ_i = the joint angle from the x_{i-1} axis to the x_i axis about the z_{i-1} axis

d_i = the distance from the origin of the $(i - 1)$th coordinate frame to the intersection of the z_{i-1} axis with the x_i axis along the z_{i-1} axis

a_i = the offset from the intersection of the z_{i-1} axis with the x_i axis to the origin of the i-th frame along the x_i axis (or the shortest distance between the z_{i-1} and z_i axes)

α_i = the offset angle from the z_{i-1} to the z_i axis about the x_i axis (using the right-hand rule)

With the above parameters and coordinate system, the equations relating one coordinate system to the one before it, the $(i - 1)$th, or the one after it, the $(i + 1)$th, or one belonging to any one of the links, can be derived PAUL81

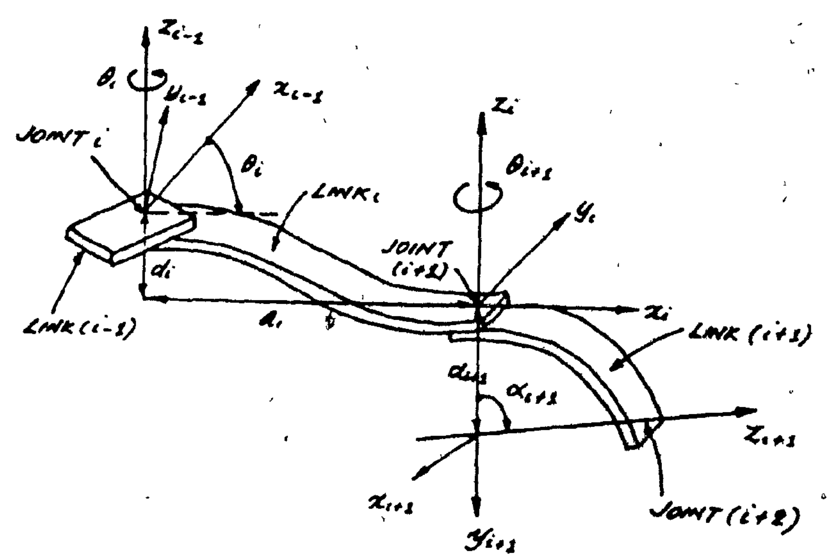

Figure 7 The Denavit-Hartenberg coordinate system

Describing the links in the above way, the Denavit-Hartenberg system then assigns an orthogonal coordinate frame to each link. Figure 7 shows how the coordinate system is set up and the relevant parameters. The coordinate frame of one link is related to the frame of the previous link by a homogeneous 4 X 4 transform, except for the first link which is described relative to the base coordinates.

Using the above terms, a point $\mathbf{P}_i$ in the i-th coordinate system, can be simply described in terms of a point $\mathbf{P}_{i-1}$ in the $(i-1)$th system using a general transformation $\mathbf{A}_i^{i-1}$. The relation is given by

$$\mathbf{P}_i = [\mathbf{A}_i^{i-1}]^{-1}\mathbf{P}_{i-1} \tag{3.1}$$

where

$$\mathbf{A}_i^{i-1} = \begin{pmatrix} \cos\theta_i & -\cos\alpha_i \sin\theta_i & \sin\alpha_i \sin\theta_i & \cos\theta_i \\ \sin\theta_i & \cos\alpha_i \cos\theta_i & -\sin\alpha_i \cos\theta_i & \sin\theta_i \\ 0 & \sin\alpha_i & \cos\alpha_i & d_i \\ 0 & 0 & 0 & 1 \end{pmatrix} \tag{3.2}$$

Thus for a six degree-of-freedom robot, the transformation matrix, ${}^0T_6$, describing the position and orientation of the end-effector is given by

$${}^0T_6 = A_1^0(\theta_1)A_2^1(\theta_2)\ldots A_6^5(\theta_6) \tag{3.3}$$

or

$${}^0T_6 = \begin{pmatrix} n_x & o_x & a_x & p_x \\ n_y & o_y & a_y & p_y \\ n_z & o_z & a_z & p_z \\ 0 & 0 & 0 & 1 \end{pmatrix} \tag{3.4}$$

where

n is the normal vector parallel to the hand. For a parallel-jaw hand, this is orthogonal to the jaws (see figure 8).

o is the sliding vector of the jaws, and is in the direction of the jaw motion

a is the approach vector of the hand, and is normal to the tool mounting plate of the arm It is akin to the normal direction of the palm of the hand.

p is the position vector of the hand relative to the origin of the base coordinate system.

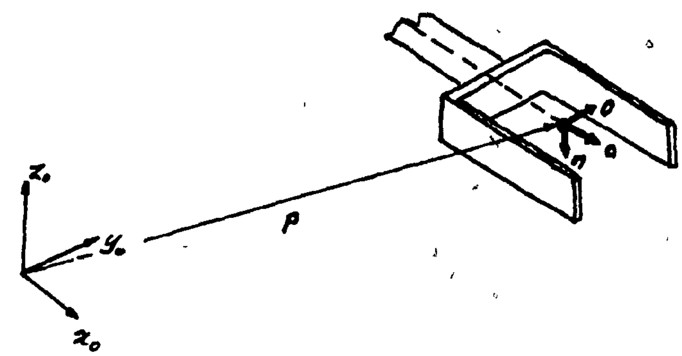

Figure 8 **n, o, a, p** vectors of a robot arm

Note that the homogeneous matrix of equation 3.2 can be decomposed into the *basic homogeneous translation matrix* and three *basic homogeneous rotational matrices* LEE82 The translational matrix is given by

$$T_{tran} = \begin{pmatrix} 1 & 0 & 0 & dx \\ 0 & 1 & 0 & dy \\ 0 & 0 & 1 & dz \\ 0 & 0 & 0 & 0 \end{pmatrix} \tag{3.5}$$

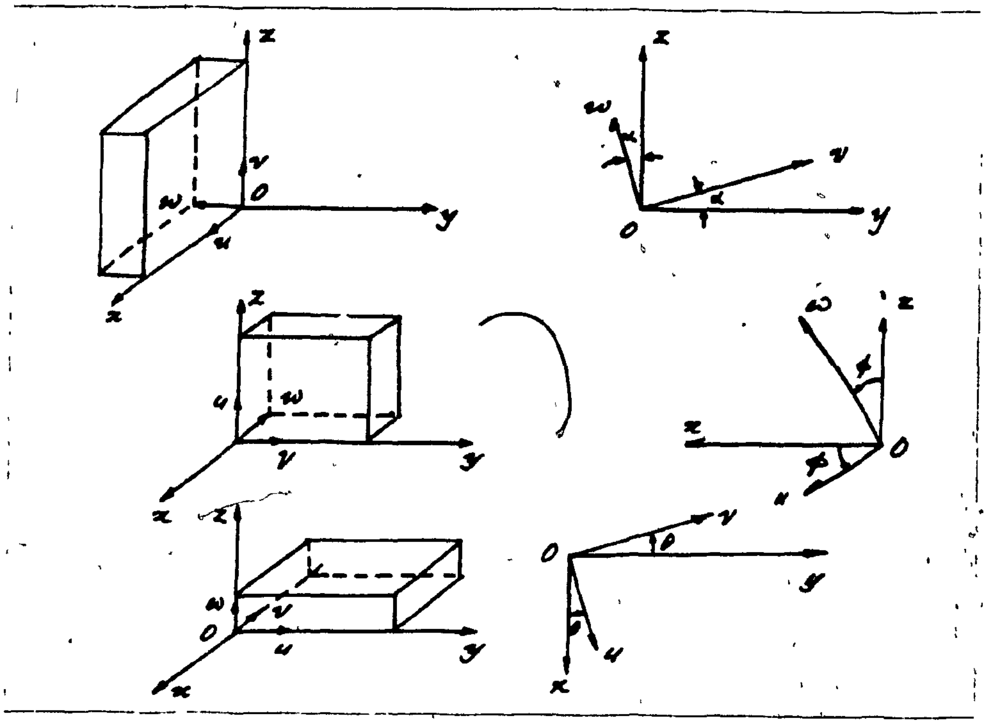

Figure 9 Orientation of a 3-D object in 3-D space

and the three basic rotational matrices are given by

$$T_{x,\alpha} = \begin{pmatrix} 1 & 0 & 0 & 0 \\ 0 & \cos\alpha & -\sin\alpha & 0 \\ 0 & \sin\alpha & \cos\alpha & 0 \\ 0 & 0 & 0 & 1 \end{pmatrix} \tag{3.6}$$

$$T_{y,\phi} = \begin{pmatrix} \cos\phi & \sin\phi & 0 & 0 \\ 0 & 1 & 0 & 0 \\ -\sin\phi & 0 & \cos\phi & 0 \\ 0 & 0 & 0 & 1 \end{pmatrix} \tag{3.7}$$

$$T_{z,\theta} = \begin{pmatrix} \cos\theta & -\sin\theta & 0 & 0 \\ \sin\theta & \cos\theta & 0 & 0 \\ 0 & 0 & 1 & 0 \\ 0 & 0 & 0 & 1 \end{pmatrix} \tag{3.8}$$

where α, ϕ and θ represents rotations about the x, y and z axes respectively (see figure 9)

and the translation

$$d = \sqrt{dx^2 + dy^2 + dz^2} \tag{3.9}$$

Robot arm *kinematics* "deals with the geometry of robot arm motion with respect to a fixed reference coordinate frame without regard to the forces/moments that cause the motion" LEE82 It deals with how the joint variables affect the position and orientation of the arm in space There are two sub-problems in the kinematics problem that in the forward direction, the direct problem, and the other in the reverse, the inverse problem The direct problem involves finding the position and orientation of the end of the arm given the joint angle vector $\theta = (\theta_1, \theta_2, \theta_3, \theta_4, \theta_5, \theta_6)$ of the robot arm Conversely given a particular position and orientation of the end of the arm, the inverse kinematics problem would be to determine the joint angles needed to attain it Robot arm *dynamics* on the other hand, deals with the mathematical formulations of the path, velocity and acceleration equations of the arm motion

3.3 Link Coordinate Assignment

Given an n-degree-of-freedom robot arm this algorithm assigns an orthonormal coordinate system to each link of the robot arm The relations among adjacent links can be represented by a 4 X 4 homogeneous *transformation matrix* of the form shown in equation 3 2 This labeling of the coordinate systems begins from the supporting base to the end-effector of the arm Note that the assignment of a coordinate system is not unique

The link coordinate assignment used in deriving the results of this study will now be presented G C S Lee LEE82 gives the following procedure for formulating the coordinate system -

D1 { *Establish the base coordinate system* } Establish a right-hand orthonormal coordinate system (x_0, y_0, z_0) at the supporting base with the z_0 axis lying along the axis of motion of joint 1

D2 { *Initialize and loop* } For each i, $i = 1, \ldots, n$, perform the steps **D3** to **D6**

D3 { *Establish joint axis* } Align the z_i with the axis of motion (rotary or sliding) of joint $i+1$

D4 { *Establish the origin of the i-th coordinate system* } Locate the origin of the i-th coordinate system at the intersection of the z_i and z_{i-1} axes or at the common intersection of common normals between the z_i and z_{i-1} axis

D5 { *Establish x_i axis* } Establish $x_i = (z_{i-1} \times z_i)/\|z_{i-1} \times z_i\|$ or along the common normal between the z_{i-1} and the z_i axes when they are parallel.

D6 { *Establish y_i axis* } Establish $y_i = (z_i \times x_i)/\|z_i \times x_i\|$ to complete the right hand coordinate system (Extend the z_i and the x_i axes if necessary for steps *D8 to D11*)

D7 { *Find the joint and link parameters* } For each i, $i = 1, \ldots, n$, perform the steps *D8 to D11*

D8 { *Find d_i* } d_i is the distance from the origin of the $(i-1)$th coordinate system to the intersection of the z_{i-1} axis and the x_i axis to the origin of the i-th coordinate system along the x_i axis

D9 { *Find a_i* } a_i is the distance from the intersection of the z_{i-1} axis and the x_i axis to the origin of the i-th coordinate system along the x_i axis.

D10 { *Find θ_i* } θ_i is the angle of rotation from the x_{i-1} axis to the x_i axis about the z_{i-1} axis It is the joint variable if joint i is rotary.

D11 { *Find α_i* } α_i is the angle of rotation from the z_{i-1} axis to the z_i axis about the x_i axis.

This assignment establishes the coordinate system shown in figure 10 and is used both for the forward and inverse kinematics calculations

3.4 A-matrices for the PUMA 260

With the above formulation for the assignment of the coordinate frames for the various

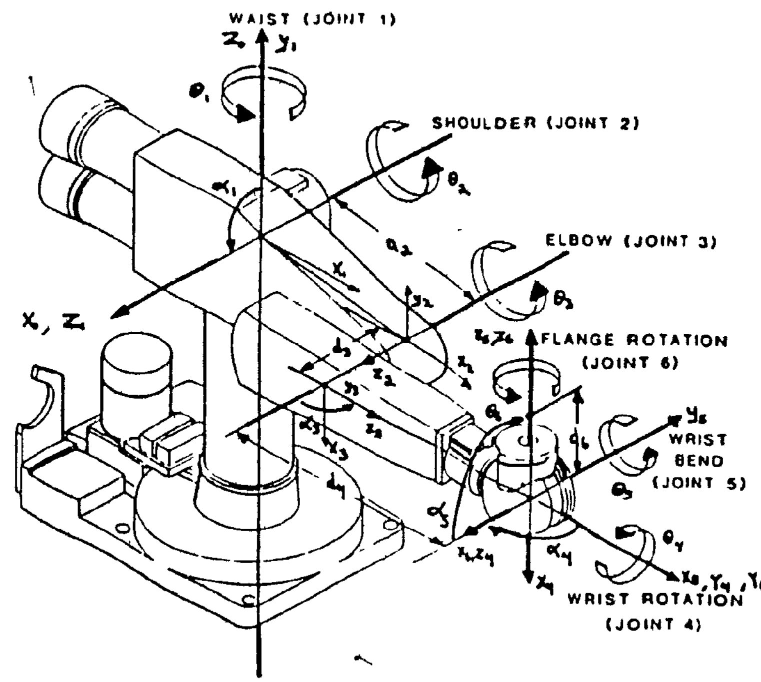

Figure 10 Orientation of the PUMA 260 robot arm

links of the PUMA 260, we arrive at the following **A**-matrices.

$$A_1^0 = \begin{pmatrix} C_1 & 0 & S_1 & 0 \\ S_1 & 0 & -C_1 & 0 \\ 0 & 1 & 0 & 0 \\ 0 & 0 & 0 & 1 \end{pmatrix}$$

$$A_2^1 = \begin{pmatrix} C_2 & -S_2 & 0 & a_2 * C_2 \\ S_2 & C_2 & 0 & a_2 * S_2 \\ 0 & 0 & 1 & 0 \\ 0 & 0 & 0 & 1 \end{pmatrix}$$

$$A_3^2 = \begin{pmatrix} C_3 & 0 & -S_3 & 0 \\ S_3 & 0 & C_3 & 0 \\ 0 & -1 & 0 & d_3 \\ 0 & 0 & 0 & 1 \end{pmatrix}$$

$$A_4^3 = \begin{pmatrix} C_4 & 0 & S_4 & 0 \\ S_4 & 0 & -C_4 & 0 \\ 0 & 1 & 0 & d_4 \\ 0 & 0 & 0 & 1 \end{pmatrix}$$

$$A_5^4 = \begin{pmatrix} C_5 & 0 & -S_5 & 0 \\ S_5 & 0 & C_5 & 0 \\ 0 & -1 & 0 & 0 \\ 0 & 0 & 0 & 1 \end{pmatrix}$$

$$A_6^5 = \begin{pmatrix} C_6 & -S_6 & 0 & 0 \\ S_6 & C_6 & 0 & 0 \\ 0 & 0 & 1 & 0 \\ 0 & 0 & 0 & 1 \end{pmatrix} \tag{3.10}$$

where

$C_i \equiv \cos\theta_i$

$S_i \equiv \sin\theta_i$

Recall that the **A**-matrices (equation 3.10) and equations 3.3 and 3.4 are used to give the forward kinematics solution of equation 3.1 which expresses the position and orientation of the end effector of the robot in terms of its joint angles θ_i. Multiplying the A-matrices in the manner described by equation 3.3, we have the entries of equation 3.4 given by

$$n_x = C_1[C_{23}(C_4C_5C_6 - S_4S_6) - S_{23}S_5C_6] - S_1[S_4C_5C_6 + C_4S_6]$$
$$n_y = S_1[C_{23}(C_4C_5C_6 - S_4S_6) - S_{23}S_5C_6] + C_1[S_4C_5C_6 + C_4S_6]$$
$$n_z = -S_{23}[C_4C_5C_6 - S_4S_6] - C_{23}S_5C_6 \tag{3.11}$$

$$o_x = C_1[-C_{23}(C_4C_5S_6 + S_4C_6) + S_{23}S_5S_6] - S_1[-S_4C_5S_6 + C_4C_6]$$
$$o_y = S_1[-C_{23}(C_4C_5S_6 + S_4C_6) + S_{23}S_5S_6] - C_1[-S_4C_5S_6 + C_4C_6]$$
$$o_z = S_{23}(C_4C_5S_6 + S_4C_6) + C_{23}S_5S_6 \tag{3.12}$$

$$a_x = C_1(C_{23}C_4S_5 + S_{23}C_5) - S_1S_4S_5$$
$$a_y = S_1(C_{23}C_4S_5 + S_{23}C_5) + C_1S_4S_5$$
$$a_z = -S_{23}C_4S_5 + C_{23}C_5 \tag{3.13}$$

$$p_x = C_1(d_6(C_{23}C_4S_5 + S_{23}C_5) + S_{23}d_4 + a_2C_2) - S_1(d_6S_4S_5 + d_2)$$
$$p_y = S_1(d_6(C_{23}C_4S_5 + S_{23}C_5) + S_{23}d_4 + a_2C_2) + C_1(d_6S_4S_5 + d_2)$$
$$p_z = d_6(C_{23}C_5 - S_{23}C_4S_5) + C_{23}d_4 - a_2S_2 \tag{3.14}$$

where

$C_{ij} \equiv \cos(\theta_i + \theta_j)$

$S_{ij} \equiv \sin(\theta_i + \theta_j)$

3.5 Inverse kinematics in the PUMA 260

The problem in inverse kinematics is to find a joint angle vector $\theta = (\theta_1, \theta_2, \theta_3, \theta_4, \theta_5, \theta_6)$ so that the desired position of the arm and orientation wrist assembly as given by **n**, **o**, **a**, **p** is attained

Using Paul's notations PAUL81, the joint angles relate to the geometry and orientation of the robot according to the equations shown below LLOYD84.

$$\theta_1 = \tan^{-1}\left[\frac{\pm p_y\sqrt{p_x^2 + p_y^2 - d_2^2} - d_2 p_x}{\pm p_x\sqrt{p_x^2 + p_y^2 - d_2^2} + d_2 p_y}\right] \tag{3.15}$$

$$-\pi \le \theta_1 \le \pi$$

$$\theta_2 = \tan^{-1}\left[\frac{\{-p_z(a_2 + d_4S_3) + (d_4C_3)(\pm\sqrt{p_x^2 + p_y^2 - d_2^2})\}}{p_2(d_4C_3) - (a_2 + d_4S_3)(\pm\sqrt{p_x^2 + p_y^2 - d_2^2} + d_2p_y}\right] \tag{3.16}$$

$$-\pi \le \theta_2 \le \pi$$

$$\theta_3 \doteq \tan^{-1}\left[\frac{p_x^2 + p_y^2 + p_z^2 - d_4^2 - a_2^2 + d_2^2}{\pm\sqrt{4d_4^2a_2^2 - (p_x^2 + p_y^2 + p_z^2 - d_4^2 - a_2^2 + d_2^2)^2}}\right] \tag{3.17}$$

$$-\pi \leq \theta_3 \leq \pi$$

$$\theta_4 = \tan^{-1}\left[\frac{C_1 a_y - S_1 a_x}{C_1 C_{23} a_x + S_1 C_{23} a_y - S_{23} a_z}\right] \tag{3.18}$$

$$-\pi \leq \theta_4 \leq \pi$$

$$\theta_5 = \tan^{-1}\left[\frac{(C_1 C_{23} C_4 - S_1 S_4) a_x + (S_1 C_{23} C_4 + C_1 S_4) a_y - C_4 S_{23} a_z}{C_1 C_{23} a_x + S_1 S_{23} a_y + C_{23} a_z}\right] \tag{3.19}$$

$$-\pi \leq \theta_5 \leq \pi$$

$$\theta_6 = \tan^{-1}\left[\frac{(-S_1 C_4 - C_1 C_{23} S_4) n_x + (C_1 C_4 + S_1 C_{23} S_4) n_y - (S_4 S_{23}) n_z}{(-S_1 C_4 - C_1 C_{23} S_4) o_x + (C_1 C_4 + S_1 C_{23} S_4) o_y - (S_4 S_{23}) o_z}\right]$$

$$-\pi \leq \theta_6 \leq \pi$$

(3.20)

3.6 Geometric constants of the PUMA 260

Figure 10 shows the PUMA 260 as labelled with the Denavit-Hartenberg convention. As it is a six-jointed robot arm, the highest number reached in the subscripts is 6. The linear dimensions of the PUMA 260 are shown in table 1. The circular measures (in degrees) refer to the hardware rotation limits of the various joints. These dimensions are supplied by Unimation in their engineering drawings of the PUMA 260. To prevent damage to the arm, the software rotation limits are set slightly less than the hardware limits, with the result that the robot cannot be maneuvered under program control beyond the software limits.

Joint i	Rotational Offset α_i	Linear Offset a_i (mm)	Link Length d_i (mm)	Lower Hardware Limit	Upper Hardware Limit
1	90°	0	0	−4°	+304°
2	0°	203.20 ± 0.38	0	−67°	+247°
3	−90°	0	126.24 ± 0.5	−236°	+56°
4	90°	0	203.20 ± 0.64	−223°	+355°
5	−90°	0	0	−122°	+122°
6	0°	0	0	−222°	+312°

Table 1. Dimensions of the PUMA 260

3.7 Trajectory control using VAL

The position and orientation of a 3-dimensional object in 3-D space is determined uniquely by specifying all its six degrees-of-freedom - three for translation (x, y, z) and three for rotation (θ, α, ϕ) (see figure 9) FOLEY83. Therefore, in an attempt to orient a tool that is held by a robot arm, one has to specify all these six parameters and apply a correction to the current orientation. The orientation of the PUMA arm is specified by VAL in two ways (see figures 10 and 11) - The first is that the position of the arm is specified in cartesian coordinates by the linear positional parameters x, y, z, (in millimeters) and the rotational orientation parameters are described by O, A, T (in degrees) O is the *yaw* angle, A the *pitch* angle, and T the *roll* angle (see figure 11) Note here that the *roll, pitch*, and *yaw* angles of figure 11 cannot be used interchangeably with the $\theta_4, \theta_5, \theta_6$ angles of figure 10

The other way in which VAL describes the orientation of the arm is by the *joint angles*, in degrees, of each joint The joint angles are obtained from the shaft encoders which are connected by gears to the axis of motion The Gray codes of the shaft encoders provide a 16-bit number to describe the position of the shaft This is the most accurate way in VAL for specifying the orientation of the arm A particular orientation of the arm described in these parameters is called a *precision point* UNIMATION82 When instructed to attain that particular orientation, the joints are servoed until those joint angles are obtained However, in this raw form, it does not lend itself easily to use Inverse kinematic transformations (see section 3 4) have to be applied to the joint angle readings to obtain the cartesian parameters of the arm The master processor of the PUMA 260 controller is a DIGITAL EQUIPMENT CORPORATION (DEC) LSI-11 (This is the VLSI implementation of DEC's PDP-11.) The LSI-11 is a 16-bit processor and in evaluating the inverse transformation, there is some loss of accuracy Each of the six 6502 slave processors expects an instruction from the LSI-11 master every 26 milliseconds This figure was arrived at by determining how fast the joint angles can be sampled, the inverse kinematic transformations performed on them, and the interpolation/extrapolation calculations between the points to be travelled such that a sufficiently smooth motion can be obtained The result of having the motion insufficiently sampled is a jerky motion of the arm This LSI-11 processor is dedicated to the VAL calculations of the cartesian motions and the inverse kinematic computations must be carried out externally

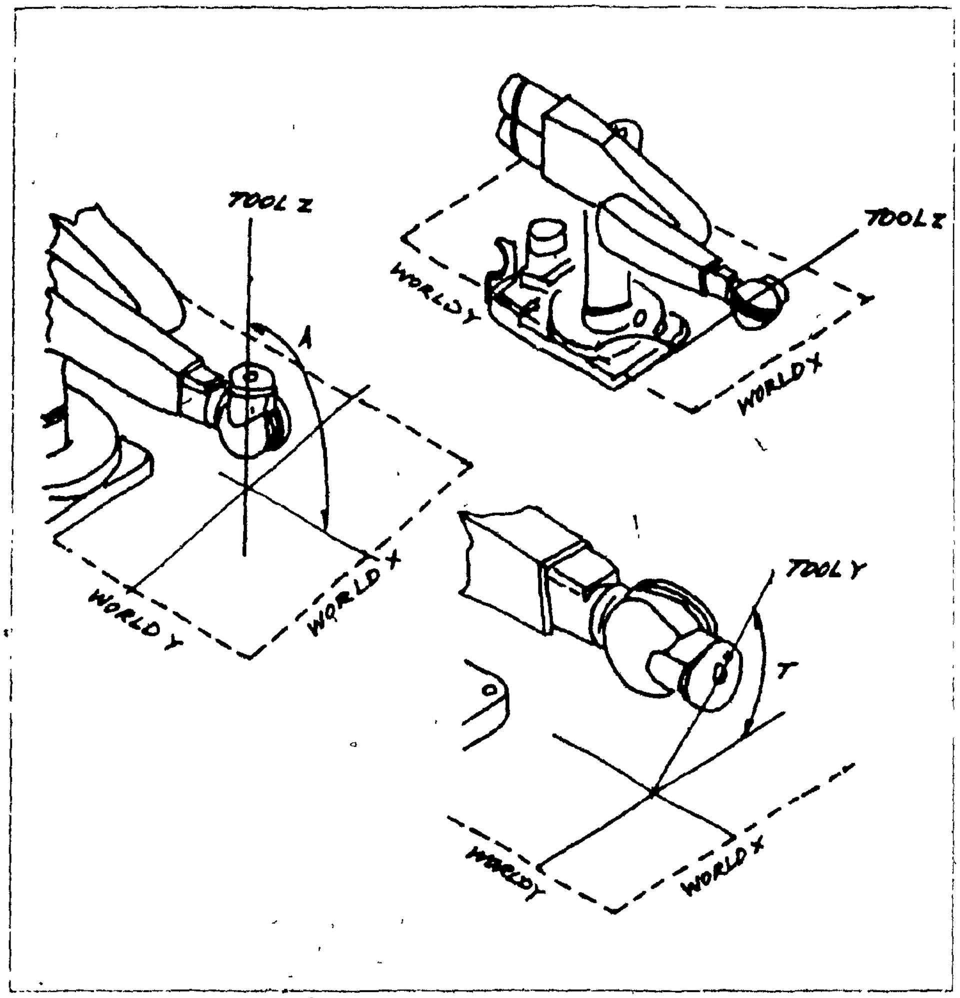

Figure 11 Orientation of the wrist assembly

on the VAX-11/780 computer

In VAL, the orientation of the arm can be found by interrogating the robot controller with the instruction WHERE The instruction will return with the current location of the robot in cartesian world coordinates and joint angle settings Below is an example of the returned string

x/JT1	y/JT2	z/JT3	O/JT4	A/JT5	T/JT6
341 560	-152 910	-78.140	-0.994	1 225	-89.984

JT1	JT2	JT3	JT4	JT5	JT6
-175 139	-160 263	24.505	95 050	93.200	45.980

(3.21)

The first string of numbers are the cartesian world coordinates, while the second are the joint angles. The command to move the robot can take one of two forms. It can be instructed to move to a new point either by actually specifying it, or by instructing it to move a certain distance *from* its current position. Note that the latter instruction does *not* require specification of the end point, only the *differences* between its current position and that of the final position. This instruction is DRAW $\langle dx \rangle, \langle dy \rangle, \langle dz \rangle$. dx, dy, and dz are the distances to be moved in the directions of the x, y and z axes respectively. Aside from the problem of not being able to change the orientation of the wrist assembly, the DRAW command *ignores* any move request specification *less* than 0 010 mm. When used in loops, this truncation error can accumulate to generate a large loss of accuracy.

The alternative to the DRAW instruction is the MOVE instruction. The parameters of the MOVE instruction, as mentioned earlier, can be specified either in world cartesian coordinates, or in terms of joint angles. All six parameters of orientation including those of the wrist assembly can be specified. Although a slightly higher accuracy is afforded, joint angles are not easily related to by a user and he has to perform the inverse kinematic relationship on the destination to calculate the required joint angles. These inverse computations are performed on the VAX-11/780 which is a 32-bit machine because the LSI-11 in its current setting does not lend itself to computation of any equations other than those inherent in the VAL language stored in Read Only Memory (ROM). Thus any additional computations have to be performed on *another* machine since it is not practical to modify the contents of the ROM without the aid of source listings

Representation of a number in an n-bit binary machine generates uncertainty in the last bit thereby causing a loss in accuracy of 1 part in 2^n Subsequent operations such as addition, subtraction, multiplication, or division result in an inaccuracy that varies with the range of numbers involved, and the number of times the operations are executed, ie, the loss in accuracy is cumulative It is not possible to generally state compactly how the loss in accuracy accumulates except that the division and multiplication operations accrue inaccuracy much faster that the operations of addition and subtraction

Robot operations till now have largely been a pick-and-place one, with a human operator guiding and teaching the robot the various task positions with the ubiquitous hand-held teach pendant We are breaking away from this archaic method of instruction, and adopting an "Expert Systems" approach to our task of hyrid IC board inspection and repair in which the task positions and trajectories are calculated by the robot programs themselves and incorporating relevant sensor inputs such as force and vision Such an implementation will make the programs more "intelligent" and able to adapt to varying conditions and types of faults Basic in this need is to provide enhanced computational capabilities for the kinematic and trajectory control of the robot arm In the preceding paragraphs we have described the coordinate system for the PUMA 260 on which the robot kinematics are based, and the calibration results in this thesis derived

4. Accuracy and Repeatability

In order to measure the accuracy and the repeatability of the robot, we use a pointer tool to aid in the measurement process. While the actual tools that will be used in the repair task will be different from the pointer tool, the differences can be easily and accurately reflected in the tool transforms. This chapter presents the experimental results of accuracy and repeatability tests done to evaluate the performance of the tactile and visual calibration techniques studied.

4.1 Tool modeling

The problem in orienting a tool comes when the robot arm has to pick up a different tool to effect a different phase of repair. While the dimensions of the tool can be defined as constant and the orientation for pick-up of the tool forced by the use of a tool rack, any future movement of the tool rack will necessitate a re-teaching effort requiring operator intervention. Since the system incorporates a computer, it is logical to add a self-calibrating step with the attendant advantage that any subsequent tool wear can be measured and *accommodated* each time the workstation is started up.

Prerequisite to the re-orientation and calibrating problem is the modeling of the tool. While each tool may be different, and thus have a different model, extensions to an algorithm for the general case will suffice for accurately describing the tool. In this particular instance, a rectangular model will be used to describe the general case of the tool. The model will thus have a linear length, breadth, and height. The advantage of having a rectangular model is that its axes are orthogonal. The major distinctions between various tools are characterized by these three offsets since the tools generally exhibit axial symmetry by design.

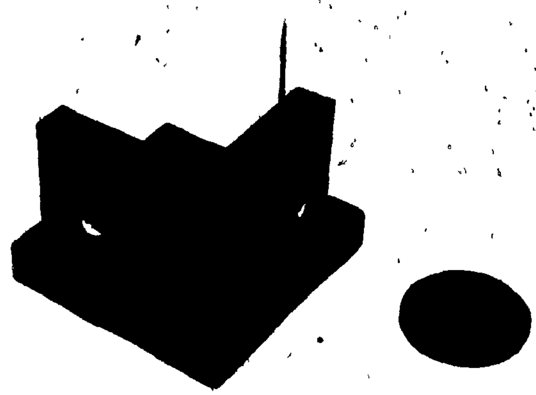

Figure 12 Calibration Contact Block

4.2 Measurement techniques

This rectangular model will be held in the jaws of the hand to simulate the holding of a tool. To enable *simple, automatic* and *consistent* determination of when the model has made contact, an electrical contact system was implemented. The model was precisely machined out of metal, and the contact is a short stub of a flexible metal strip mounted on an insulating block (see figure 12). The use of an elastic metal strip will give consistent indication of contact if the elastic limit is not exceeded. Once the elastic limit is exceeded, the deformation becomes irreversible, and the response becomes no longer linear. For linear deformation, the spring equation is

$$F = -kx \tag{4.1}$$

where F is the force applied on the spring, k the spring constant and x the distance stretched

To ensure that contact between the model and the spring is non-deformative, the arm is made to move at its slowest possible speed, and the CPU made to respond immediately to an input to its I/O (input/output) module. Given that the SIGNALI instruction of VAL is *interrupt* driven, that the clock rate of the LSI-11 is 8.0 MHz, and that it takes about 30 clock cycles to service the interrupt, it would mean that the CPU can acknowledge the signal in about 3.75 microseconds. Since each of the joints receives an instruction from the LSI-11 every 26 milliseconds, this millisecond interval becomes the primary factor in determining exactly when the arm stops moving upon receipt of an interrupt driven command to stop.

By driving the arm sufficiently slowly, (at 0.01 of the VAL monitor speed of 100.0), the arm moves at about 10 millimeters per 10 seconds. This works out to about 1 millimeter per second, and the distance travelled in 26 milliseconds is about 26×10^{-03} millimeters, or 26 micrometers (microns). Thus any spring element that can be extended better than 26 microns without irreversible deformation will suffice for this application. This also implies that the resolution of electrical contact, using this constant velocity scheme *cannot* be better than 26 microns. This is the dead distance before the system can respond. Exploratory techniques based on polling could refine this precision even further. The encoder has a 16-bit resolution, and is coupled to the servo with a step-down gear ratio allowing the robot an ultimate angular resolution of 0.010 of the arc.

4.3 Choice of programming languages

The use of a particular computer language is dictated in large part by the task at hand, the ease with which it can be used, and very importantly, the support afforded by the computing facilities at which the work is carried out. Here at the Computer Vision and Robotics Laboratory, much of the research carried out is very computationally intensive, especially in the numerical evaluation of mathematical expressions As most of DEC's computers are targeted for use in scientific environments and that FORTRAN is the most widely used language in such environments it is no accident that they have a version of FORTRAN *optimized* to run on their machines As such, much of the code for the trajectory computations is written in FORTRAN. It is estimated that any code written with this FORTRAN is only about 3 – 5 times slower than code written in assembler Also, FORTRAN lends itself very well to numerical computations because of the fact the language was designed specifically to perform numerical computations For that reason too, there exists considerable software support in FORTRAN The International Mathematics and Scientific Library (IMSL) routines, for example are written in FORTRAN This represents considerable support software for matrix manipulations and solutions and also for statistical analysis, a number of which were used in this study

While FORTRAN is extremely versatile in numerical computations, it is extremely unwieldy when it comes to character-string manipulation To efficiently handle terminal emulation and character string handling at the VAX-11/780 end, the language **C** was chosen **C** is widely acknowledged as a very versatile, and powerful language The language has some very interesting features especially manipulation at the bit and byte (hence, character level) levels For this reason alone the authors of the widely-used operating system (OS), UNIX, have chosen to use this language to implement most of the OS Except for a very small part of UNIX which is machine-dependent, all of the code is portable This means that when it is transported to another machine all that is needed is to re-compile the code that is written in **C** with a **C** compiler for the new machine, and re-write the small amount of machine-dependent code The program that handles the serial communication between the Unimate controller and the VAX-11/780 ROUTINES C, is written in **C** It handles the *Virtual Machine System*

(VMS, the OS of the VAX-11/780) calls to open the communication channel with the Unimate controller, and at the same time allows the port communications to be interrupt-driven. Being interrupt-driven allows for efficient handling of communications without constant polling by the CPU. It was originally written by P. Merrill MERRILL83, and updated by the author to allow for the execution of numerous functions of VAL used in carrying out these experiments.

All VAL instructions can divided into three distinct classes: those that can be executed in *monitor* mode, those that can be executed in *program* mode, and those that can be executed in *both* modes. A monitor mode instruction means that it can be executed at any time, as opposed to a program mode instruction which can only be executed as part of a *VAL program*. The WHERE instruction, for example, can only be executed in the monitor mode, whereas the SIGNALI[2] instruction can only be executed in program mode. The SPEED instruction can be executed in both modes. Recall that the SIGNALI instruction is used in these experiments. Although the SIGNAL instruction can be used instead, it does not allow for interrupt-driven detection of the terminating condition.

The need to execute program mode instructions means that execution is temporarily transferred to the Unimate Controller. To do this, the SIGNALI instruction is embedded in a VAL program. Together with its interrupt service routine, the two programs are prepared under VAL on the floppy disk drive of the Unimate Controller. Except for the SIGNALI instruction, other non-interrupt-driven instructions are executed directly from the VAX-11/780. Before the execution of any program-mode VAL instruction, the VAL files containing these instructions are made to load from the floppy disk into the semi-conductor memory of the Unimate Controller. Thus when a program mode VAL instruction must be executed, the VAL program containing that instruction is run. ROUTINES.C handles communications (eg

[2] The I in the SIGNALI refers to the interrupt version of the SIGNAL instruction. The CPU is interrupted immediately upon receipt of the condition. SIGNAL and SIGNALI are intrinsic VAL instructions.

error handling, terminating conditions) between the Unimate Controller and the VAX-11/780 by matching strings generated by the VAL programs For programs that communicate *via* ROUTINES C with the Unimate Controller, error handling, terminating and other conditions are described by error codes These error codes are generated by ROUTINES C from the character strings sent by the Unimate Controller and are handled during run time

4.4 Accuracy and Precision

Webster's Dictionary WEBSTER81 defines *accuracy* as conforming to the truth or standard W D Cooper COOPER78 defines it as the "closeness with which an instrument reading approaches the true value of the variable being measured" Webster's WEBSTER81 defines *repeatability* as being reproducible In every day usage, there is a tendency to use these two words interchangeably, but incorrectly An instrument can be very repeatable *and* highly inaccurate This says that when the instrument is used to measure a sample a number of times, it will obtain the same reading nearly all of the time, but this reading is far from what would be measured compared with the use of a standard Using terminology from statistics, the measurements from such an instrument are said to have a small *deviation* A large deviation, on the other hand would imply that the repeatability of the machine is poor. Mathematically, the mean, $\bar{X}$, (or μ) and the standard deviation, σ, is defined as

$$\bar{X} = \frac{\sum_{i=1}^{N} X_i}{N} \tag{4.2}$$

$$\sigma = \sqrt{\sum_{i=1}^{N} \frac{X_i^2}{N} - \bar{X}^2} \tag{4.3}$$

The difference between the mean of the measurements with an instrument and the correct value is indicative of its accuracy Thus, an instrument with a very small difference between the mean of its measurements and the correct value, while at the same time having a small deviation is said to be highly accurate and repeatable

The PUMA 260 is specified to have a positional *repeatability* of $\pm$ 0.05mm. The manual does not however, specify a figure for the *accuracy* of the arm, and also under what conditions is the repeatability figure measured. Initial positioning experiments on the robot reveal that its positional accuracy is about 5-6 times worse than the figure for positional repeatability

Although current generation of robots are more repeatable than accurate, their limit of accuracy is indeed the lower limit of *controllable* movement. This fact is exploited in the calibration procedures

4.5 Tactile Domain

Initial experiments were performed by having the tip of the robot arm move between two *precision points*, one of which will be referred to as the starting location, and the other the destination. The two locations were chosen such that there was variation in only one of the cartesian axes in this case the x, and not all three. The Unimate Controller was made to run in an interrupt-driven mode in which contact with the electrical contact will stop the motion. The robot is then interrogated for its position. Motion is made between two points 5 centimeters apart. The robot is made to move at 0.01 of the VAL monitor speed of 100.0 to minimize non-elastic permanent deformation of the electrical contact, and also the dead distance travelled before the interrupt can be serviced. After the motion is stopped, the robot is made to go back to its starting location, and the experiment is repeated

Figures 13, 14, 15, 16, 17, 18 show the results of the experiment performed 50 times

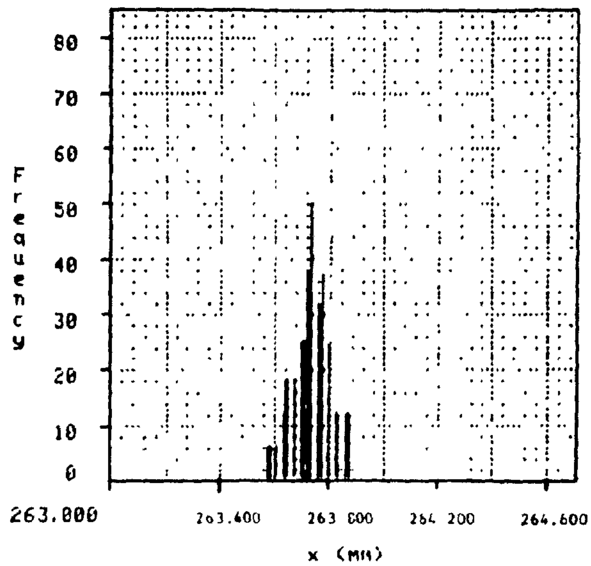

Figure 13 Variation in x readings ($\bar{x}$ = 263 738 mm σ = 0 068 mm)

Figure 13 shows the variations in the readings of the x-position of the end effector Figures 14. 15. 16. 17. 18. show those belonging to y. z. O. A and T respectively. Note that x. y. z are measured in millimeters. while O. A. T are measured in degrees

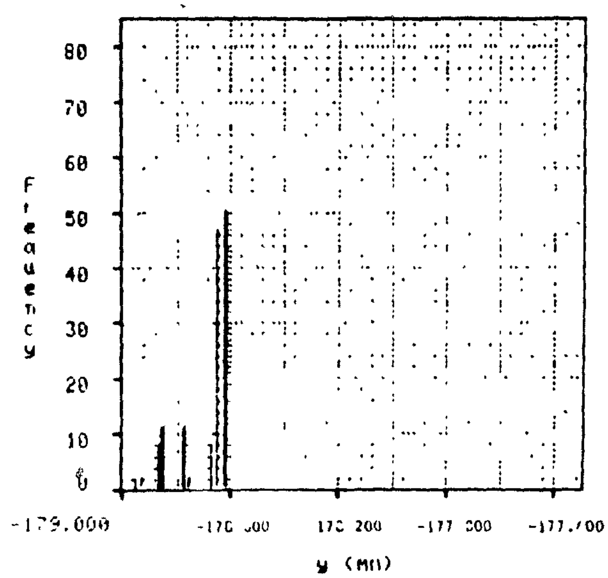

Figure 14 Variation in y readings ($\bar{y}$ = - 178 693 mm. σ =0 100 mm)

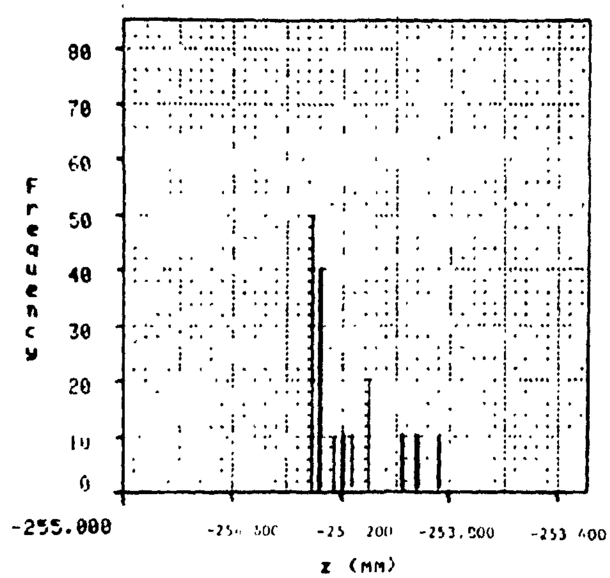

Figure 15 Variation in z readings ($\bar{z}$ = - 253 648 mm σ = 0 471 mm)

The graph of figure 13 shows a mean of $\bar{x}$ = 263 738 mm, and a deviation of σ = 0 068 mm There is a distinct peak at 263 74 mm, but there is a spread in the readings on both sides of the peak The readings do not occur at all intervals There exists a minimum interval between the readings The smallest interval in the readings of figure 13 is 0 020 mm The readings of the y position (see figure 14) show two main peaks at y = -178 610 mm, and at y = -178 650 mm and some scattering beyond this Minimum movement is 0 020 mm $\bar{y}$ is at -187 693 mm, with a σ of 0 100 mm z readings showed a considerable spread across nearly 0 6 mm, with no definitive peak Minimum movement occurred at intervals of 0 020 mm This, and subsequent graphs, indicate that 0 020 mm represents the limit of the linear resolution of the PUMA 260 It is important to note that the average positions in the base frame are arbitrarily chosen and it is the deviation that is important since it indicates how repeatable the motion is The results depicted in figures 13, 14, and 15 are all associated with a test motion along the x-axis of the robot but because of the robot geometry, this demands a coordinated motion of the joints to realize the linear motion in x

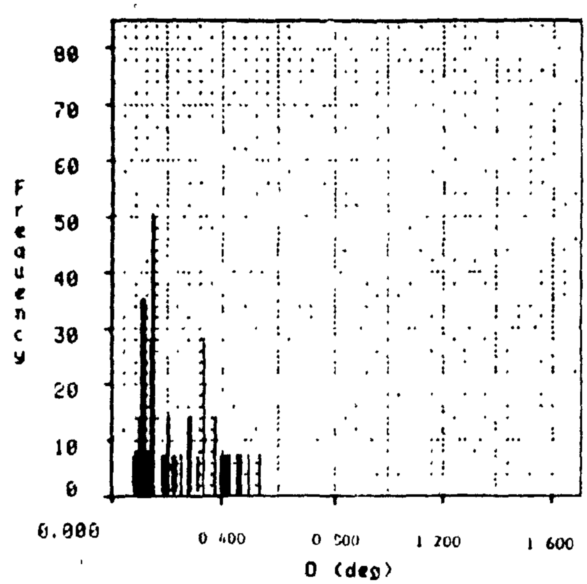

Figure 16 Variation in O readings ($\bar{O} = 0.218°, \sigma = 0.122°$)

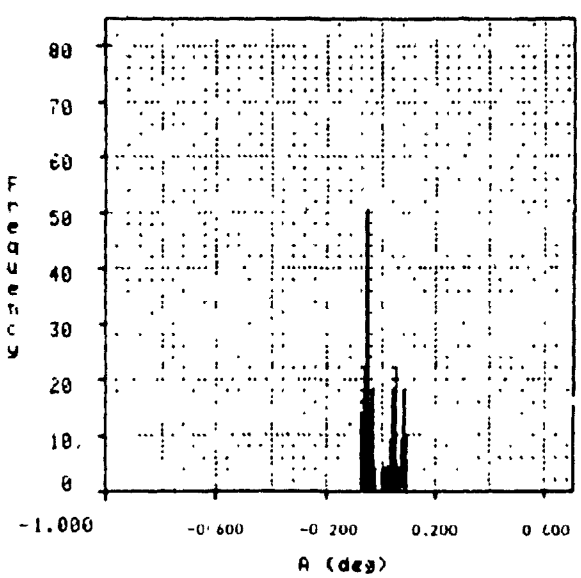

Figure 17 Variation in A readings ($\bar{A} = -0.005°, \sigma = 0.059°$)

The results for orientation of the wrist assembly during the x-axis motion tests are shown in figures 16, 17 and 18 The O readings varied across nearly a full 0.5° with no definitive

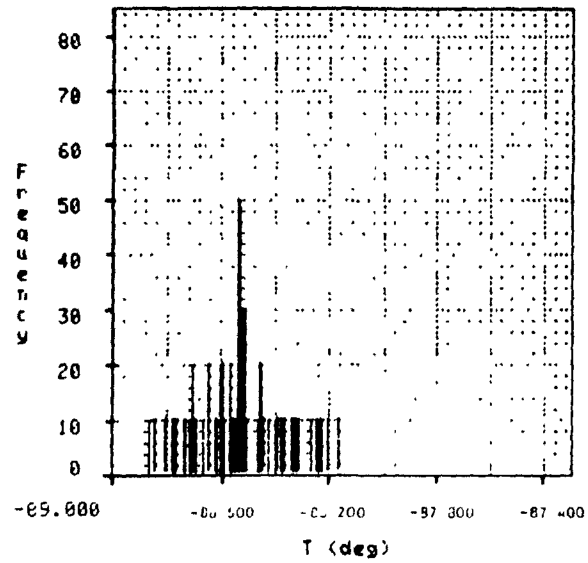

Figure 18 Variation in T readings ($\bar{T} = -88.517^\circ$, $\sigma = 0.163^\circ$)

peak. On the same scale, the A readings were clustered tightly together resulting in a deviation of 0.060°. The orientation of T showed a scattering similar to that of O with a deviation of 0.16°.

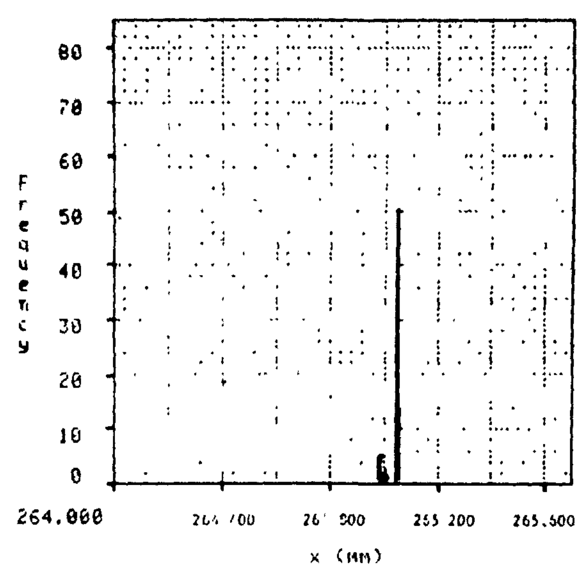

Figure 19 Variation in x readings ($\bar{x} = 265.038$ mm, $\sigma = 0.020$ mm)

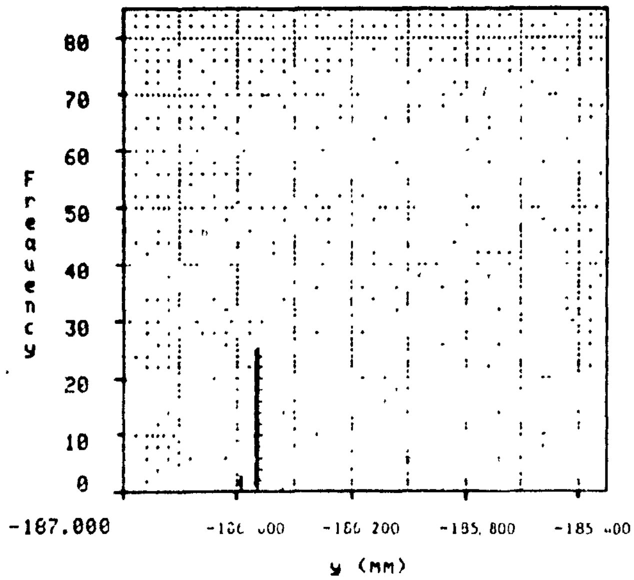

Figure 20 Variation in y readings ($\bar{y}$ = - 186 544 mm, σ =0 012 mm)

The robot was then made to move in a straight line between two points parallel to the y-axis of the base frame Figures 19, 20, 21, 22, 23, and 24 shows the results of the experiment for such a motion Figure 19 showed that while the mean of the x reading was 265 038 mm, the deviation was 0 020 mm and that the smallest interval between the peaks occurred at intervals of 0 020 mm from each other There is very little scatter in the readings beyond the two peaks indicating good repeatability Examination of the variation in the y position readings of figure 20 show remarkable repeatability in the re-positioning of the arm along this axis A deviation of 0 004 mm for the y-position readings reflects this It also shows a minimum movement of 0 020 mm

The z readings plotted in figure 21 show a mean, $\bar{z}$ of - 246 548 mm, and a deviation of 0.015 mm. Again, it shows very good repeatability in the z-axis, and that the minimum movement is 0 020 mm

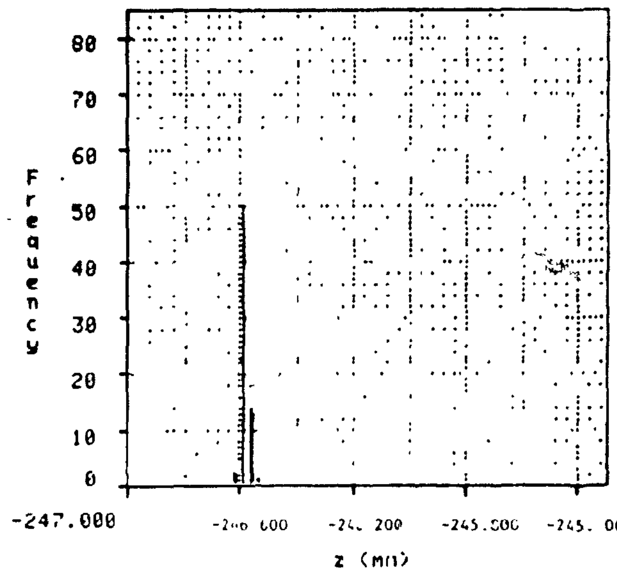

Figure 21 Variation in z readings ($\bar{z} = -246.584$ mm $\sigma = 0.015$ mm)

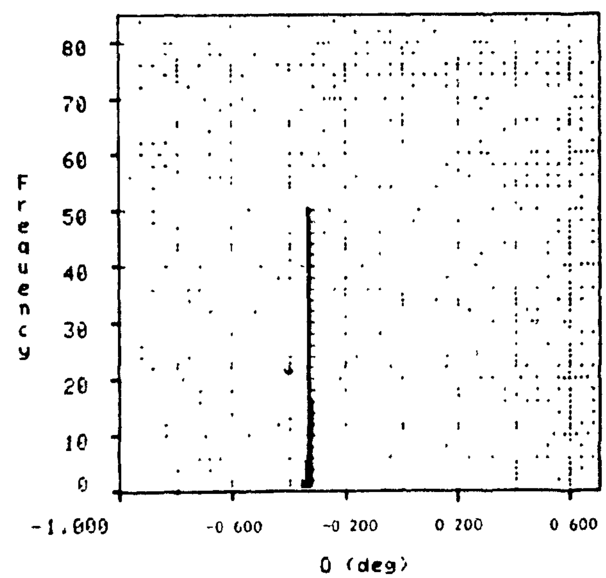

Figure 22 Variation in O readings ($\bar{O} = -0.335°, \sigma = 0.006°$)

The graph for the readings of the yaw angle, O, (see figure 22) show the readings grouped very tightly around the peak at $-0.335°$ with little spread. Interestingly enough it shows a minimum angular movement of 0.005°. It does occasionally move 0.006° (which may be due to numerical roundoff), and also 0.011° stemming from 0.005° + 0.006° movements. The

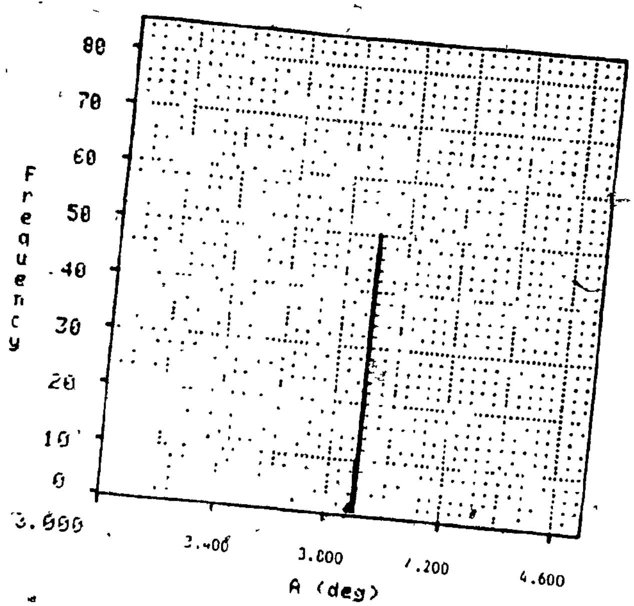

Figure 23 Variation in A readings ($\bar{A} = 3.898^\circ, \sigma = 0.005^\circ$)

deviation in the readings of the yaw angle, O, is 0.006°. The readings for the pitch angle, A, (see figure 23)exhibit a similar tight clustering of the readings around 3.898°. Minimum angular movement is again 0.005°. The pitch angle readings have a deviation of 0.005°.

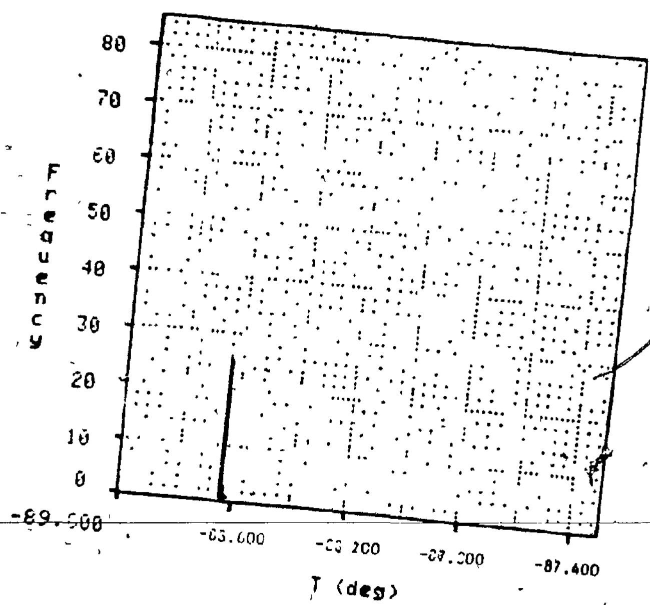

Figure 24 Variation in T readings ($\bar{T} = -88.637^\circ, \sigma = 0.006^\circ$)

The readings of the roll angle (see figure 24) indicate a mean, $\bar{T}$, of $-88.637°$, and a small deviation, σ, of $0.006°$. The minimum angular movement for this joint is $0.005°$; and there is just a single main peak, with a little scattering on either side. It is interesting to note that the orientation angles, O, A, and T, all exhibit the same very tight clustering resulting in a deviation of $0.005°$ of the arc.

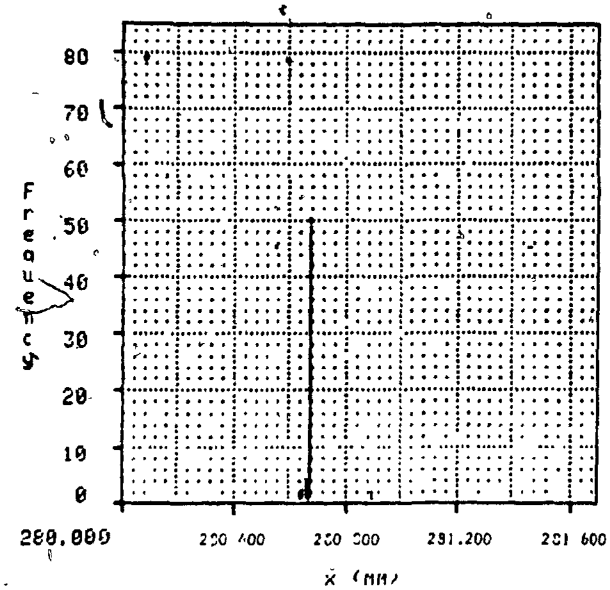

Figure 25 Variation in x readings ($\bar{x}$ = 280 685 mm σ = 0 043 mm)

Figures 25, 26, 27, 28, 29, 30 show the experimental results to move the PUMA 260 between 2 points 5 centimeters apart, along a line parallel to the z-axis of the base frame. In this set of experiments, the readings of the x-position (see figure 25) shows a single main peak with little scatter The readings averaged at $\bar{x}$ = 280.685 mm, with a deviation of 0.043 mm. Minimum movement is 0 020 mm Figure 26 shows the readings for the y-position. The existence of two main peaks (at -184 440 mm and 0 030 mm away at -184 470 mm) and some scatter at the higher end, resulted in a deviation of 0.057 mm.

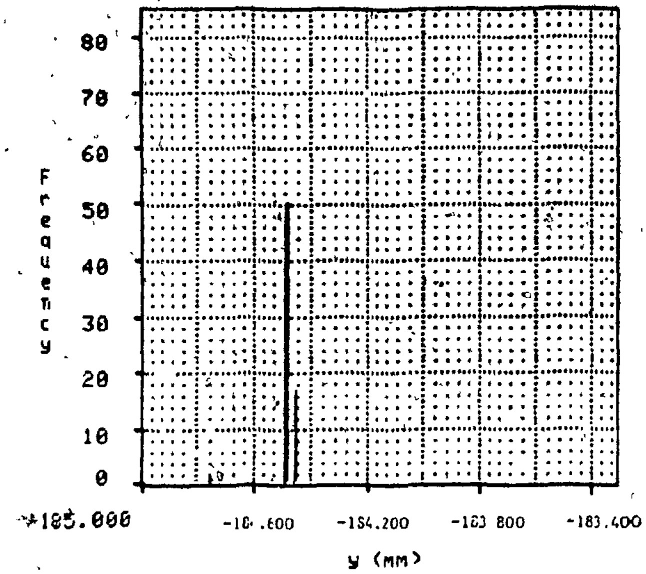

Figure 26 Variation in y readings ($\bar{y}$ = - 184 482 mm σ =0 057 mm)

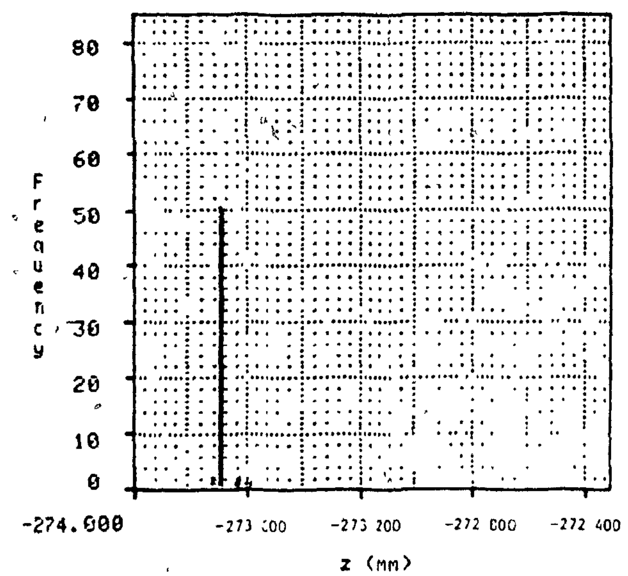

Figure 27 Variation in z readings ($\bar{z}$ = - 273 684 mm σ = 0 023 mm)

The graph for the readings of the z-position (see figure 26) show a single main peak. The average $\bar{z}$ is at -273.684 mm. and small resulting deviation of 0.023 mm

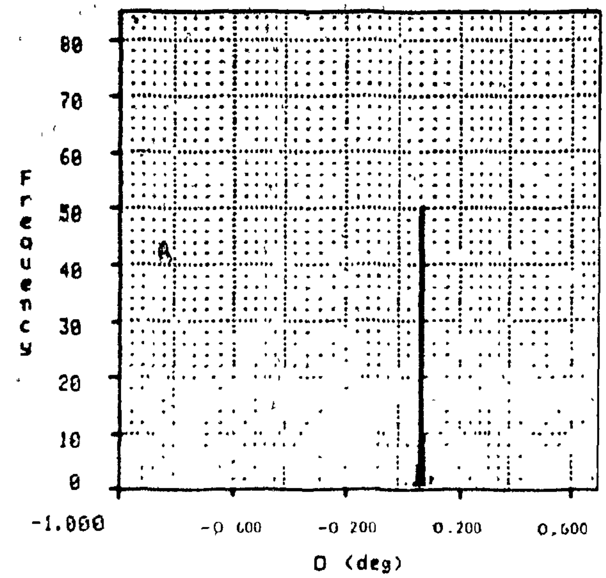

Figure 28 Variation in O readings ($\bar{O} = 0.084^\circ, \sigma = 0.010^\circ$)

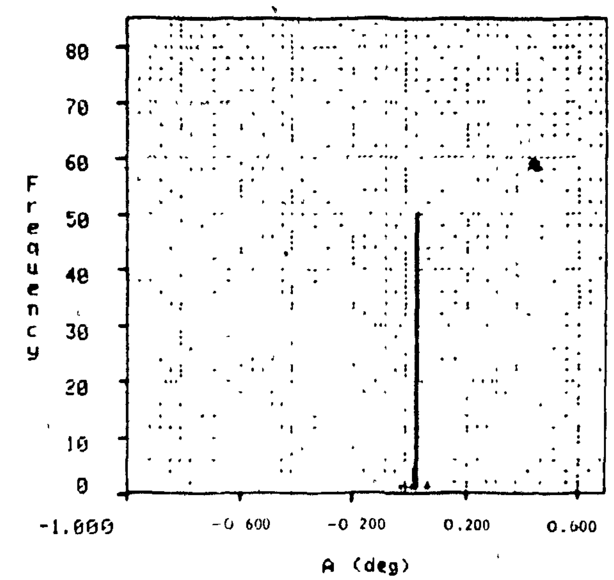

Figure 29 Variation in A readings ($\bar{A} = 0.043^\circ, \sigma = 0.013^\circ$)

The behavior of the wrist assembly is very much the same as in the two earlier parts of the experiment O and A show the presence of a single peak with a small amount of scatter on either side of the peak O averaged at 0.084°, while A averaged at 0.043° σO is 0.010° and σA is 0.012 The readings for T exhibited two main peaks nearly 0.010° apart The average is at 91 303° and deviation is 0.006° The results of these tests with x, y and z axis motions suggest that the maximum precision (minimum σ) results along the test axis motion

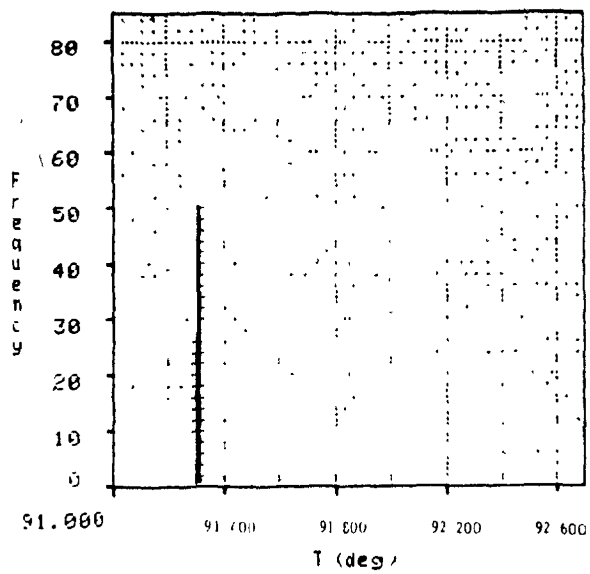

Figure 30 Variation in T readings ($\bar{T} = 91\ 303^\circ, \sigma = 0\ 006^\circ$)

4.6 Tool Orientation

To evaluate the enhanced control capability of the PUMA 260, we have to determine how well the robot can reach a commanded position and orientation For the purposes of formulating an experiment we will attempt to orient the tool frame such that it will be parallel with the base frame This orientation of the tool model is performed by first discovering a point of contact, $P1(x_1, y_1)$, in the x direction (see figure 31) Another point, $P2(x_2, y_2)$, further down the x-axis is then determined Note that although the DRAW command is used to perform the move, the actual orientation of the arm is determined by interrogating the controller with the command WHERE, and not through the use of dead reckoning[3] This

[3] Dead reckoning is the term of the navigational technique in which one s position is not determined absolutely

is necessary to avoid the significant roundoff errors introduced by the DRAW algorithm for movement

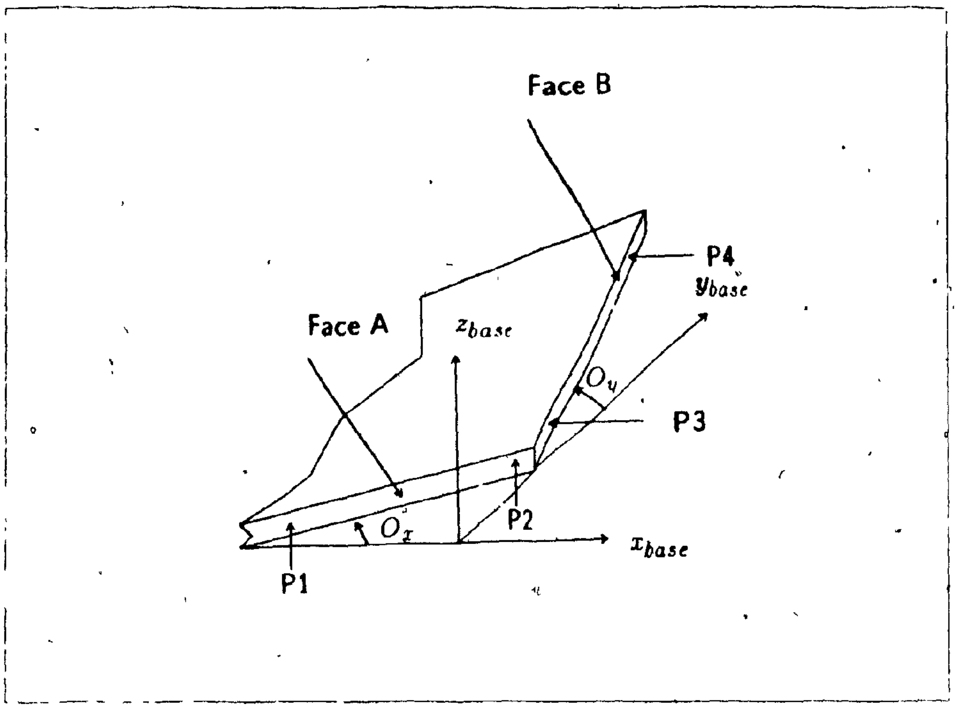

Figure 31 Discovering the O correction of the model

The angle made by the face A of the edge (see **figure 32**) with the x-axis of the base frame is given by

$$\delta O_x = \tan^{-1}\left(\frac{y_2 - y_1}{x_2 - x_1}\right) \tag{4.4}$$

The robot is maneuvered to round the corner of the model to operate on face B. The procedure is repeated for the y-axis with the determination of two more points, P3 and P4. Let δO_y be the angle made by face B with the x-axis. If face A of the model is orthogonal to

---

each time but rather only at the initial starting position. Subsequent positions are determined by measuring how far and along which direction one has travelled. Adding this information to the initial position the current position is obtained.

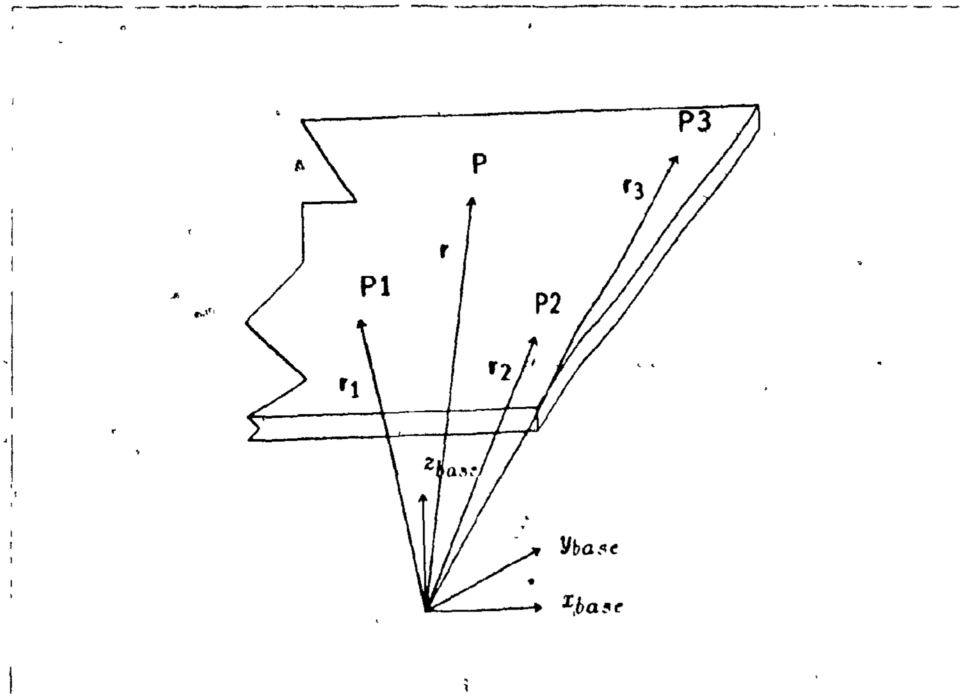

Figure 32 Discovering the wrist rotation angle

face B, then the angle δO_x is equal to the angle δO_y. Thus to align the P1-P2 edge with this the x-axis of the base frame, the correction angle δO_x has to be applied to the wrist rotation angle O.

Next the equation of the bottom face has to be found. To do this, the robot is manœuvered to have the model positioned directly over the electrical contact. It is then made to move down slowly until a contact is made. Motion is stopped to interrogate the robot for its position. The model is then raised and made to follow a triangular course to discover to two further points (see figure 32). Now given three points P_1, P_2, P_3 in space it is desired to find the equation of a plane that contains all these three points. Since the three points are not co-linear, the three points are sufficient to define a plane. Let their position vectors be denoted by $\mathbf{r_1}, \mathbf{r_2}, \mathbf{r_3}$. Also let $\mathbf{r}$ be the position vector of any point P, in the plane, then

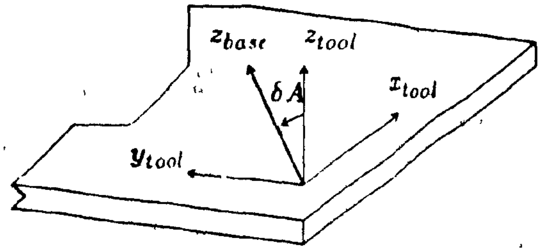

Figure 33 Discovering the wrist bend angle

$$\mathbf{P_1P} \cdot (\mathbf{P_1P_2} \times \mathbf{P_1P_3}) = 0 \tag{4.5}$$

and

$$(\mathbf{r} - \mathbf{r_1}) \cdot (\mathbf{r_2} - \mathbf{r_1}) \times (\mathbf{r_3} - \mathbf{r_1}) = 0$$

or

$$(\mathbf{r} - \mathbf{r_1}) \cdot \mathbf{Z_{tool}} = 0 \tag{4.6}$$

Therefore

$$\mathbf{Z_{tool}} = (\mathbf{r_2} - \mathbf{r_1}) \times (\mathbf{r_3} - \mathbf{r_1}) \tag{4.7}$$

The angle made by this $\mathbf{z_{tool}}$ and the z-axis of the base frame (see figure 33) is the angle δA. This is the wrist bend correction angle, the angle that when applied to the current orientation of the wrist, would cause the vector perpendicular to its plane to line up with the

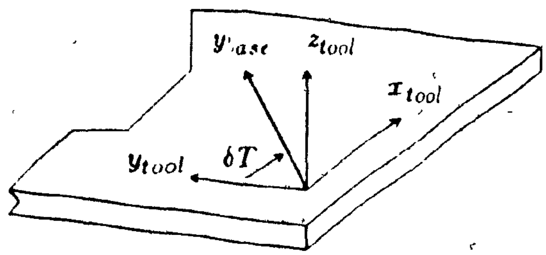

Figure 34 Discovering the flange rotation angle

z-axis of the base frame The correction angle, δA, is obtained from the equation

$$\mathbf{z_{base}} \cdot \mathbf{z_{tool}} = |\mathbf{z_{base}}| \, |\mathbf{z_{tool}}| \cos \delta A \tag{4.8}$$

Manipulating it we have

$$\delta A = \cos^{-1}\left[\frac{\mathbf{z_{base}} \cdot \mathbf{z_{tool}}}{|\mathbf{z_{base}}| \, |\mathbf{z_{tool}}|}\right] \tag{4.9}$$

The correction angle, δT, that is to be applied to the current flange rotation angle, is the angle formed between the vector $\mathbf{z_{tool}}$ and the y axis of the base frame (see figure 34) δT is obtained from

$$\delta T = \cos^{-1}\left[\frac{\mathbf{y_{base}} \cdot \mathbf{z_{tool}}}{|\mathbf{y_{base}}| \, |\mathbf{z_{tool}}|}\right] \tag{4.10}$$

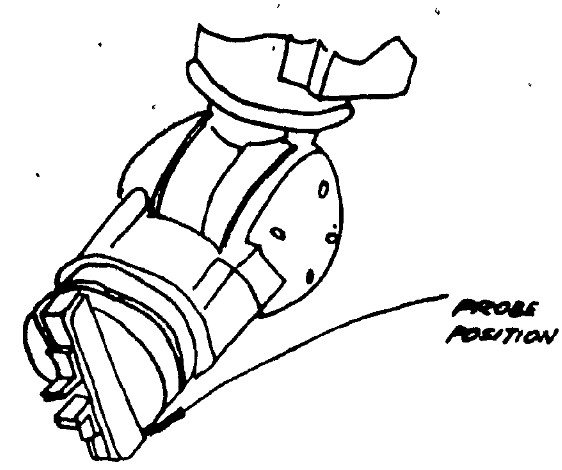

Figure 35 Discovering the linear corrections

4.7 Corrections for linear displacements

It is important to note here that the above procedure only performs corrections on the orientation of the wrist* This operation re-orients the wrist bend angle O, the wrist rotation angle A, and the flange rotation angle T of the wrist assembly There remains the linear corrections of δx, δy and δz to be measured and applied to the final positional correction to be performed on the model For this, it necessary to first define a suitably fixed benchmark on the arm (or wrist itself) from which the corrections can be calculated A point on the back face (see figure 35) of the standard gripper was chosen to provide this constant This point is rigid, and in any application, will be placed a short distance away from the tip of the tool It is important to keep this distance short because of the problems of numerical instability involved in taking the inverse Jacobian when the arm is moved to its extreme positions

To this end the linear displacements (δx, δy, and δz) from the reference (a corner on the back-face of the standard gripper) to the corner of the model are obtained The linear distances obtained in this manner are then stored in a *calibration* file that will be referenced later On subsequent recalibrations and performances of this motion the readings of the position of the corner on the back face of the standard gripper is compared with that in the calibration file Any discrepancies are then translated into linear corrections (δx δy and δz) to be applied to any final positions

Correction was first performed to re-orient the O, A, and T angles of the wrist assembly After this correction the coordinate axes of the model become aligned with the coordinate axes of the base of the robot This allows the linear correction factors to be applied to the transformation of the final point Thus the final correction matrix is given by

$$T_{tran} = \begin{pmatrix} 1 & 0 & 0 & \delta x \\ 0 & 1 & 0 & \delta y \\ 0 & 0 & 1 & \delta z \\ 0 & 0 & 0 & 1 \end{pmatrix} \qquad (4.11)$$

If the tool is similar to the model in that it can be modeled as a cuboid, then a corner can be thought of as the intersection of the planes forming that corner This holds even if the planes are not orthogonal to each other The orthogonal case is a *special* case of the general one A numerical advantage of modeling it as an intersection of planes is that it is a *linear* equation in x, y and z Because it is a set of linear equations, it can be solved very efficiently through the use of matrices

A note has to be made here about method for the re-orientation of the model of the tool None of the positions of the robot used in these experiments are critical Only the approximate starting location of the search need be known Even this position does not have to be known to any accuracy All that is required are the precise orientations of the robot arm when electrical contact occurs Programming a new starting location can be performed very easily through the use of the interactive facilities provided by the program and the teach pendant The use of the above techniques allow tremendous flexibility when it comes to re positioning the peripherals of the workstation There is absolutely no need to re-program all points of the robot task These can all be corrected from a few key reference points Only the starting location of the search for each peripheral is needed

4.8 An Independent Measurement

To test out the above procedure of aligning the tool frame with that of the base frame. the repeatability of the corrected positioning of the PUMA arm was checked with a *Baty* dial gauge micrometer that has a resolution of 0 010 mm The procedure consisted of carrying out the searches to evaluate corrections to the tool frame angles and translations and verifying the resulting tool axes alignment with the dial gauge The repeatability of this sequence was verified along each of the tool axes Since the origin of the robot coordinate system lies somewhere in the solid mass of metal forming the base of the robot we describe the results as a measure of its repeatability

The micrometer was used to measure the repeatability of the robot in aligning its tool x-axis and y-axis with the x- and y-axis of the base frame respectively as explained for figure 31 The results for the alignment of the x-axis of the tool frame with that of the base frame are shown in figure 36 The total spread in the readings is 0 020 mm with a deviation of 0 014

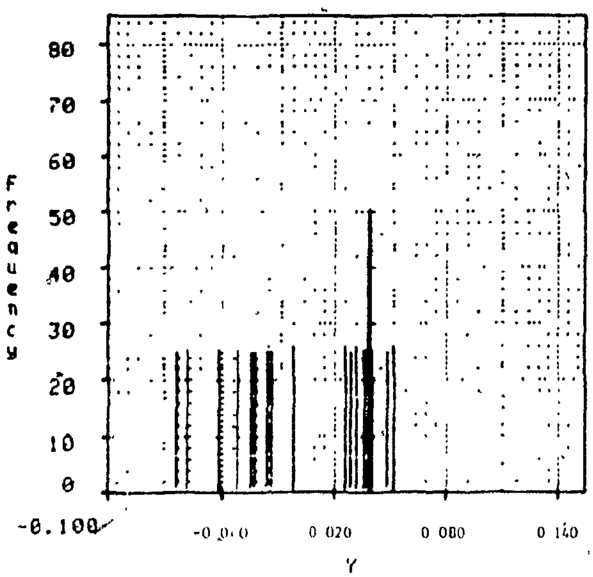

Figure 37 Variation in y readings ($\sigma = 0.037$ mm)

mm Alignment of the y-axis (see figure 37), on the other hand, showed a deviation of 0.037 mm

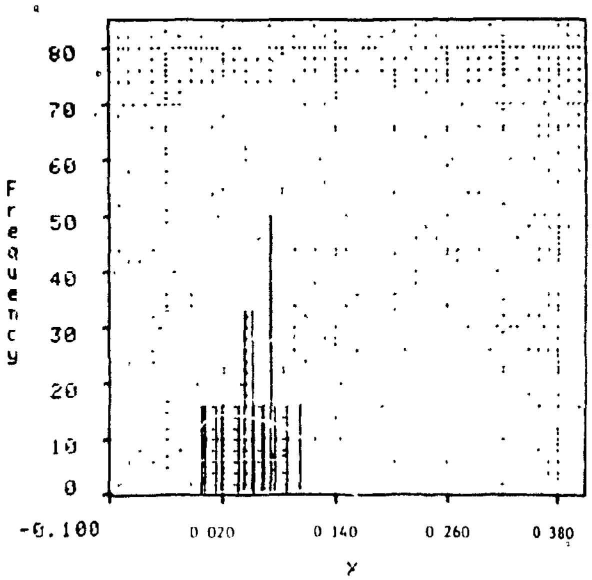

Figure 36 Variation in x readings ($\sigma = 0.014$ mm)

Because of the shape of the experimental tool, the z-axis response was treated differently. Here the flat face of the model was measured using three non-collinear points in the $x-y$ plane (on the bottom side of the model, see figure 32). The position of the micrometer dial gauge is fixed and the lower flat side of the model is brought into contact with it. This is repeated for two more points chosen to lie in the plane of contact which should maintain a constant z value. The differences between the first point, **P1** and the second point, **P2** are shown in figure 38, that of **P2** and **P3** in figure 39, and that of **P3** and **P1** in figure 40. Figure 38 shows a tight clustering around the main peak and a secondary peak beyond. The **P1** - **P2** readings have a deviation of 0.010 mm. **P2** - **P3** readings shown in figure 39 are somewhat more spread out with a deviation of 0.015 mm. The scatter of **P3** - **P1** readings (see figure 40) has a deviation of 0.020 mm. These small deviations serve to show that the tool plane is very well aligned to within the specified repeatability of the robot.

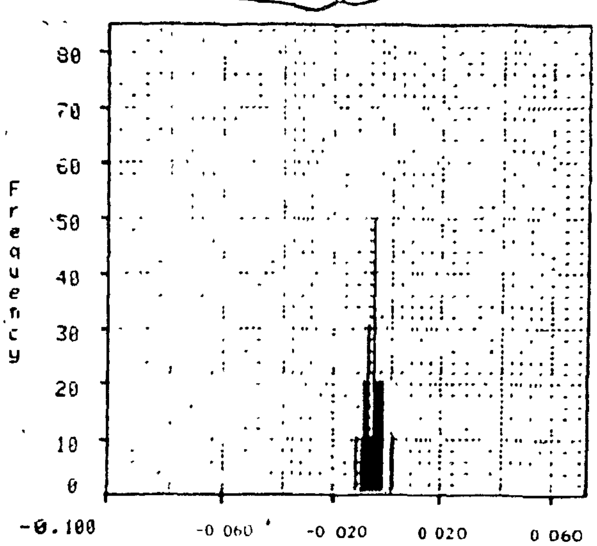

Figure 38 Variation in **P1** - **P2** readings ($\sigma = 0.010$ mm)

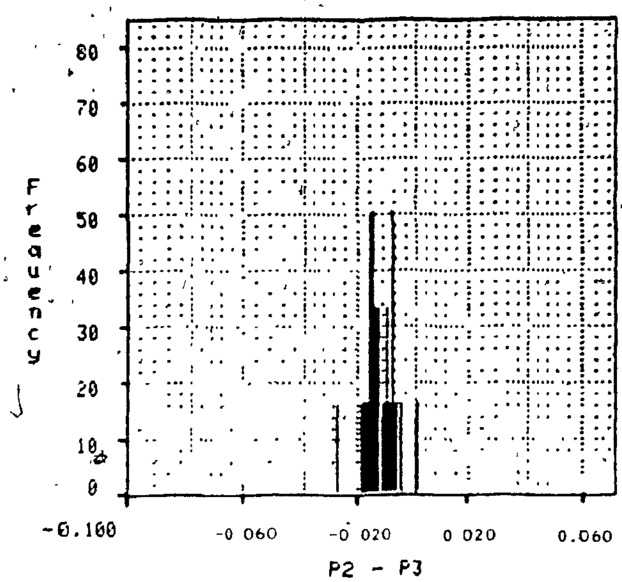

Figure 39 Variation in **P2** - **P3** readings (σ = 0 014 mm)

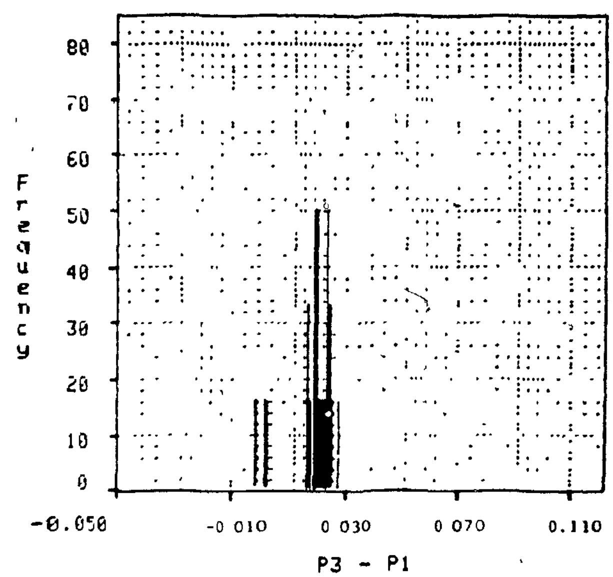

Figure 40 Variation in **P3** - **P1** readings (σ = 0 020 mm)

4.9 Warped Tool

The re-orientation process is next tested out on its ability to re-orient a purposely distorted model of a tool (see figure 41) The model is fashioned to have a sharp, definitive bend. Note that the plane to be corrected for is the shaded portion lying entirely beyond the bend. The rest of it is held in the grippers of the PUMA arm. The robot is then maneuvered to align the tool frame of the shaded part with that of the base frame. **P1** and **P2** are first measured to obtain the alignment of the x-axis of the tool frame. The alignment of the y-axis of the tool frame with that of the base frame is next found by measuring the differences in position between points **P3** and **P4**.

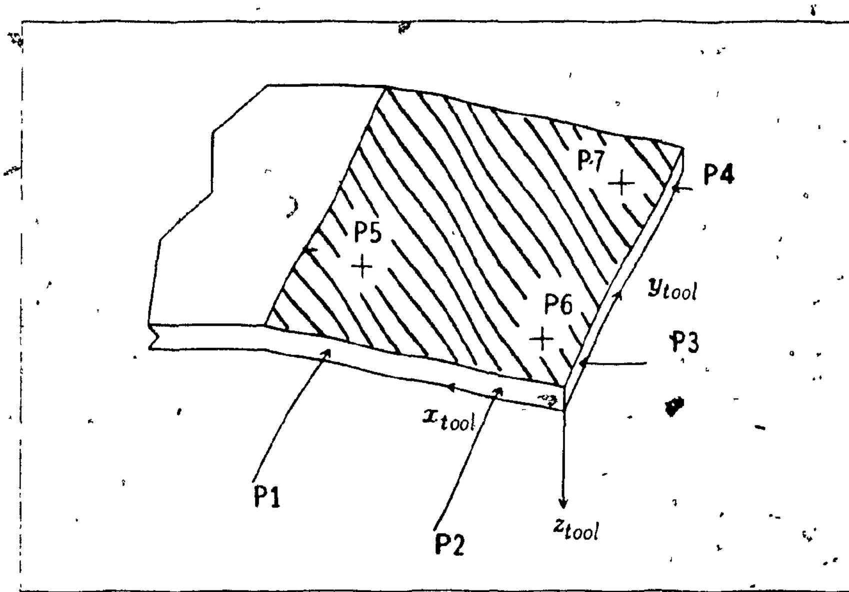

Figure 41 Warped Tool

Figure 42 shows the variation in the micrometer dial gauge readings of **P1** and **P2** obtained in the experiment to determine the alignment of the x-axis of the tool frame with that of the base frame The existence of two main peaks at -0.025 mm and at 0.040 mm with most of the readings falling in between them resulted in a deviation of 0.011 mm. The alignment of the y-axis resulted in the readings shown in figure 43 There are a number of closely clustered

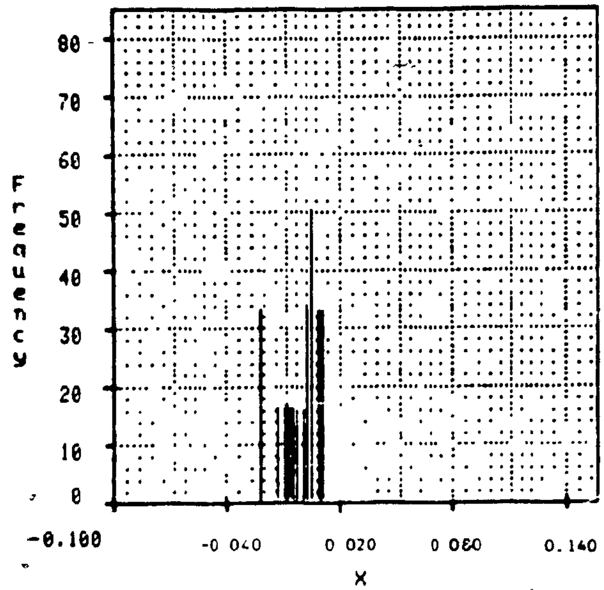

Figure 42 Variation in x readings (σ = 0 011 mm)

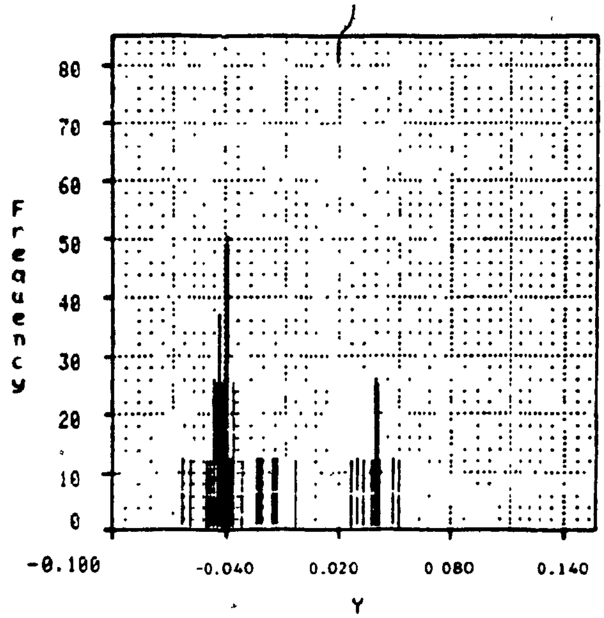

Figure 43 Variation in y readings (σ = 0 038 mm)

peaks The deviation of the readings of the differences between points **P3** and **P4** is 0.038 mm

The experimental procedure to measure the alignment of the bottom face of the tool with respect to the base frame is now performed for the warped tool using three points **P5**, **P6**, and **P7** shown in figure 41. Based on these measurements. the tool frame axes are realigned with the base frame The success of this realignment is verified by moving the warped tool to a micrometer and measuring the points **P5, P6,** and P7. Figures 44, 45, and 46 show the readings of the micrometer dial gauge in verifying the alignment. Figure 44 shows two main peaks with some scatter in the **P5** - **P6** readings resulting in a deviation of 0.017 mm. **P6** - **P7** (see figure 45) shows a single main peak The deviation is 0.011 mm. The **P7** - **P5** readings (see figure 46) show a scatter very similar to that of the **P6** - **P7** readings and have a deviation of 0 024 mm

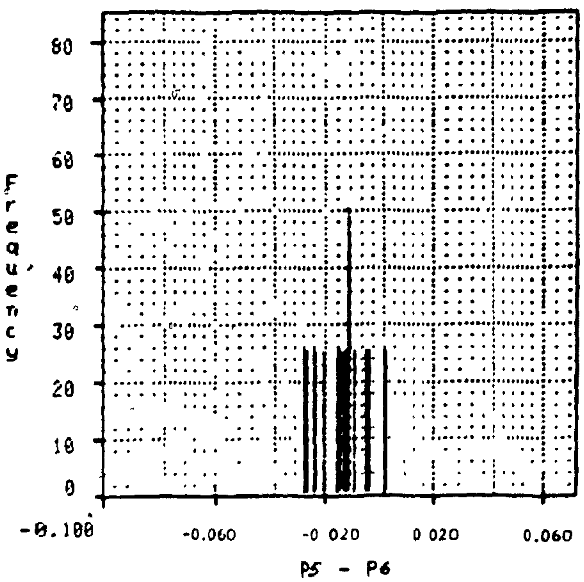

Figure 44 Variation in **P5** - **P6** readings (σ = 0 017 mm)

4.10 Calibration of a Pneumatic Grinder

While the above experiments were carried out with a model representing a tool, it is

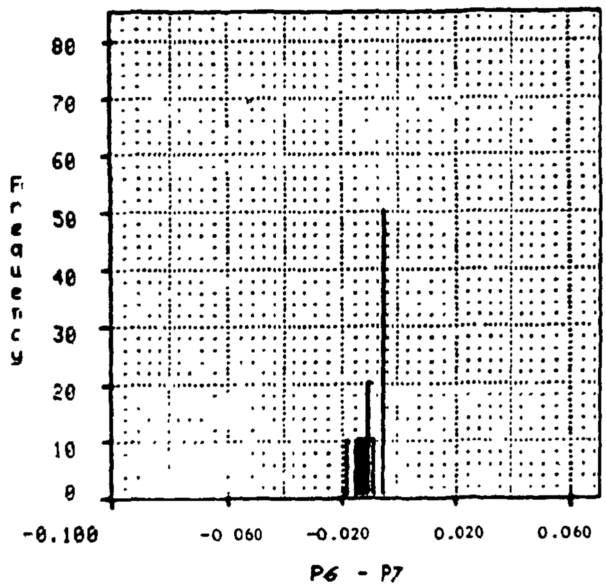

Figure 45 Variation in **P6 - P7** readings ($\sigma = 0.011$ mm)

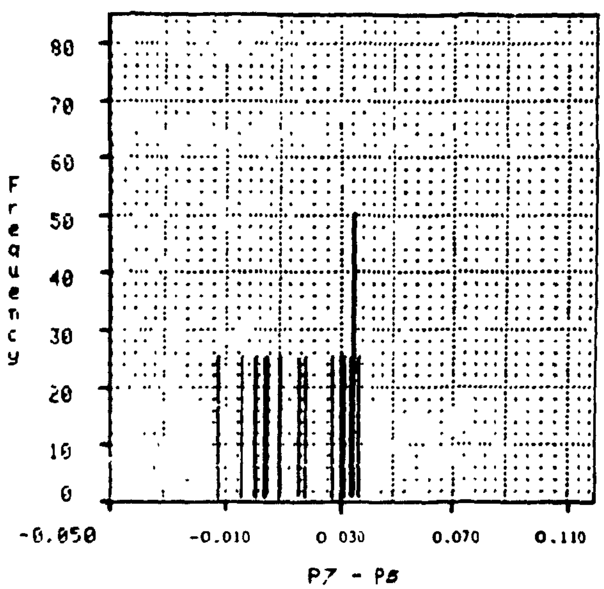

Figure 46 Variation in **P7 - P5** readings ($\sigma = 0.024$ mm)

necessary to determine how the automatic calibration procedures perform with a real tool, one which will be used in the course of the repair task The geometries of other tools will no doubt be somewhat different, but if their geometries can be accurately modelled, the necessary modifications to the calibration procedures will be few

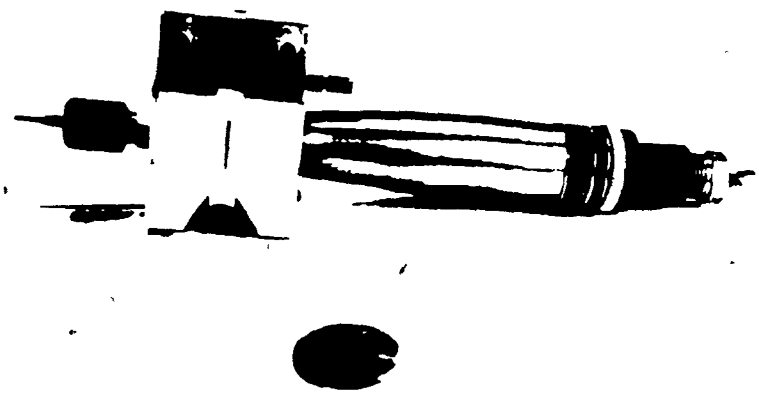

Figure 47 The pneumatic grinder

To carry out the experiment, a pneumatic grinder was chosen as the tool. As the tactile calibration is electrical in nature, it is necessary to have an electrically conducting tool, a tool that is conducting right to its very tip of tooling The pneumatic grinder is such a tool (see figure 47)

For the purpose of measuring the tip of the tool to verify the calibration procedures, all the wrist angles of O, A and T will be fixed orthogonal to each other, and aligned with the base coordinate frame of the robot With these constraints, the many of the trigonometric terms of the inverse kinematic equations of the wrist assembly (see equations 3 15 to 3 20) will simplify to 0 or ± 1

The calibration study was carried out with a special pointer tool shown in figure 48. Any subsequent tool, in this case the pneumatic grinder, will be calibrated against this special pointer tool The differences in geometry between this tool and the pointer with their appro-

Figure 48 Calibration Pointer Tool

priate signs, is then inserted into the appropriate locations of the homogeneous transform of equation 4.11 to successfully adapt the robot program to its new tool.

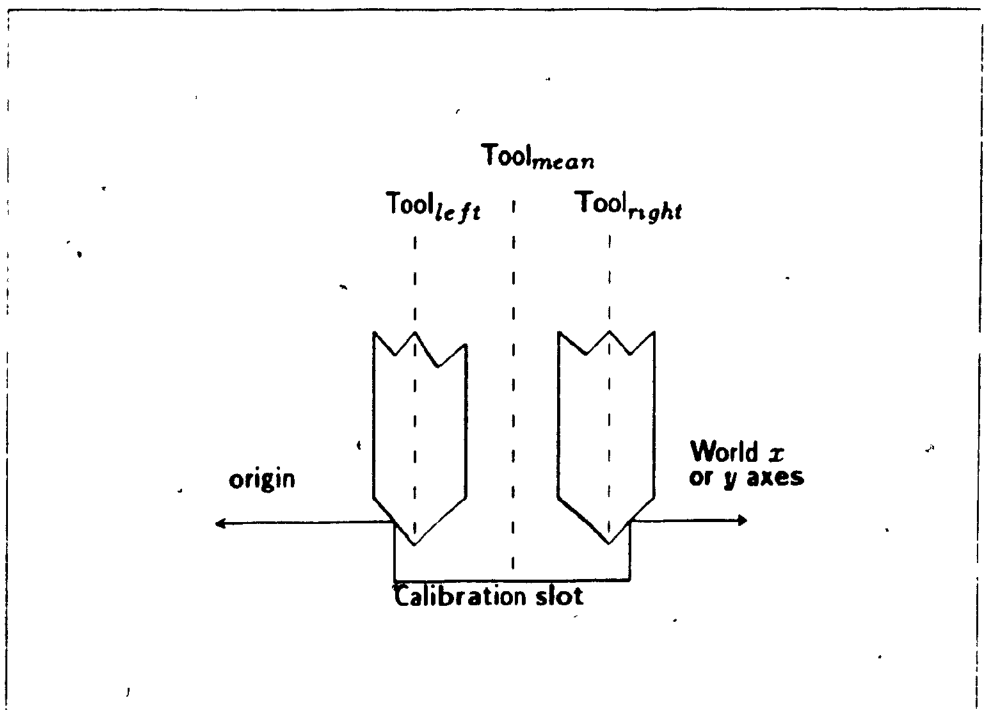

Figure 49 Determining the tool dimensions with the use of a calibration slot

The calibration procedure was carried out as follows The tool coordinate system was first aligned with the world coordinate system by interrogating the robot controller system and applying the necessary corrections By maneuvering the pointer tool to the obtain electrical contact with the left and right edges of a calibration slot (see figure 49), the mean tool position, P_{mean}, was obtained and stored For this test, the robot motion was selected to travel along one of the base coordinate axes and the calibration slot was positioned accordingly. The process was repeated using the grinder tool and its mean position, G_{mean}, was obtained. This difference, $P_{mean} - G_{mean}$ constitutes the tool calibration offset along one of the tool axes By rotating the tool by 90° about its z axis and repeating this procedure, both the grinder tool x and y offsets were obtained. Because of the tool shape, a simple electrical contact along the tool z axis is sufficient to determine its z dimension.

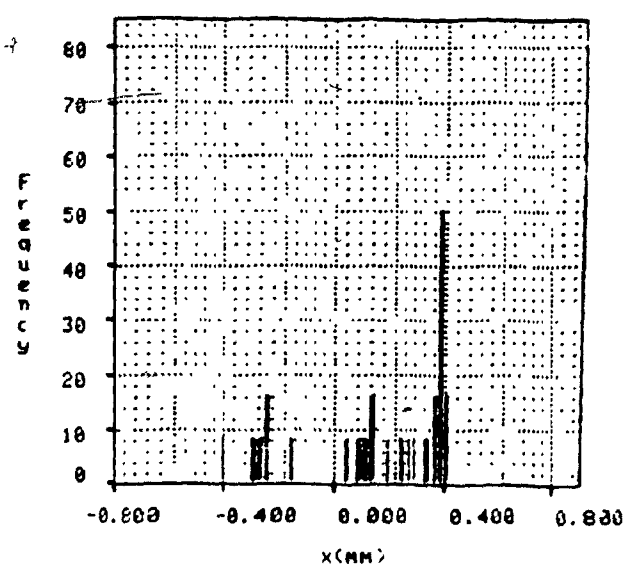

Figure 50 Variation in x readings ($\sigma = 0.242$ mm)

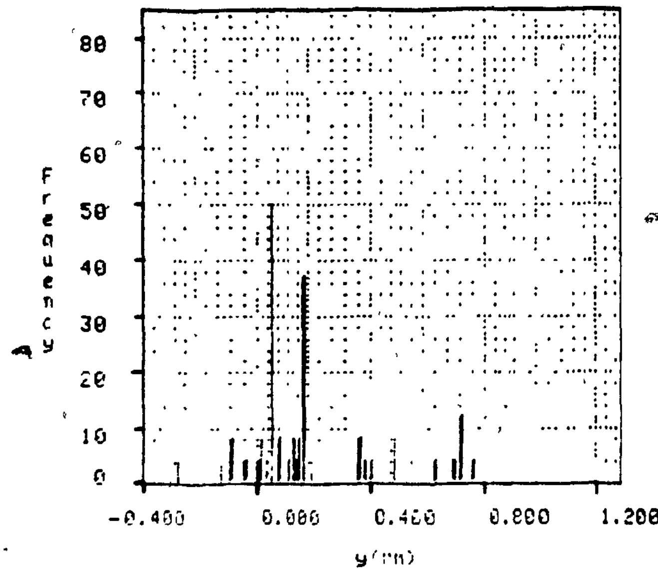

Figure 51 Variation in y readings ($\sigma = 0.237$ mm)

The test program positions the special pointer tool against a micrometer Using successive 90° tool rotations, the test program positions the special pointer against a single micrometer to obtain a set of x, y and z reference values which were selected to be zero for convenience. Then the pointer tool was exchanged for the grinder tool, and the previous motions repeated using the grinder tool offsets previously obtained. The micrometer readings were collected and the experiment repeated twenty times

Figures 50, 51, 52, show the performance of the calibration process in the x, y and z dimensions of the tool They show the differences between the measured dimensions of the grinder and that calculated by the calibration procedure The differences in readings of the x dimension of the tool have a deviation of 0 242 mm In the y dimension, the differences have a deviation of 0 237 mm The differences in the z dimension of the tool have a deviation of 0 136 mm. The results show that the tool when calibrated, can be placed to better 0.25 mm of its targeted position. This variation is considerably larger than the 0.02 mm to 0.03 mm

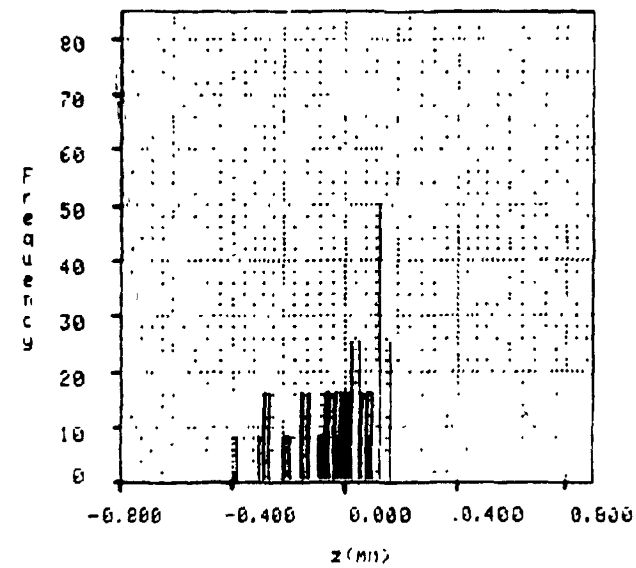

Figure 52 Variation in z readings ($\sigma = 0.136$ mm)

repeatabilities obtained in the previous sections. It could be due in part to the flutes of the grinding tip. Another possibility is the magnification resulting from the cantilever pivoting due to the considerable size of the grinder tool itself. This overall precision is acceptable for the grinding tasks

4.11 Calibrating the vision system

The vision system accompanying any robotic task has to be calibrated to coordinate what is being viewed by the camera (or cameras) and the actual movements of the robot arm It allows the robot to see its surroundings and interpret it with the right perspective Consider a camera viewing a robotic workstation as shown in figure 53 It can see both the cube (or any object grasped) at the end of the robot arm and the origin of base frame, labelled x_{base}, y_{base}, and z_{base} in figure 53. Let the homogeneous transformation describing the coordinate system established at the center of the cube in relation with the camera to be $\mathbf{T_1}$ If now

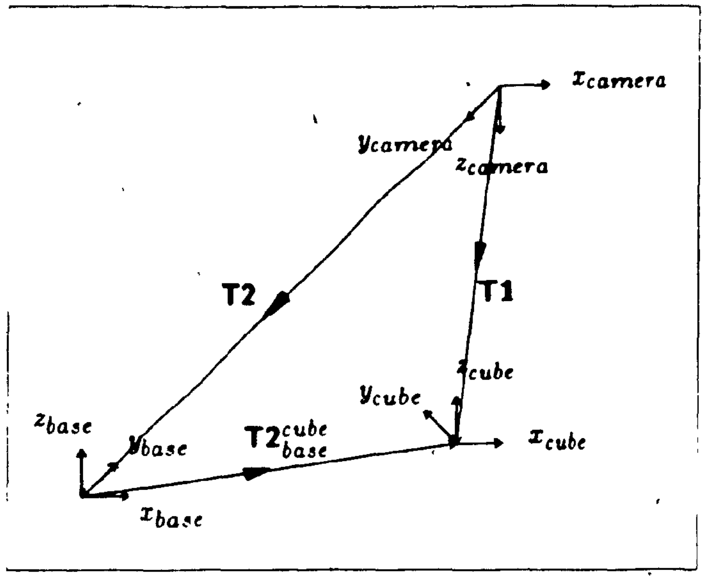

Figure 53 Coordinating eye-hand movements in the PUMA 260

T_2 is the homogeneous transformation of the origin of the base coordinate system as seen by the camera, then the position of the center of the cube with respect to the base coordinate system is given by

$$T^{cube}_{base} = (T_2)^{-1} \cdot T_1 \tag{4.12}$$

Solution of the above equation requires knowledge the entries of the matrices A number of methods can be employed to do this With the use of just one camera, the robot is used to move the cube through a known course to cause a change in the position of the cube in the image seen by the camera from which the inverse transformation can be computed BALLARD82 The use of two or more cameras in this method lends it greater versatility and also a larger field of view

Although a wide-angle (of view) lens may be desirable, there exists an accuracy trade-off in its use This loss of resolving power is an inverse function of the focal length of the lens on

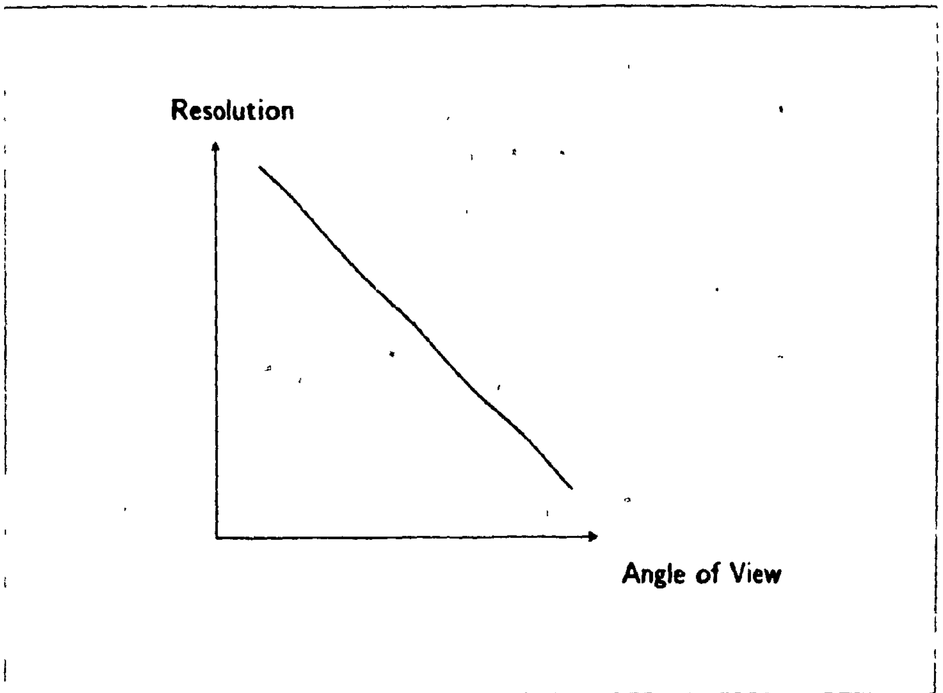

Figure 54 Angle of view and resolution trade-off

the camera Figure 54 illustrates this loss of resolving power The center-to-center distance between the sensing elements of the CCD array is fixed in the manufacturing process of the CCD array The result of this is that an image whose length is smaller than this distance cannot be resolved Because it will cause an output on only *one* element the length of the object *cannot* be computed The equation describing this is given by

$$\frac{1}{f} = \frac{1}{d_i} + \frac{1}{d_o} \tag{4.13}$$

where f is the focal length of the lens used on the camera. d_i the distance from the lens to the image plane. and d_o. the distance to the object plane. The equation relating the height of the object. h_o. to the height of the image h_i is given by

$$\frac{h}{d} = \frac{h}{d} \qquad (4.14)$$

and the limiting condition under which determination of the length is no longer possible is defined by

$$h = \text{center to center distance of sensing elements} \qquad (4.15)$$

If r_1 is the resolution of a lens with focal length f_1, and r_2 is the resolution with focal length f_2 with the same resolution CCD array, the equation relating these is given by

$$\frac{r_1}{r_2} = \frac{f_2}{f_1} \qquad (4.16)$$

Of the cameras that are in the laboratory, the Fairchild CCD3000 camera has a resolution of 488 pels vertically and 380 pels horizontally. The vertical center-to-center distance between sensing elements is 18 microns, and that for the horizontal is 30 microns. The Hitachi KP-120U CCD camera has a resolution of 320 pels horizontally and 244 pels vertically. This corresponds to a center-to-center distance between sensing elements of 20.6 microns and 36 microns respectively. The recently acquired *Sony* XC-37 cameras, which weighs just ¿45 grams, has 280 pels horizontally and 350 pels vertically, with corresponding distances between sensing elements of 23 microns and 13.4 microns.

A compromise can be reached in the trade-off between the angle of view and the resolution through the use of *multiple* cameras with different angles of view. A wide-angle lens can be used to view the general scene. This view, in turn, is over-lapped in crucial areas by several telephoto lenses. Correlation between the multiple views is easily achieved by examining a point common in the wide-angle and narrow-angle views. To determine the repeatability in the discovery of a point in the view of a camera. the image is displayed on a monitor. and the point is tracked by a user While the position of the point will be tracked by a computer program in future. it is sufficiently indicative of the repeatability to use a human user to track the point Computer algorithms used to perform this tracking function are still inferior to humans performing the same task

4.12 Visual Domain

The graphs for the visual tracking experiments are shown in figures 55 and 56 The experiment determines how closely a human user can track a high contrast pattern of a 3 cm cross draw in ink on white paper and seen by the Fairchild CCD3000 camera through a Wild Leitz microscope at 6 times magnification and displayed in grey scale on a CONRAC monitor. The results are shown in figure 55. There is a 100% probability of tracking to within one pixel In fact. the probability of tracking to the target pixel itself is better than 70%. The deviation in the number of pixels along the x-axis is just 0.4; better than half a pixel Figure 56 shows the result of tracking the y-coordinate of the target point. It also has a deviation of 0.4 pixels

The resolution of the combined optical and electronic imaging system is dependent upon both the focal length of the optics and the center-to-center distance. d_{c-c}. between the sensing elements of the CCD array. Thus for a particular focal length. f. and d_{c-c} the angular resolution. θ. is given by

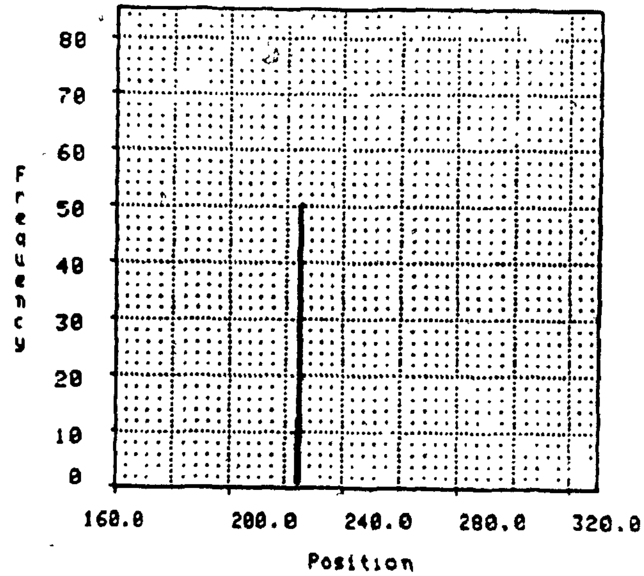

Figure 55 Variation in x (pixels) readings ($\bar{x} = 223.8$ $\sigma = 0.4$)

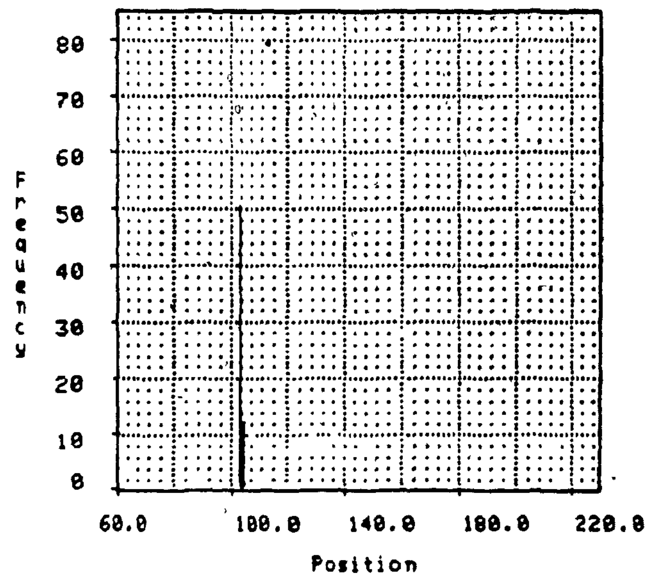

Figure 56 Variation in y (pixels) readings ($\bar{y} = 103.2$. $\sigma = 0.4$)

$$\theta = \tan^{-1}\left(\frac{d_{c-c}}{f}\right) \tag{4.17}$$

For a lens of 18 mm focal length and a d_{c-c} of 36 X 10^{-06} mm (the worst case for the Hitachi KP-120U). this corresponds to an angular resolution of 0.95°. With a target at 30 cm away (a common distance given the current laboratory set-up) the resulting linear resolution is 500 microns, or 0.5 mm

The problem of tracking a target point visually in 3-D space can be reduced to a number of sub-problems of tracking in 2-D space. For an optimally placed set of views, (in this case, this would be an orthogonal placement of camera positions) the limit of volumetric resolution would be a cube of 500 micron sides. This figure can be improved upon by increasing the focal length of the lens used with the camera, but the result of this choice is a smaller angle of view.

The optical system together with the CCD sensing array was tested for any barreling or pin-cushion distortion. A machined and polished edge with two scribed marks a known small distance apart, was viewed through the microscope and electronic imaging system It was first placed at the lower edge of the screen and the displacement in the number of pixels noted. It was then moved to the center of the screen, and the experiment repeated Finally it was moved to the top of the screen. Any distortion would result in a change in the number of pixels. However, the results showed no evidence of distortion at any magnification.

The overall camera calibration can be evaluated experimentally by viewing a calibrated scale and calculating the overall scaling coefficients in the x and y directions These measurements resulted in scaling factors of 580 microns and 450 microns per image pixel in the x and y directions respectively for a target placed 320 mm away from the focal plane. In terms of viewing angles, this works out to a field of view of 20.3° vertically and 24.7° horizontally

Aside from the standard 18 mm focal length lens, the camera can be attached to one of the viewing ports of the *Wild Leitz* binocular microscope The microscope has a a 6-50 times magnification capability. With a camera whose sensing elements have a 36 micron center-to-center distance, its resolution was measured at 67 microns under 6 times magnification and 8 microns at 50 times magnification. The image under high magnifications becomes less well-defined

With the above techniques, we have a choice whether to calibrate a tool in the visual domain or in the tactile domain. This choice lends considerable latitude to the calibration procedure While a tool with a relatively simple geometry such as the pneumatic grinder was used to test out the calibration procedures, there were some tools with a complexity in geometry that would preclude the use of tactile sensing for its calibration In such instances, the availability of camera sensing serves to overcome the limitations of calibration in the tactile domain By viewing the tool from a number of different positions, its geometry can accurately be characterized Besides use in the visual calibration of tools, camera vision can also be used to gauge distances or dimensions of components that do not lend themselves easily to tactile sensing These visual sensing techniques MALOWANY85 have been successfully applied to printed circuit board assembly MANSOURI85 and electronic assembly by robots MICHAUD85

4.13 Evaluations and Future Extensions

This was primarily a study to characterize the sources and magnitudes of the various errors in positioning the PUMA 260 robot arm. The above methods for the measurements and tool characterizations are satisfactory since the program execution speed is not a limiting factor Rather, it is the nature of the slow robot motions that is required However, improvements can be made in communication between the host computer and the Unimate controller. The implementation through the VAL terminal mode gives rise to some very clumsy constructs which could be simplified with a more powerful robot language such as RCCL Communication is also enhanced because RCCL allows for direct interrupt servicing capability Future extensions of the calibration programs will include utilities to calibrate new tools, a database with various tool transforms and the locations of the various task positions.

5. Conclusion

The Computer Vision and Robotics Laboratory is currently involved in the application of automated visual inspection and repair of hybrid integrated circuit boards The task is to develop an "intelligent" workstation, based on the expert-systems approach, so that the repair process with relevant inputs from the visual and tactile domains, can decide and effect a course of action in the inspection and repair process.

In this context of development, it is necessary to depart from the traditional method of teaching the robot all its task positions Rather, these positions are to be calculated by the robot programs themselves, according to the task requirements and tools required To this end, the calibration procedures were formulated based on electrical contact and camera vision

The repeatability of the robot's motion was measured using electrical contact under a variety of conditions of motion The positioning experiments here have shown that the PUMA 260 is indeed capable of the 50 micron repeatability as described in the manufacturer's specifications Nearly all applications can be tailored so as to depend on the positional repeatability of a robot arm, rather than its positional accuracy The positional accuracy of the robot cannot be specified very precisely without taking the geometry of the robot into account. If the robot suffered a collision in which a link becomes slightly distorted, the robot will still (if it is able to operate) be able to maintain the *same* repeatability, but will no longer be as accurate as before the collision

The repeatability has been shown to be better than 0.040 mm. The minimum linear movement resolution is 0.020 mm The experiments also show that a tool can be positioned at a targeted location, when calibrated, to within 0.3 mm The wrist assembly is found to have a positional resolution of 0.005° with the deviation generally around 0.006°. With a 5 cm tool length, for example, this works out to an arc length of less than 5 microns

The implementation of the coordinate system for the PUMA 260 allows the kinematics equations of the robot to be solved. not on the robot controller. but on a VAX-11/780 computer in conjunction with the application programs The numerical evaluation of the kinematic equations for the motions were performed on the VAX-11/780 with the resulting joint angles transmitted to the Unimate controller for the execution of the motion. These programs are available for general use in calibrating other tools as necessary. This enhanced kinematic computational capability is further advanced with the use of self-calibrating procedures Different tool geometries can readily be accommodated into the kinematic equations so that the working point of the tool can be located at the same position despite a change of tools These techniques were experimentally verified by demonstrating the ability to exchange pointer and grinder tools in a robot "test" program

The visual tracking experiments were carried out with the use of the Hitachi CCD camera whose vertical center-to-center distance between active sensing elements is 36 $X\ 10^{-06}$ mm. showed an extremely high probability of tracking to within one pixel of the target point. The actual distance resolved in the world coordinate system is dependent upon the focal length. and hence the magnification of the lens used For an 18 mm focal length lens (the lens used in some of the experiments). the resolution in the world coordinates is 0.05° of the arc At 32 cm from the CCD plane. a distance commonly encountered in the current workstation setting. this translates to a resolution 500 microns. or 0.50 mm In actual measurements. the camera was able to resolve 580 microns and 450 microns per image pixel in the x and y directions respectively This corresponds to a viewing angle of 20.3° vertically and 24.7° horizontally.

A camera having a 36 micron center-to-center distance between sensing elements was used in conjunction with the *Wild Leitz* microscope which has a 6-50X zoom capability. At the lowest magnification of 6 times. the resolution that can be obtained is 67 microns. At the highest magnification of 50 times, an 8 micron resolution was achieved. Under high magnifications, however, the image becomes less well defined and tracking becomes difficult. "Smooth" surfaces no longer appear smooth under such high magnifications.

To track in 3-D space, multiple views, from a mobile camera or multiple fixed cameras, are proposed. Using an 18 mm focal length lens, the volumetric resolution of a point 320 mm away corresponds to a cube of 500 microns, or 0.50 mm per side. Higher linear resolutions can be achieved through the use of lenses with longer focal lengths if the smaller angle of view is acceptable.

6. References

Achmatowicz, M. J., "Industrial Robots in General Motors - 1982 Update." Proceedings of the Canadian Conference on Robotics. pp 2-3. Mississauga, Ontario. September 1982

Agin, G. J. & Gleason, G. J., "A Modular Vision System for Sensor-Controlled Manipulation and Inspection." Proceedings of the 9th International Symposium on Industrial Robots. Society of Manufacturing Engineers. pp 57-70. Detroit. 1979.

Albertson, P., "Verifying Robot Performance." Robotics Today. pp 33-36. October 1983

Albus, J. S., "Theory and Practice of Hierarchical Control." 23rd IEEE Computer Society International Conference. September 1981

Ambler, A. P, et al., "A Versatile Computer-Controlled Assembly System." Proceedings of the 3rd International Joint Conference on Artificial Intelligence. pp 298-307. 1973.

Anderson, R. H., Gillard, C. W. & Huang, C. C., "Application of Laser Interferometry to Robotics." Proceedings of the SPIE. - The International Society for Optical Engineering - Vol 360. San Diego, California. pp 207-214. 1982.

Ballard, D. H. & Brown, C. M., "Computer Vision." Prentice-Hall. ISBN 0-13-165316-4. 1982.

Balzer, R., "A 15 Year Perspective on Automatic Programming." IEEE Transactions on Software Engineering. Volume SE-11. Number 11. pp 1257-1267. November 1985

Bardelli, R., Dario, P., Rossi, D. R. & Pinotti, P. C., "Piezo and Pyroelectric Polymers Skin-Like Tactile Sensors for Robots and Prostheses." Conference Proceedings of 13th International Symposium on Industrial Robots and Robots VII. Vol. 2. pp (18-45) - (18-56). Chicago. April. 1983

Barnard, S. T., Kushner, T. R. & Siegel, D., "Inspection of Printed Circuit Boards for

Part Integrity." SRI International Technical Note 274, Project 3588, pp 1-25, December 1982

Bejczy, A. K., "Smart Sensors for Smart Hands," Proceedings of conference on 'Smart Sensors', AIAA/NASA, Hampton, Vermont, November 1978

Berger, A., Dunbar, P. & Roberts, C., "Machine Vision Character Recognition in the Electronics Packaging Industry, Three Case Studies," Conference Proceedings of Vision '85, pp 1-15 to 1-35, March 25-28, 1985, Detroit, Michigan

Besl, P. J., Delp, E. J. & Jain, R., "Automatic Visual Solder Joint Inspection," IEEE Journal of Robotics and Automation, Volume RA-1, Number 1, pp 42-56, March 1985

Blade Runner, 20th Century Fox film release, Ridley Scott (director), 1982.

Bolhouse, V. C., Machine Vision Applications for High Volume Electronics Manufacturing," Conference Proceedings of Vision '85, pp 5-75 to 5-98, Detroit, Michigan, March 25-28, 1985

Bolles, R. & Paul, R. P., "The Use of Sensory Feedback in a Programmable Assembly System," The Stanford Artificial Intelligence Laboratory, Stanford University, AIM-220, Oct 1973

Bonner, S. & Shin, K. G., "A Comparative Study of Robot Languages," IEEE COMPUTER, Volume 15, Number 12, pp 82-99, ISSN 0018-9162, December 1982.

Bortz, A. B., "Robots in Batch Manufacturing," Robotics Age, Vol. 6, No. 1, pp 12-18, January 1984.

Boudreault, Y. & Malowany, A. S., "A CMOS Convolution Chip for Robotics Applications," 13th International Symposium on Mini and Microcomputers and their Applications, pp 1-4, McGill University, Montréal, Canada, June 3-5, 1985

Britannica, Encycloædia Britannica, 15th edition, Macropædia, Volume 2, Arizona-

Bolivar, Encyclopædia Britannica Inc (publisher). Essay on *Automation*, ISBN 0-85229-378-X, 1981

Britannica, Encycloædia Britannica, 15th edition, Macropædia, Volume 15, Proboscidea-Rubber, Encyclopædia Britannica Inc (publisher), Essay on *Robot Devices*, ISBN. 0-85229-378-X, 1981

Brooks, R., "Solving the Find-Path Problem by Good Representation of Free Space," IEEE Transaction on Systems, Man and Cybernetics, Volume SMC-13, Number 3, March-April 1983

Bronowski, J., "The Assent of Man," Little, Brown (publisher), 1974, 1973c, ISBN. 0316-109-304.

Brown, D. R., Fowler, D. V., Park, W. T. & Robinson, A. E., "Applications of Artificial Intelligence/Robotics," Proceedings of the SPIE, - The International Society for Optical Engineering - Vol 360, pp 50-57, San Diego, California, 1982

Brown, D. & Morgen, B., "Surface Mountable Components - An Update," Electronic Packaging & Production, pp 76-80, January 1984.

Brown, S. D. & Mittman, B., "A Description of the APT Language," CACM 6 (11), pp 649-658, November 1963

Carlisle, B., Roth, S., Gleason, J. & McGhie, D., "The PUMA/VS-100 Robot Vision System," Proceedings of the 1st International Conference on Robot Vision and Sensory Control, pp 149-160, Stratford-upon-Avon, UK, April 1981.

Chao, C. S., "Real-Time Microprocessor Control of a Hexapod Vehicle," Ph. D. Dissertation, The Ohio State University, 1979

Connah, D. M. & Fishbourne, C. K., "Using laser for scene analysis," Proceedings of the 2nd International Conference on Robot Vision and Sensory Controls, Stuggart, Germany, pp 223-240, November 1982

Cooper, W. D., "Electronic Instrumentation and Measuring Techniques," 2nd. Edition, Prentice-Hall, 1978

CONTEXTVISION, Teknikringen 1, S-583 30, Linköping, Sweden, 1985.

Crowley, J. L., "Dynamic World Modelling for an Intelligent Mobile Robot," International Conference on Pattern Recognition, Vol. 1, pp 207-210, Montréal, 1984.

Dekker, M. G., "Introduction to Terrain-Vehicle Systems," University Michigan Press, Ann Arbor, Michigan, 1969

Denavit, J. & Hartenberg, R. S., "A Kinematic Notation for Lower-Pair Mechanisms Based on Matrices," Journal of Applied Mechanics, pp 215-221, June 1955.

Dinstein, I., Merkle, F., Lam, T. D. & Wong, K. Y., "Imaging System Response Linearization and Shading Correction," International Conference on Robotics, pp 204-109, Atlanta, Georgia, March 1984

Duda, R. & Hart, P., "Pattern Classification and Scene Analysis," Wiley (publisher), New York, 1973

Empire Strikes Back, The, 20th Century Fox film release, George Lucas (director), 1981.

Engelberger, J. F., "Robotics in Practice," IFS Publications Ltd., Kempston, England, 1980.

Fairchild, "CCD3000, Video Communications Camera, Automation Camera Series", Fairchild Company Brochure 1983.

Feldman, J. et al., "The Use of Vision and Manipulation to Solve the Instant Insanity Puzzle," Proceedings of the Second International Conference on Artificial Intelligence, pp 359-364, London, England, 1971.

Foley, J. D. & Van Dam, A., "Fundamentals of Interactive Computer Graphics," Addison-Wesley, 1983

Foulloy, L. P. & Kelley, R. B., "Improving the Precision of a Robot," International Conference on Robotics, pp 62-67, Atlanta, Georgia, 1984

Freedman, P., Carayannis, G., Gauthier, D. & Malowany, A. S., "A Session Layer for a Distributed Robotics Environment," Proceedings of the COMPINT '85 Conference, pp 549-565, Montreéal, Canada, September 1985

Fu, K. S., "Pattern Recognition for Automatic Visual Inspection," IEEE COMPUTER, Volume 15, Number 12, pp 34-41, ISSN 0018-9162, December 1982

D. Gauthier, G. Carayannis, P. Freedman, A. Malowany, "A Session Layer Design for the CVaRL Local Area Network," McGill University, Dept of Electrical Engineering, TR-85-7R, February 1985.

Gilbert, E. G. & Johnson, D. W., "Distance Functions and Their Application to Robot Path Planning in the Presence of Obstacles," IEEE Journal of Robotics and Automation, Volume RA-1, Number 1, pp 21-30, March 1985.

Goertz, R. C., "Manipulators Used for Handling Radioactive Materials," Human Factors in Technology, Chapter 27, edited by E. M. Bennett, McGraw-Hill, 1963.

Gonzalez, R. C. & Safabakhsh, R., "Computer Vision Techniques for Industrial Application and Robot Control," IEEE COMPUTER, Volume 15, Number 12, pp 34-41, ISSN 0018-9162, December 1982

Goto, T., Takeyasu, K. & Inoyama, T., "Precise Insert Operation by Tactile-Controlled Robot HI-T-HAND Expert-2," Proceedings of the 4th International Symposium on Industrial Robots, pp 149-159, Tokyo, Japan, May 1972.

Gupta, K. K. & Zucker, S. W., "Path Planning in a Three Dimensional Environment," International Conference on Pattern Recognition, Vol. 1, pp 196-198, Montréal, 1984.

Hackwood, S., Beni, G., Hornak, L. A., Wolfe, R. & Nelson, T. J., "A Torque-Sensitive Tactile Array for Robotics," The International Journal of Robotics Research, Volume 2, Number 2, ISSN 0278-3649, MIT Press, pp 46-50, Summer 1983.

Harmon, S. Y., "Advanced Automation for the Battlefield," Proceedings of the SPIE - The International Society for Optical Engineering - Vol. 360, San Diego, California, pp 67-73, 1982.

Hayati, S. & Mirmirani, M., "Puma 600 Robot Arm Geometric Calculations," International Conference on Robotics, pp 1-8, Atlanta, Georgia, 1984.

Hayes-Roth, F., "The Machine as a Partner of the new Professional," (Letters to the Editor), IEEE Spectrum, Vol 21, Number 6, pp 28-31, June 1984.

Hayward, V. & Paul, R. P., "Real Time Manipulator Control Under Unix," TR-EE 83-42, Purdue University, West Lafayette, Indiana, October 1983

Hayward, V. & Paul, R. P., "Introduction to RCCL: A Robot Control 'C' Library," First IEEE Conference on Robotics, pp 293-297, Atlanta, Georgia, USA, March 1984.

Hohn, R. E., "Application Flexibility of a Computer-Controlled Industrial Robot," Society of Manufacturing Engineering (SME) Technical Paper, MR 76-603, 1976.

Ho, C. S., "Precision of Vision Systems," Conference Proceedings of the Workshop on Industrial Application of Machine Vision, IEEE Computer Society, pp 153-159, Los Angeles, 1982.

Hopcroft, J. E., Schwartz, J. T. & Sharir, M., "Efficient Detection of Intersection among Spheres," The International Journal of Robotics Research, Volume 2, Number 4, ISSN 0278-3649, MIT Press, pp 77-80, Winter 1983.

Hovanesian, J. D. & Hung, Y. Y., "Three Dimensional Shape Recognition by Moire Correlation." Proceedings of SPIE - The International Society of Optical Engineering. Vol. 360. pp 88-89. San Diego. California. 1982.

Hughes Aircraft Corporation, Brochure on the "Probeye Thermal video System." Industrial Products Division. Probeye Marketing. 6155 El Camino Real. Carlsbad. CA 92008. USA.

Jarvis, J. F., "A Method of Automating Visual Inspection of Printed Wiring Boards." IEEE Transaction on Pattern Analysis and Machine Intelligence. Volume PAMI-2. Number 1. pp 77-82. January 1980.

Jarvis, R. A., "A Computer Vision and Robotics Laboratory." IEEE COMPUTER. Volume 15. Number 6. pp 55-61. ISSN 0018-9162. June 1982

Jones, B. M. & Saraga, P., "Parallel Projection Optics in Simple Assembly." Proceedings of the 1st International Conference on Robot Vision and Sensory Controls. pp 99-112. Stratford-upon-Avon. UK. April 1981

Jones, R. D., "Hybrid Circuit Design and Manufacture." Marcel Dekker (Publisher). 1982.

Jordan, S. Z. A., "Robotic Intelligence." Proceedings of the Canadian Conference on Robotics. pp 38-43. September 1982. Mississauga. Ontario.

Kak, A. & Rosenfeld, A., "Digital Picture Processing." Academic Press. 1976.

Kempf, K. G., "Robot Command Languages and Artificial Intelligence." Robots VI. Conference Proceedings. pp 369-383. Detroit. Michigan. March 1982.

Klein, C. A., Olson, K. W. & Pugh, D. R., "Use of Force and Attitude Sensors for Locomotion of a Legged Vehicle over Irregular Terrain." The International Journal of Robotics Research. Volume 2. Number 2. ISSN 0278-3649. MIT Press. pp 3-18. Summer 1983.

Lee, G. C. S., "Robot Arm Kinematics, Dynamics and Control," IEEE COMPUTER, Volume 15, Number 12, pp 62-79, ISSN 0018-9162, December 1982.

Leigthy, R. D., "Army's Activities in Artificial Intelligence/Robotics," Proceedings of SPIE - The International Society for Optical Engineering, Robotics and Industrial Inspection, Volume 360, pp 39-49, August 1982, San Diego, California.

Leonard, P. F., Svetkoff, D. J., Kelley, R. W. & Rohrer, D. K., "Machine Vision Applications in Electronic Manufacturing," Conference Proceedings of Vision '85, pp 5-99 to 5-116, Detroit, Michigan, March 25-28, 1985

Levine, M. D., O'Handley, D. A. & Yagi, G. M., "Computer Determination of Depth Maps," Computer Graphics and Image processing, Vol. 2, pp 131-150, October 1973

Levine, M. D., Eskenazi, C., Zucker, S. W., "Automated Visual Inspection of Electronic Circuits," Canadian Conference on Robotics, Mississauga, Ontario, September 1982

Levine, M. D., "Vision in Man and Machine," McGraw Hill, March 1985.

Levinthal, E. C., "DARPA Program - Intelligent Task automation," Proceedings of SPIE - The International Society for Optical Engineering, Robotics and Industrial Inspection, Volume 360, pp 32-38, San Diego, California, August 1982.

Ligthart, G. & Groen, F. C. A., "A Comparison of Different Autofocus Algorithms," IEEE 6th International Conference on Pattern Recognition, pp 597-600, 1982.

Lloyd, J. E. & Studenny, J., "Kinematics Equation and Solutions for the McGill Vision/Robotics PUMA 260," Department of Electrical Engineering, McGill University, CVaRL Technical Report, TR 84-3, June 1984.

Loewenstein, D., "Computer Vision and Ranging Systems for a Ping Pong Playing Robot," Robotics Age, Vol. 6, No 8, pp 21-25, August 1984.

Lowry, M. R. & Miller, A., "Analysis of Low-level Computer Algorithms for Implementation on a Very Large Scale (VLSI) array." Proceedings of the SPIE. - The International Society for Optical Engineering - Vol. 360, pp 143-150, San Diego, California, August 1982

Lozano-Perez, T., "Robot Programming." Proceedings of the IEEE, Vol. 71, No. 7, pp 821-841, July 1983.

Mansouri, A. R. & Malowany, A. S., Proceedings of the 1985 IEEE Microprocessor Forum, pp 115-122, Atlantic City, New Jersey, April 2-4, 1985.

Malowany, A. S., Levine, M. D. & Thong, W. K., "Calibrating a Robotic Workstation." IEEE Electronicom '85, Toronto, October 5-7, 1985.

Mason, M. T., "Compliance and Force Control for Computer Controlled Manipulators." Robot Motion Planning and Control, Brady et al (editors), MIT Press, Cambridge, 1982

Marcoux, P., "Surface Mount Assemblies Shrink Circuitry." Electronic Packaging & Production, pp 82-86, January 1984

Markstein, H. W., "Pick-and-Place Swings Toward Surface Mount." Electronic Packaging & Production, pp 56-63, January 1984

McConney, R., "An Environment for Programming a PUMA 260 Workcell." M. Eng. thesis, Department of Electrical Engineering, McGill University, (to be submitted in March 1986).

McGhee, R. B., "Control of Legged Locomotion Systems." Proceedings of the IEEE Joint Automatic Control Conference, pp 205-215, New York, 1977.

Michaud, C., Malowany, A. S. & Levine, M. D., "Electronic Assembly by Robots." Graphics Interface '85, Montréal, Québec, pp 391-397, May 27-31, 1985.

Milgram, D. L. et al, "Algorithms and Hardware Technology for Image Recognition."

DARPA Order 3206, University of Maryland, Maryland, March 1978

Merrill, P., "Automated Visual Inspection of Solder Joints," M. Eng Thesis, McGill University, 1984

Mosher, R. S., "Exploring the Potential of a Quadruped," International Automotive Engineering Congress Paper no 690191, Society of Automotive Engineers, New York, 1969

Mudge, T. N., Voltz, R. A. & Atkins, D. E., "Hardware/Software Transparency in Robotics Through Object Level Design," Proceedings of the SPIE, - The International Society for Optical Engineering - Vol 360, pp 216-223, San Diego, California, 1982

Mueller, R. K. & Rylander, R. L., "'Seeing' Acoustically," IEEE Spectrum, Volume 19, Number 2, pp 28-33, February 1982

Nilsson, N. J., "Principles of Artificial Intelligence," Tioga (publisher), Palo Alto, California, 1980

Nimrod, N., Margalith, A. & Mergler, H. W., "A laser-based rangefinder for robotic applications," Proceedings of the 2nd International Conference on Robot Vision and Sensory Controls, pp 241-252, Stuggart, Germany, November 1982

Nitzan, D., "Assessment of Robotic Sensors," Proceedings of the 1st International Conference on Robot Vision and Sensory Control, pp 1-11, Stratford-upon-Avon, UK, April 1981.

Okada, T., "Development of an Optical Distance Sensor for Robots," The International Journal of Robotics Research, Volume 1, Number 4, ISSN 0278-3649, MIT Press, pp 3-14, Winter 1982.

Orin, D. E., "Supervisory Control of a Multilegged Robot," The International Journal of Robotics Research, Volume 1, Number 1, ISSN 0278-3649, MIT Press, pp 79-91, Fall 1982

Parthasarathy, S., Birk, J. & Dessimoz, J., "Laser Rangefinder for Robot Control and

Inspection." Proceedings of the SPIE. - The International Society for Optical Engineering - Vol 336, pp 2-11, Arlington, Virginia, 1982

Paul, R. P. & Shimano, B. E., "Compliance and Control." The 1976 Joint Automatic Control Conference, pp 649-699, 1976.

Paul, R. P., "WAVE: A Model-Based Language for Manipulator Control." *The Industrial Robot* **4** 1, pp 10-17, March 1977

Paul, R. P., "Modelling, Trajectory Calculation and Servoing of a Computer-controlled Arm." Stanford Artificial Intelligence Laboratory, Stanford University, AIM 313, 1978.

Paul, R. P., Shimano, B. & Mayer, G., "Differential Kinematic Control Equations for Simple Manipulators." IEEE Transactions on Systems, Man, and Cybernetics, Vol SMC-11, No 6, pp.456-460, June 1981

Paul, R. P., "Robot Manipulators: Mathematics, Programming, and Control." MIT Press, Cambridge, 1981

Pavlidis, T., "Algorithms for Graphics and Image Processing." Computer Science Press, ISBN 0-914894-65-X AACR2, 1982

Pease, W., "An Automatic Machine Tool." Scientific American, 187 (3), pp 101-115, September 1952

Pfister, S. L., "Robotics - Development of the Second Industrial Revolution." Conference Proceedings of Robots VI, pp 3-14, Detroit, Michigan, March 1982.

Pipitone, F. J. & Marshall, T. G., "A Wide-Field Scanning Triangulation Rangefinder for Machine Vision." The International Journal of Robotics Research, Volume 2, Number 1, pp 39-49, ISSN 0278-3649, MIT Press, Spring 1983.

Porter, G. B. III & Mundy, J. L., "Non-contact profile sensing system for visual inspection." Proceedings of the SPIE. - The International Society for Optical Engineering - Vol 336. pp 67-83. Arlington. Virginia. 1982.

Pugh, A., "Robotic Technology." Edited by A. Pugh. Published by Peter Peregrinus. 1983.

Raibert, M. H. & Craig, J. J., "Hybrid Position/Force Control of Manipulators." Robot Motion Planning and Control. Brady et al (editors). MIT Press. Cambridge. 1982

Raibert, M. H. & Tanner, J. E., "Design and Implementation of a VLSI Tactile Sensing Computer." The International Journal of Robotics Research. Volume 1. Number 3. pp 3-18. ISSN 0278-3649. MIT Press. Fall 1982.

Rausa, M., Poseika, R. & Goldenberg, A., "Integrated Manufacturing Systems." Canadian Conference on Robotics Proceedings. pp 38-43. September 1982. Mississauga. Ontario

Return of the Jedi, The. 20th Century Fox film release. George Lucas (director). 1983.

Rioux, M., Laser Range Finder based on Synchronized Scanners. Applied Optics. Volume 23. Number 21. pp 3837-3844. November 1984.

Roberts, L. G., "Machine Perception of Three-Dimensional Solids." Report No 315. Lincoln Laboratory. Massachusetts Institute of Technology. 1963

Roberts, L. G., "Homogeneous Matrix Representation and Manipulation of N-Dimensional Constructs." Document No MS1045. Lincoln Laboratory. Massachusetts Institute of Technology. 1965

Rosenberg, J., "A History of Numerical Control 1949-1972: The Technical Development. Transfer to Industry. and Assimilation." U.S C. Information Sciences Institute. Marina del Ray. California. Report No ISI-RR-72-3. 1972.

Ross, D., "Automatically Programmed Tool System: The APT Joint Effort". pp 70. Mechanical Engineering. 81 (5). May 1959.

Sanderson, A. C. & Perry, C., "Sensor-based Robotic Assembly Systems: Research and Applications in Electronic Manufacturing." Proceedings of the IEEE. Vol. 71. No 7. pp 856-871. July 1983

Schwartz, J. T. & Sharir, M., "On the piano movers' problem: III. Coordinating the Motion of Several Independent Bodies The Special ~~Case of~~ Circular Bodies Moving Amidst Circular Barriers." The International Journal of Robotics Research. Volume 2. Number 3. pp 46-75. ISSN 0278-3649. MIT Press. Fall 1983.

Seltzer, D. S., "Tactile Sensory Feedback for Difficult Robot Tasks." Robots VI. Conference Proceedings. pp 467-478. Detroit. Michigan. March 1982.

Shneier, M., Kent, E. & Mansbach, P., "Representing Workspace and Model Knowledge for a Robot with Mobile Sensors." International Conference on Pattern Recognition. Vol. 1. pp 199-202. Montréal. 1984.

Soroka, B. I., "What Can't Robot Languages Do?." Conference Proceedings of 13th International Symposium on Industrial Robots and Robots VII. Vol. 2. pp (12-1) - (12-8). Chicago. April. 1983

Star Wars. 20th Century Fox film release. George Lucas (director). 1979

Stauffer, R. N., "Robot Accuracy." Robotics Today. Volume 7. Number 2. pp 43-49. April 1985

Sterling, W. M., "Automatic Non-Reference Inspection of Printed Wiring Boards." Proceedings of IEEE Conference on Pattern Recognition and Image Processing. pp 93-100. August 1979.

Sun, S. S., "A Theoretical Study of Gaits for a Legged Locomotion Systems," Ph D. Dissertation. The Ohio State University. 1974.

Synder, W. E. & St. Clair, J., "Conductive Elastomers as Sensors for Industrial Parts

Handling Equipment." IEEE Transactions on Instrumentation and Measurement. IM-27(1). 1978

Taylor, R. H., Summers, R. D. & Meyers, J. M., "AML: A Manufacturing Language." The International Journal of Robotics Research. Volume 1. Number 3. pp 19-41. ISSN 0278-3649. MIT Press. Fall 1982

Thibadeau, R. H., "Automated Visual Inspection as Skilled Perception." Conference Proceedings of Vision '85. pp 5-1 to 5-19. Detroit. Michigan. March 25-28. 1985.

Thomas, L., "The Lives of a Cell Notes of a Biology Watcher." Penguin Books. (publisher). 1978c. 1974. ISBN 0140047433

Thomas, L., "The Medusa and the Snail. More Notes of a Biology Watcher." Viking Press (publisher) 1979. ISBN 0670465682

Trepagnier, P., "Recent Developments in Visual Gaging." Conference Proceedings of Vision '85. pp 3-12 to 3-23. Detroit. Michigan. March 25-28. 1985

Udupa, S.M., "Collision Detection in Computer Controlled Manipulators." 5th International Joint Conference on Artificial Intelligence. pp 737. MIT. 1977.

Unimation. 200 Series. Volume I - Equipment Manual. Version 260 V13G. August 1983.

Unimation. 260 Series. Volume II - Programming Manual. "User's Guide to VAL." Version 260 V13G. August 1983.

Valetz, M. C., "An Introduction to Multi Robot Control Using Production Systems." IEEE Workshop on Languages for Automation. pp 22-27. IEEE Computer Society. December 1983.

VanderBrug, G. J., "RAIL. A Language for Vision and Robotics." Proceedings of COMPSAC81. IEEE Computer Society. 1981.

Watson, P. C. & Drake, S. H., "Pedestal and Wrist Force Sensors for Automatic Assembly," Proceedings of the 5th International Symposium on Industrial Robots, pp 501-511, Chicago, Illinois, September 1975.

WEBSTER'S, "Webster's New Collegiate Dictionary," G. C. Merriam (publisher), 1981.

Whitney, D. E., "Force Feedback Control of Manipulator Fine Motions," The 1976 Joint Automatic Control Conference, pp 649-699, 1976.